CZECH TECHNICAL UNIVERSITY IN PRAGUE

Faculty of Electrical Engineering

BACHELOR'S THESIS

Filip Novák

Escape Behaviour in Self-localised Swarms of Micro Aerial Vehicles

August 2020

Department of Cybernetics

Thesis supervisor: **Ing. Martin Saska, Dr. rer. nat.**

CTU CZECH TECHNICAL UNIVERSITY IN PRAGUE

BACHELOR'S THESIS ASSIGNMENT

I. Personal and study details

Student's name: **Novák Filip** Personal ID number: **474570**

Faculty / Institute: **Faculty of Electrical Engineering**

Department / Institute: **Department of Cybernetics**

Study program: **Cybernetics and Robotics**

II. Bachelor's thesis details

Bachelor's thesis title in English:

Escape Behaviour in Self-Localised Swarms of Micro Aerial Vehicles

Bachelor's thesis title in Czech:

Únikové chování ve vzájemně lokalizovaných rojích miniaturních dronů

Guidelines:

The aim of the thesis is to design, implement and experimentally verify a method for fast escaping a swarm of micro aerial vehicles (MAV) from an approaching obstacle (a predator). Work plan:

- To understand boids model of flocking of micro-aerial vehicles [4] and the system of MRS group at CTU designed for stabilization of MAV groups [1,6].
- To design and implement an escape behaviour (such as the one in [2,3]) with shock propagation within the MAV group.
- To integrate the designed system into the Robot Operating System (ROS), verify its behavior with MAV models in Gazebo, and adapt the system for using with the relatively localized MAV system of Multi Robot Systems group at CTU in Prague [5].
- To compare the obtained method with classical boids model.
- To compare achieved behaviour with and without possibility of communicating the state (escaping state/normal state) of particular MAVs
- If weather and platforms availability allow, to prepare a HW outdoor experiment.

Bibliography / sources:

[1] V Spurny, T Baca, M Saska, R Penicka, T Krajnik, J Thomas, D Thakur, G Loianno and V Kumar. Cooperative Autonomous Search, Grasping and Delivering in a Treasure Hunt Scenario by a Team of UAVs. Journal of Field Robotics 36(1):125-148, 2019.
[2] H. Min and Z. Wang, Design and analysis of group escape behavior for distributed autonomous mobile robots, in IEEE ICRA, 2011.
[3] Jan Bulušek. Active and passive escape behavior designed for groups of autonomous helicopters. CTU thesis. 2014.
[4] R. Olfati-Saber, "Flocking for multi-agent dynamic systems: Algorithms and theory," IEEE Transactions on Automatic Control, vol. 51, no. 3, pp. 401–420, 2006.
[5] V Walter, N Staub, A Franchi and M Saska. UVDAR System for Visual Relative Localization With Application to Leader–Follower Formations of Multirotor UAVs. IEEE Robotics and Automation Letters 4(3):2637-2644, July 2019.
[6] T Baca, D Hert, G Loianno, M Saska and V Kumar. Model Predictive Trajectory Tracking and Collision Avoidance for Reliable Outdoor Deployment of Unmanned Aerial Vehicles. In 2018 IEEE/RSJ International Conference on Intelligent Robots and Systems (IROS). 2018.

Name and workplace of bachelor's thesis supervisor:

Ing. Martin Saska, Dr. rer. nat., Multi-robot Systems, FEE

Name and workplace of second bachelor's thesis supervisor or consultant:

Date of bachelor's thesis assignment: **15.02.2020** Deadline for bachelor thesis submission: **14.08.2020**

Assignment valid until: **30.09.2021**

Ing. Martin Saska, Dr. rer. nat.	doc. Ing. Tomáš Svoboda, Ph.D.	prof. Mgr. Petr Páta, Ph.D.
Supervisor's signature	Head of department's signature	Dean's signature

III. Assignment receipt

The student acknowledges that the bachelor's thesis is an individual work. The student must produce his thesis without the assistance of others, with the exception of provided consultations. Within the bachelor's thesis, the author must state the names of consultants and include a list of references.

.

Date of assignment receipt

Student's signature

Author statement for undergraduate thesis:
I declare that the presented work was developed independently and that I have listed all sources of information used within it in accordance with the methodical instructions for observing the ethical principles in the preparation of university theses.

Prague, date............................. ....
Signature

Acknowledgements

I would like to thank my thesis supervisor Ing. Martin Saska, Dr. rer. nat. for his advice. Special thanks belongs to my family, who supports me throughout my life. Last thanks is for members of Multi-Robot Systems group and other people who helped me with this thesis.

Abstract

This thesis deals with the design, implementation and verification of system for escaping a swarm of micro aerial vehicles from a dynamic obstacle. The system is based on the Boids swarming model with implemented escape behaviour algorithm and is adapted for using a method of relative localization of micro aerial vehicles developed by Multi-Robot Systems group at Czech Technical University in Prague. The designed system is tested in realistic simulator Gazebo and verified by conducting real-world experiments. The achieved behaviour is compared with standard Boids model and also with and without the possibility of communication between particular micro aerial vehicles.

Keywords

swarm, boids, escape behaviour, MAV, drone, dynamic obstacle

Abstrakt

Tato práce se zabývá návrhem, implementací a ověřením systému pro únik roje bezpilotních helikoptér od pohybující se překážky. Systém je založen na rojovém modelu Boids s implementací algoritmu únikového chování a je schopen použít metodu relativní lokalizace bezpilotních helikoptér vyvíjenou ve skupině Multirobotických systémů na Českém vysokém učení technickém v Praze. Navržený systém je testován v realistickém simulátoru Gazebo a ověřen při reálných experimentech. Dosažené chování je porovnáno s klasickým rojovým modelem Boids bez implementovaného algoritmu únikového chování a též je srovnáno chování systému s možností komunikace mezi jednotlivými bezpilotními helikoptérami a bez této možnosti.

Klíčová slova

roj, boids, únikové chování, MAV, dron, dynamická překážka

Contents

List of Figures

List of Tables

Chapter 1

Introduction

Nowadays, there is a great boom in modern autonomous technologies. Rapid development concerns on all types of robots - ground, water and of course aerial. This thesis focuses on Micro Aerial Vehicles (MAV) as a subtype of aerial robots. An example of a MAV is displayed in Figure 1.1. Due to MAVs size restriction, more individual robots are often needed to accomplish the given task.

The use of a group of MAVs grows every year. A group of MAVs can be used for searching for lost people in a wide area, e.g. children in a forest, localization of fires and initial fire-fighting action, measuring air pollution over the city, measurement of radiation, monitoring animals, ensuring security and surveillance of large areas, recording concerts from multiple angles and also helping to ensure security at large events such as festivals, where more small cameras provide images of the situation is better than one high quality camera.

With such wide use of MAVs, the group of MAVs must be able to avoid static obstacles as well as dynamic ones. A dynamic obstacle can also be called a moving obstacle or a predator. Numerous objects can be considered such predators - another aerial vehicle, people moving around the group of MAVs regardless of their intentions, hostile devices trying to assault the group and also animals. Avoiding dynamic obstacles can be called *Escape behaviour* [1] and has an important role, because it can protect the group of MAVs and the predator. For example, if children come close to the group of MAVs, they could get hurt.

To control the group of MAVs it is necessary to implement a system for their stabilization. Basis of such a system called *Boids* was introduced by Craig W. Reynolds in [2]. This system is designed for dimensionless particles and the dynamics of these particles were not considered. The group of robots called *swarm* is also described by Vito Trianni in [3]. A system dealing with a group of robots is the subject of research in many scientific studies [4][5][6][7].

Figure 1.1: An example of Micro Aerial Vehicle (MAV)

A system based on Boids is designed in [8]. This system contains implementation for static obstacle avoidance and was verified in realistic simulator Gazebo [9] and by conducting real-world experiments. However, Escape behaviour is not implemented in this system and for proper functionality, the system requires communication to share position and velocity between individuals in a group.

Systems for control of MAVs group with included Escape behaviour is presented in [10][11]. These systems were verified in simulators, but verification in real-world experiments is missing. As a result, the use of these systems is not realistic, and thus serve only as a theoretical assumption for further work.

This thesis proposes a design of a system for stabilization of MAVs group (swarm) that will be based on [2][8]. Escape behaviour based on [1][10][11] will also be integrated as one of the main parts of the system. As mentioned above, these systems still need communication for proper functionality. For this purpose, the system developed by Multi-robot Systems group at Czech Technical University called UVDAR system [12][13] will be integrated to reduce the requirements for communication.

The motivation for this thesis is the creation of autonomous system used for a group of MAVs that is able to use the UVDAR system for relative localization without the need for communication. The goal for the system designed in this thesis is to avoid dynamic obstacles thanks to the implementation of Escape behaviour. The designed system will be prepared for experiments in real conditions.

The system designed in this thesis will be tested in realistic simulator Gazebo in order to imitate real conditions and verified by conducting real-world experiments. The behaviour of a system with implemented Escape behaviour and a system using classic Boids algorithm are compared in exhaustive simulation testing. The behaviour of systems using Escape behaviour with or without the ability of communication are similarly compared.

Chapter 2

Swarm of MAVs

There are several definitions of a swarm in technical literature [4][5][6]. In general, this literature defined a swarm as a group of individuals that move together, cooperate and work on an assigned task, but this swarm definition is not specific enough for our purposes. A more detailed definition is formulated by Vito Trianni who presented swarm as follows [3, p. 39-40]:

> *"Additionally, the controller the robotic system should be distributed, flexible and robust, in order for the system is efficient and reliable. Decentralization, locality, flexibility, robustness and emergence are what we consider the main features of a swarm robotic system."*

There are five terms mentioned in the citation above - *decentralization*, *locality*, *flexibility*, *robustness* and *emergence*. *Decentralization* means the absence of a specific leader to control the behaviour of other swarm members. Each swarm member has to make its own decisions based on observation of the surroundings and the requirement of the current task. *Locality* refers to a limited sensing range and communication ability. Adaptation to new conditions and environment is ensured by *flexibility*. If any of the swarm members fails, the swarm system must be able to continue operating, a property which is called *robustness*. The last term mentioned is *emergence* which is described by Vito Trianni [3, p. 46]: *"The control is distributed, and all parts of the system contribute to the emergence of the organisation. The global order is the result of the numerous interactions among the system components."* The system in this thesis will be designed to meet this definition of a swarm.

The behaviour of a swarm may be inspired by observing equivalent situations in nature. In artificial intelligence, the behaviour inspired by group of birds is called *flocking*. Boids system based on flocking was presented in [2] by Craig W. Reynolds and will be used as the basis of the system designed in this thesis. It consists of three principles: keeping the swarm together (Flock centering), preventing collisions (Collision avoidance) and maintaining swarm's direction and speed (Velocity matching).

In order to perform compact flocking of real MAVs, it is necessary that a MAV knows the state of the surrounding MAVs. The state contains information about position, velocity and direction of movement. The easiest approach is to implement communication between members of the swarm and broadcast states of each member in a global frame, which is the same for all swarm members. In real environment, both the broadcasting in large groups and precise localization are difficult to achieve with sufficient reliability. For such position estimation it is necessary to use a global sensor (such as Global Navigation Satellite System (GNSS)), which can easily lose the signal and its precision is insufficient for compact flocking. The loss of signal typically happens during a flight through a forest, urban areas or when flying indoors. To share MAV states it is also necessary to ensure reliable communication, ad hoc network for the variable size of the swarm and to ensure a sufficient transfer rate for keeping the current information about the surroundings. To achieve robustness w.r.t. such challenges, the UVDAR system [12] will be used to localize other MAVs.

Figure 2.1: A flock of birds exhibits swarm-like behaviour [14]

2.1 Boids

The Boids algorithm consists of three basic rules that are applied to neighbours in distance less than r_B from an agent. We will define the state of the agent in terms of its position $\vec{p}_A$ and velocity $\vec{v}$ in the global frame, both of which are vectors in $\mathbb{R}^3$.

- **position** - $\vec{p}_A = (x, y, z)$
- **velocity** - $\vec{v} = (v_x, v_y, v_z)$

The proposed system is intended to be used onboard of each agent in a decentralised way. Therefore, each of the following rules must be evaluated separately for each agent. To describe the relationship between neighbours, relative position $\vec{p}_{j,i}$, will be introduced. It is a vector with origin in the current position of agent j and ends in current position of another agent i.

- **relative position** - $\vec{p}_{j,i} = \vec{p}_{Ai} - \vec{p}_{Aj}$

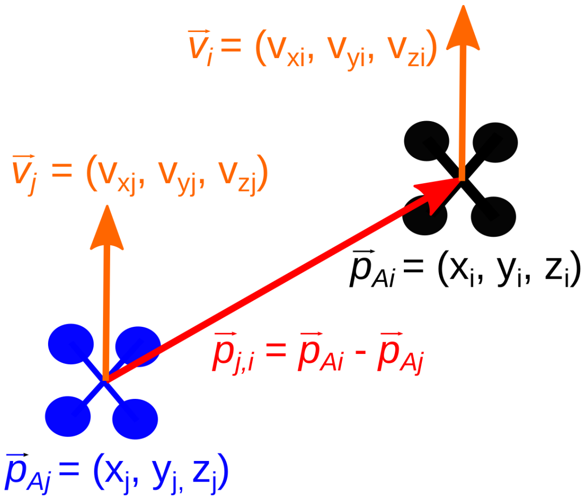

Figure 2.2: Parameters of the agent state

The first rule of the Boids model states that individual agents are attracted to each other within the distance r_B. This is ensured by the Cohesion force (Figure 2.3). This force keeps the agents together and if any of the agents are separated, the force pulls them back into the swarm. Its magnitude increases with the distance of the individual agent from other members of the swarm (agents).

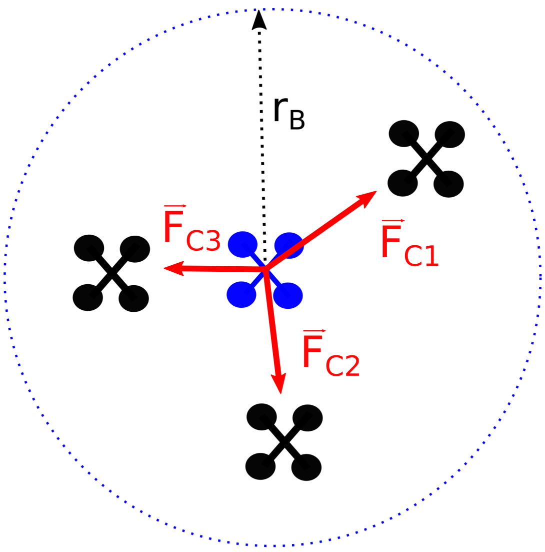

Figure 2.3: Cohesion force $\vec{F}_C$

The second rule prevents collisions among the agents and protects them from getting too close to each other. If the agents approach one other, the Separation force actives (Figure 2.4). Its magnitude increases with decreasing distance between agents. The direction of this force is opposite to the direction of the Cohesion force associated with the same neighbour.

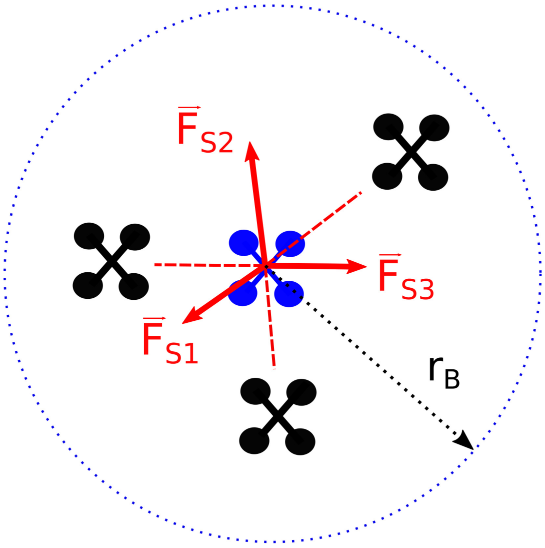

Figure 2.4: Separation force $\vec{F}_S$

The last rule applies the Alignment force (Figure 2.5) which takes into account the velocity of the surrounding members of the swarm. This force promotes unification of velocities of the swarm members.

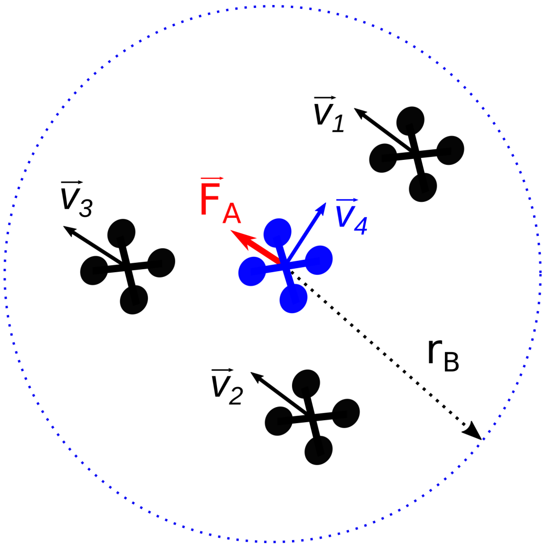

Figure 2.5: Alignment force $\vec{F}_A$

2.1.1 Cohesion force

As mentioned above, the task of the Cohesion force $\vec{F}_C$ is to keep agents in a compact group (flock). To calculate the Cohesion force it is necessary to know the relative positions $\vec{p}_i$ of other n swarm members that are located in the proximity of the agent. According to [8], the Cohesion force can be defined as

$$\vec{F}_C = \frac{1}{n}\sum_{i=1}^{n} \vec{F}_{Ci}, \tag{2.1}$$

$$\vec{F}_C = \frac{1}{n}\sum_{i=1}^{n} k_C \vec{p}_i, \tag{2.2}$$

where $k_C = 1\ \mathrm{m}^{-1}$.

Due to the high tendency of agents to collide with each other detected in initial tests in Gazebo simulator, the definition of the Cohesion force in [8] has been modified in the proposed system as follows:

$$\vec{F}_C = \frac{1}{n}\sum_{i=1}^{n} \epsilon_i \frac{\vec{p}_i}{||\vec{p}_i||}, \tag{2.3}$$

where parameter ϵ_i is defined as

$$\epsilon_i = \begin{cases} 0, & p_{2i} < d_{min} \\ k_{1C}(p_{2i} - d_{min})^2, & d_{min} < p_{2i} < d_C \\ k_{2C} \log\left(k_{3C}(p_{2i} - d_C) + 1\right) + c, & \text{otherwise} \end{cases} \tag{2.4}$$

$$p_{2i} = ||\vec{p}_i|| - l, \tag{2.5}$$

$$c = k_{1C}(d_C - d_{min})^2, \tag{2.6}$$

the values of parameters d_{min}, d_C, k_{1C}, $k_{2C} \in \mathbb{R}^+$ are summarised in Table 2.1, $k_{3C} = 1\ \mathrm{m}^{-1}$ and $l = 1$ m. For comparison, both the original and the modified Cohesion force are plotted in Figure 2.6.

Parameter	Value
d_{min}	4 m
d_C	6 m
k_{1C}	0.1 m^{-2}
k_{2C}	1

Table 2.1: Values of parameters of the Cohesion force identified empirically in simulations

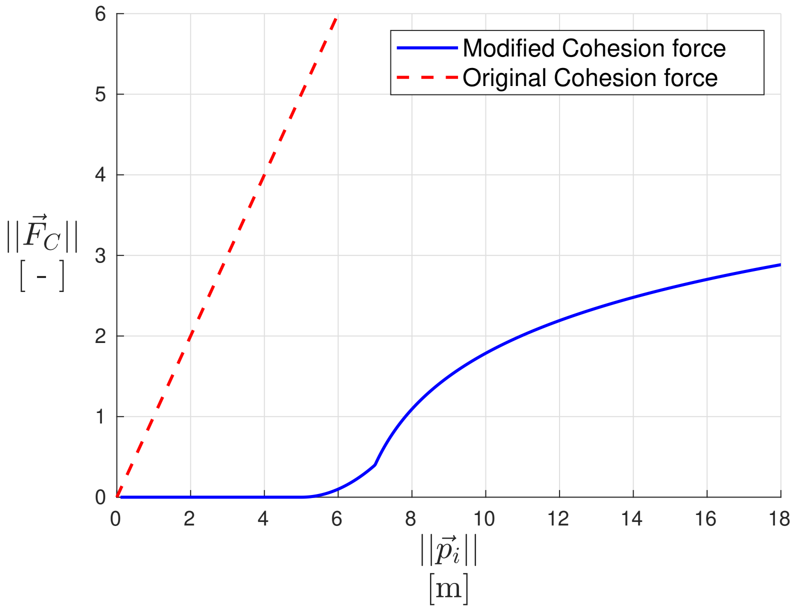

Figure 2.6: Graph of the original and the modified Cohesion force $\vec{F}_C$ for parameters in Table 2.1

2.1.2 Separation force

The separation force $\vec{F}_S$ is very important because it prevents collisions between agents. To determine its magnitude for one agent, it is necessary to know the relative positions $\vec{p}_i$ of the surrounding n swarm members. In [8], the Separation force is defined as

$$\vec{F}_S = \frac{1}{n}\sum_{i=1}^{n}\vec{F}_{Si}, \tag{2.7}$$

$$\vec{F}_S = -\frac{1}{n}\sum_{i=1}^{n}\epsilon_i\ \vec{p}_i, \tag{2.8}$$

with parameter ϵ_i defined as

$$\epsilon_i = \begin{cases} k_S\left(\dfrac{\sqrt{||\vec{p}_i||}}{||p_i||} - \dfrac{\sqrt{d}}{d}\right), & ||\vec{p}_i|| \leq d \\ 0, & ||\vec{p}_i|| > d \end{cases} \tag{2.9}$$

where $k_S = 1\ \mathrm{m}^{\frac{1}{2}}$ and $d = 8$ m.

After analysing the simulation results it was necessary to change the definition of the Separation force to improve the swarm behaviour of real robotic systems. The new proposed Separation force is as follows

$$\vec{F}_S = -\sum_{i=1}^{n} \epsilon_i \frac{\vec{p}_i}{||\vec{p}_i||}. \tag{2.10}$$

Parameter ϵ_i is defined as

$$\epsilon_i = \begin{cases} 0, & d_{max} < p_{2i} \\ k_{1S}(p_{2i} - d_{max})^2, & d_S < p_{2i} < d_{max} \\ k_{2S}\left(\frac{\sqrt{p_{2i}}}{p_{2i}} - \frac{\sqrt{d_{max}}}{d_{max}}\right) + c, & \text{otherwise} \end{cases} \tag{2.11}$$

$$p_{2i} = \begin{cases} ||\vec{p}_i|| - l, & ||\vec{p}_i|| > l + l_{min} \\ l_{min}, & \text{otherwise} \end{cases} \tag{2.12}$$

$$c = k_{1S}(d_S - d_{max})^2 - k_{2S}\left(\frac{\sqrt{d_S}}{d_S} - \frac{\sqrt{d_{max}}}{d_{max}}\right), \tag{2.13}$$

where $l = 1$ m, $l_{min} = 0.0001$ m and the values of parameters d_{max}, d_S, k_{1S}, $k_{2S} \in \mathbb{R}^+$ are given in Table 2.2.

Parameter	**Value**
d_{max}	4 m
d_S	2 m
k_{1S}	0.075 m^{-2}
k_{2S}	1.45 $m^{\frac{1}{2}}$

Table 2.2: Values of parameters of the Separation force identified empirically in simulations

Graph of the modified Separation force $\vec{F}_S$ for $n = 1$ is shown in Figure 2.7 together with the original Separation force for comparison.

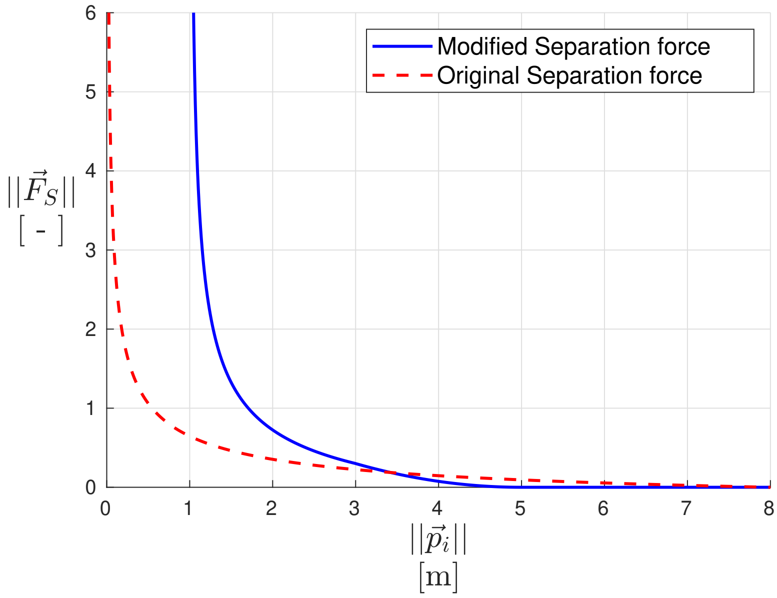

Figure 2.7: Graph of the original and the modified Separation force $\vec{F}_S$ for parameters in Table 2.2

2.1.3 Alignment force

The Alignment force $\vec{F}_A$ unifies the direction of movement of all individuals in the swarm. A deeper analysis shows that it also increases the collision protection, since it forces the direction of the movement of all members in the swarm to become parallel. In [8], the Alignment force is defined as

$$\vec{F}_A = \frac{1}{n}\sum_{i=1}^{n} \vec{F}_{Ai}, \tag{2.14}$$

$$\vec{F}_A = \frac{1}{n}\sum_{i=1}^{n} \vec{v}_i. \tag{2.15}$$

In this thesis, the Alignment $\vec{F}_A$ force defined in equation (2.15) is considered as dimensionless.

During system testing in the simulation, the calculation formula was modified by adding a constant factor $k_A \in \mathbb{R}$ as

$$\vec{F}_A = \frac{1}{n}\sum_{i=1}^{n} k_A \vec{v}_i, \tag{2.16}$$

where parameter $k_A = 0.1$ s·m^{-1} was identified as a reasonable value for swarm of MAVs with the given size and motion dynamics. In Figure 2.8, the modified Alignment force is plotted along with the original version for comparison.

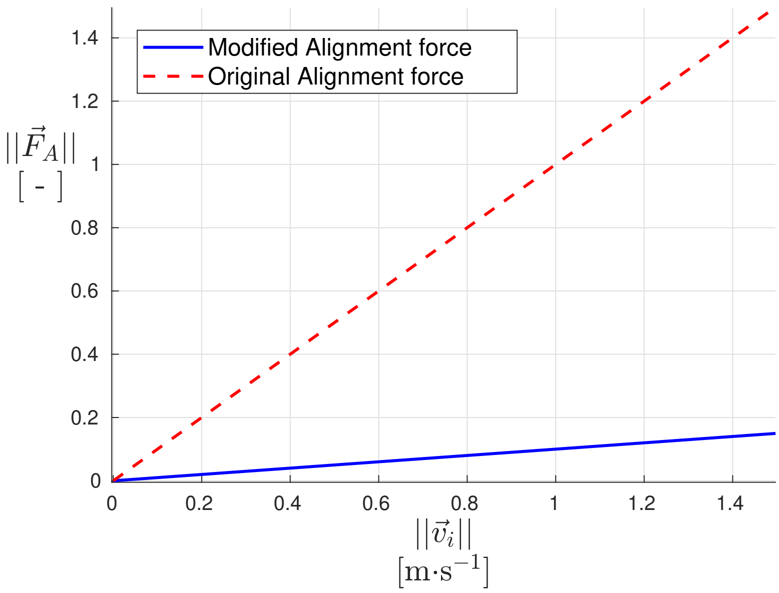

Figure 2.8: Graph of the original and the modified Alignment force $\vec{F}_A$ for $k_A = 0.1$ s·m^{-1}

2.2 Obstacles

A swarm controller suitable for real-world deployment should also ensure safe movement in an environment with obstacles. There are many different kinds of obstacles such as trees, buildings, cars, etc. that agents have to avoid. The method used for obstacle avoidance is presented in [7] and was used in [8].

The method in [7] is based on β-agents that are placed on the closest point of an obstacle to the agent. This point is approached as a virtual agent. Similarly to the Boids algorithm, swarm members have to keep a safe distance from this virtual agent. This is achieved by including a force that is called the Obstacle repulsive force $\vec{F}_{O1}$. The second force called the Obstacle orthogonal force $\vec{F}_{O2}$ is perpendicular to the Obstacle repulsive force $\vec{F}_{O1}$ (see Figure 2.9) and has characteristics of the Alignment force $\vec{F}_A$. The Obstacle repulsive force $\vec{F}_{O1}$ and the Obstacle orthogonal force $\vec{F}_{O2}$ comprise the components of the Obstacle force $\vec{F}_O$.

Definitions of forces $\vec{F}_{O1}$ and $\vec{F}_{O2}$ are based on the knowledge of the relative positions $\vec{p}_O$ of the obstacles. In this thesis, this information is obtained from the laser range scanner RPLIDAR A3 [15] integrated in Robot Operating System (ROS) [16] which provides the relative positions of the obstacles as a point cloud sampling their surfaces. Point cloud is a set of data points n in space. Each point i from the point cloud is considered as an obstacle where β-agent is placed. This method of obtaining data has the advantage of being universally applicable to different types of obstacles. Whether the obstacle is a tree, a building or a car, its representation is still point cloud.

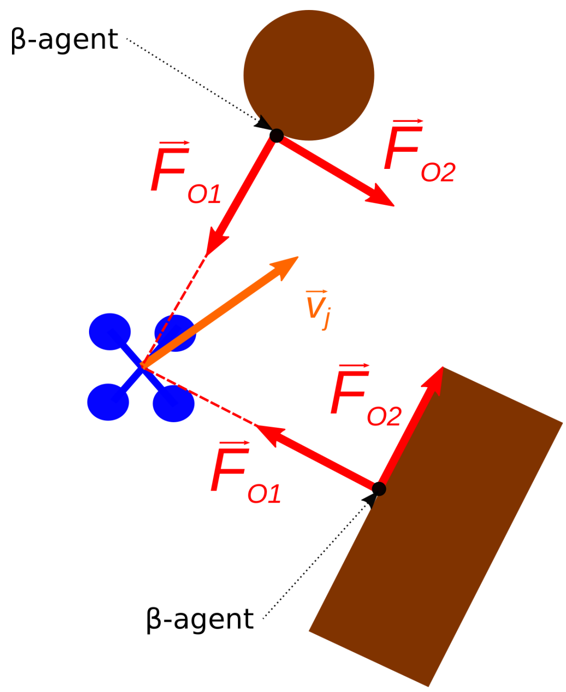

Figure 2.9: Diagram of the Obstacle force $\vec{F}_O$

2.2.1 Obstacle repulsive force

The Obstacle repulsive force $\vec{F}_{O1}$ is obtained as

$$\vec{F}_{O1} = -\epsilon_1 \frac{\vec{p}_O}{||\vec{p}_O||}. \tag{2.17}$$

The parameter ϵ_1 is determined as

$$\epsilon_1 = \begin{cases} k_{O1}\left(\frac{\sqrt{p_{O2}}}{p_{O2}} - \frac{\sqrt{d_{O,max}}}{d_{O,max}}\right), & p_{O2} < d_{O,max} \\ 0, & \text{otherwise} \end{cases} \tag{2.18}$$

$$p_{O2} = \begin{cases} ||\vec{p}_O|| - r_O, & ||\vec{p}_O|| > r_O + l_{min} \\ l_{min}, & \text{otherwise} \end{cases} \tag{2.19}$$

where $l_{min} = 0.0001$ m and parameters $k_{O1},\ r_O,\ d_{O,max}, \in \mathbb{R}^+$. Graph of its magnitude $||\vec{F}_{O1}||$ for parameters $k_{O1} = 4\ \text{m}^{\frac{1}{2}}$, $r_O = 1.5$ m and $d_{O,max} = 6$ m is shown in Figure 2.10.

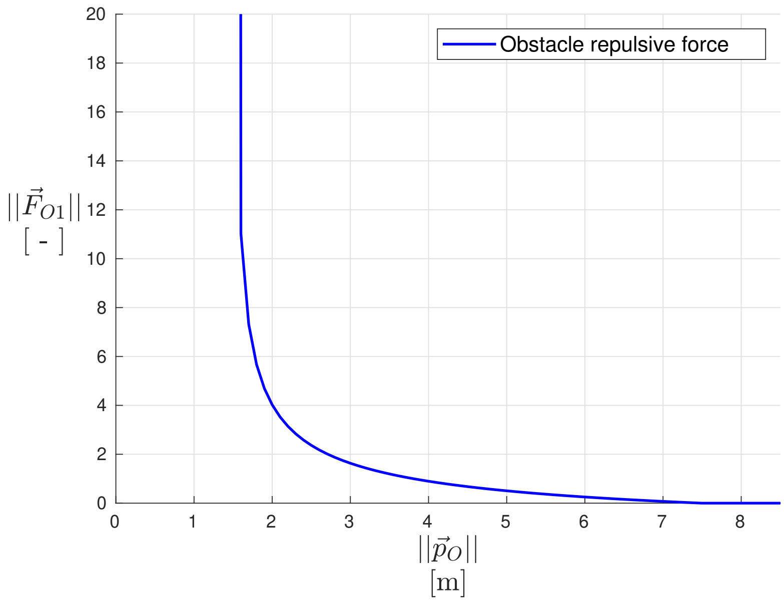

Figure 2.10: Graph of the Obstacle repulsive force $\vec{F}_{O1}$ for $k_{O1} = 4\ \mathrm{m}^{\frac{1}{2}}$, $r_O = 1.5$ m and $d_{O,max} = 6$ m

2.2.2 Obstacle orthogonal force

For the calculation of the Obstacle orthogonal force it is essential to create a projection matrix P as follows

$$P = I - \frac{\vec{p}_O}{||\vec{p}_O||}\left(\frac{\vec{p}_O}{||\vec{p}_O||}\right)^T, \tag{2.20}$$

where I symbolizes identity matrix. Projection matrix P is applied to velocity $\vec{v}$ of the agent.

$$\vec{v}^P = P\vec{v}. \tag{2.21}$$

The Obstacle orthogonal force $\vec{F}_{O2}$ is obtained as

$$\vec{F}_{O2} = \epsilon_2 \frac{\vec{v}^P}{||\vec{v}^P||}. \tag{2.22}$$

Parameter ϵ_2 is determined as

$$\epsilon_2 = \begin{cases} k_{O2}\left(\frac{\sqrt{p_{O2}}}{p_{O2}} - \frac{\sqrt{d_{O,max}}}{d_{O,max}}\right), & p_{O2} < d_{O,max} \\ 0, & \text{otherwise} \end{cases} \tag{2.23}$$

$$p_{O2} = \begin{cases} ||\vec{p}_O|| - r_O, & ||\vec{p}_O|| > r_O + l_{min} \\ l_{min}, & \text{otherwise} \end{cases} \tag{2.24}$$

where $l_{min} = 0.0001$ m and parameters $k_{O2},\ r_O,\ d_{O,max} \in \mathbb{R}^+$. Parameters are set to values $k_{O2} = 4\ \mathrm{m}^{\frac{1}{2}}$, $r_O = 1.5$ m, $d_{O,max} = 6$ m and the magnitude of the Obstacle orthogonal force $||\vec{F}_{O2}||$ is shown in Figure 2.11.

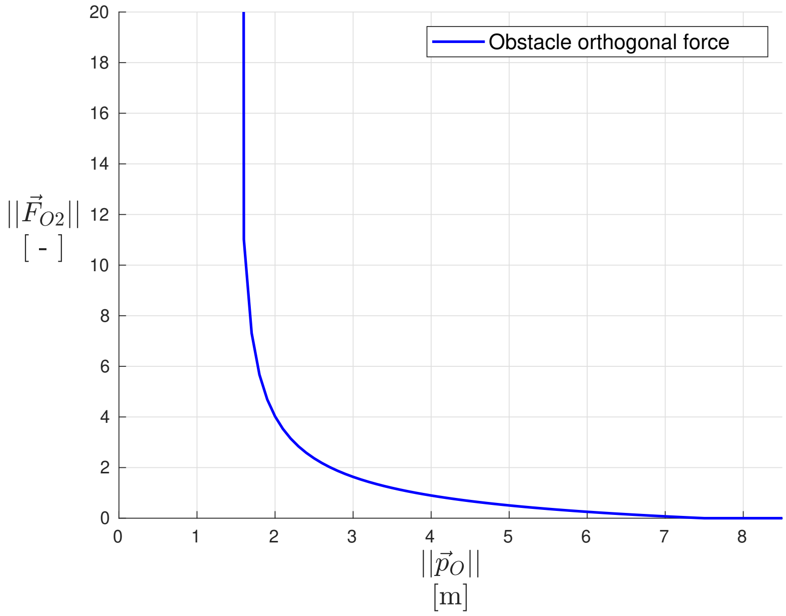

Figure 2.11: Graph of the Obstacle orthogonal force $\vec{F}_{O2}$ for $k_{O2} = 4\ \mathrm{m}^{\frac{1}{2}}$, $r_O = 1.5$ m, $d_{O,max} = 6$ m

2.2.3 Obstacle force

For n points in point cloud, the Obstacle force $\vec{F}_O$ is defined as the sum of Obstacle repulsive forces $\vec{F}_{O1,i}$ and Obstacle orthogonal forces $\vec{F}_{O2,i}$.

$$\vec{F}_O = \frac{1}{n} \sum_{i=1}^{n} \vec{F}_{O1,i} + \vec{F}_{O2,i}. \tag{2.25}$$

2.3 Effects of the forces

The Total force $\vec{F}_T$ acting on an agent is given by combining all of the presented forces - Cohesion, Separation, Alignment and Obstacle force, as

$$\vec{F}_T = \vec{F}_C + \vec{F}_S + \vec{F}_A + \vec{F}_O. \tag{2.26}$$

It is necessary to mention that all presented forces $\vec{F}$ are dimensionless quantities, with the mass of one agent being assumed to be $m = 1$. The acceleration $\vec{a}_i$ and velocity $\vec{v'}_i$ used to determine the new position $\vec{p}_{A,i+1}$ from current position $\vec{p}_{A,i}$ also are considered as dimensionless quantities in the equations in this section. The result of applying the Total force $\vec{F}_{T,i}$ on an agent is acceleration $\vec{a}_i$ of the agent.

$$\vec{a}_i = \frac{\vec{F}_{T,i}}{m} \tag{2.27}$$

The acceleration $\vec{a}_i$ is added to the current velocity of the agent $\vec{v}_i$ using the following formula:

$$\vec{v'}_i = k_{vv}\vec{v}_i + k_{va}\int_{t_i}^{t_{i+1}} \vec{a}_i \, \mathrm{d}t', \tag{2.28}$$

where $k_{vv} = 1$ s·m^{-1}, $k_{va} = 1$ s^{-1}, t_i is the time of last swarm control step and t_{i+1} is the time of the new control step. Because acceleration $\vec{a}_i$ is assumed to be constant between t_i and t_{i+1}, we can rewrite (2.28) as

$$\vec{v'}_i = k_{vv}\vec{v}_i + k_{va}\vec{a}_i(t_{i+1} - t_i). \tag{2.29}$$

Finally, the desired position $\vec{p}_{A,i+1}$ of the agent, which should be reached by the position controller, is determined as

$$\vec{p}_{A,i+1} = \vec{p}_{A,i} + k_{pv}\left(\int_{t_i}^{t_{i+1}} \vec{v'}_i(t')\mathrm{d}t'\right), \tag{2.30}$$

$$\vec{p}_{A,i+1} = \vec{p}_{A,i} + k_{pv}\left(\int_{t_i}^{t_{i+1}} k_{vv}\vec{v}_i + k_{va}\vec{a}_i(t'_{i+1} - t_i) \, \mathrm{d}t'_{i+1}\right), \tag{2.31}$$

$$\vec{p}_{A,i+1} = \vec{p}_{A,i} + \vec{v}_i(t_{i+1} - t_i) + \frac{1}{2}k_{pa}\vec{a}_i(t_{i+1} - t_i)^2, \tag{2.32}$$

where $k_{pv} = 1$ m·s^{-1} and $k_{pa} = k_{pv}k_{va} = 1$ m·s^{-2}.

2.4 Pseudocode

The swarming algorithm presented in this chapter based on the Boids model is written in the following pseudocode (Algorithm 1).

Algorithm 1 Swarming algorithm running on one agent

```
time_previous = CURRENT_TIME()
period = SET_PERIOD()                                        ▷ Set the period of the loop
mass = 1
while TRUE do
                                                             ▷ Get the necessary states
    my_state = GET_MY_STATE()
    other_agents = GET_STATE_OF_OTHER_AGENTS()
    obstacles = GET_OBSTACLES()
    time = CURRENT_TIME()
                                                             ▷ Calculate the forces
    Cohesion_force = CALCULATE_COHESION_FORCE(other_agents)
    Separation_force = CALCULATE_SEPARATION_FORCE(other_agents)
    Alignment_force = CALCULATE_ALIGNMENT_FORCE(other_agents)
    Obstacle_force = CALCULATE_OBSTACLE_FORCE(obstacles)
    Total_force = Cohesion_force + Separation_force + Alignment_force +
    + Obstacle_force
                                                             ▷ Determine the new desired position
    acceleration = Total_force/mass
    velocity_new = my_state.velocity + 1/2 acceleration(time − time_previous)
    position_new = my_state.position + velocity_new(time − time_previous)
                                         ▷ Call position controller to reach the new desired position
    POSITION_CONTROLLER_GO(position_new)
    time_previous = time
    WAIT(period)
end while
```

Chapter 3

Localization

Localization of other swarm members is component for compact flocking of agents using Boids algorithm presented in Chapter 2. All rules require knowledge of states (positions or velocities) of other agents. In this thesis, two ways of localization are presented. The first way is based on getting information from GNSS such as a GPS module and sharing it between the agents. The second approach uses a system developed by the Multi-robot Systems (MRS) group at Czech Technical University in Prague (CTU) called UVDAR system [12].

3.1 GPS with states sharing

The Global Positioning System (GPS) is one of the most common global positioning systems in outdoor applications. An ideal environment for using GPS is an open area with a view of the sky and without any obstacles disturbing the received GPS signal. Examples of such areas are meadows and fields. However, when agents move in a forest, urban area or indoors, a GPS sensor can lose accuracy or the signal completely therefore geolocation data become unavailable.

If data from a GPS module are available, agent has to share them with other swarm members to achieve swarming without other relative localization sensors. A system developed by MRS group for this task is based on ROS and it enables such communication between individual agents. In simulations, state sharing is implemented by sending data on position and velocity to a ROS topic that other agents can subscribe to. In real-world deployment this data can be transferred between agents through a wireless network.

Nevertheless, sharing states between the agents makes the system run on one agent dependent on the correct function of systems of the other agents. Dropouts of communication could lead to incorrect functioning of the whole system. In order to achieve fully decentralised control, a direct vision-based relative localization system was designed to estimate the position of swarm members. This system is called UVDAR system and it is presented in the next section.

3.2 UVDAR system

As mentioned above, UVDAR is a system for onboard relative localization which is being developed by the MRS group. A great advantage of using the UVDAR system is that communication is not required, due to the system being purely vision-based. The system consists of onboard UVDAR sensor and blinking ultraviolet (UV) markers (LEDs).

Each agent in the swarm carries the onboard UVDAR sensor. For the setup used in this thesis, the UVDAR sensor consists of two modified cameras which are able to capture the ultraviolet markers (Figure 3.1) and distinguish their blinking frequency. The markers are attached to the end of the MAV (agent) arms and have unique flicker frequency for each MAV. A diagram of the UVDAR system is in Figure 3.2.

Figure 3.1: Comparison between the visible and UV camera footage from UVDAR, collected during an experiment. The UV image is significantly easier to process to retrieve information on the observed MAV. [12, p. 2638]

A description of the UVDAR system can be found in [12] and [13]. In principle, cameras capture the images of their surroundings. The images are then processed to detect the ultraviolet markers. The individual agents are recognized by their unique blinking frequency and the relative positions of other MAVs are determined by heading and distance estimation presented in [12][13].

Because the UVDAR system uses UV LEDs, it can be used at any time of the day. Additionally, external infrastructure is not required, which means that the system can also be used in a forest, urban areas and indoors. When agent is behind an obstacle, it can not be localized as shown in Figure 3.3a. In areas with a low density of obstacles, it is not a problem, since after a few moments the agent likely reappears in view again. However, if the density of obstacles is high, agent can lose the rest of the swarm. If the agent is only partially covered by the obstacle (Figure 3.3b) and only one marker is captured,

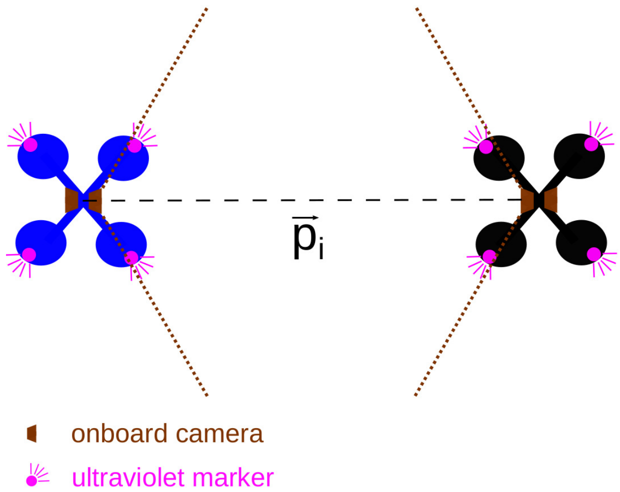

Figure 3.2: Diagram of the UVDAR system on quadrotor MAVs

the distance to the agent can not be determined. On the other hand, the approximate heading to the agent is still estimated. Example using this information can be a situation when an agent loses the swarm and is unable to estimate the position of any other swarm member. The UVDAR sensor captures one ultraviolet marker and estimates the heading to a swarm member carrying this marker. Then the agent can move in the direction of the estimated heading, where the swarm member is expected to be located.

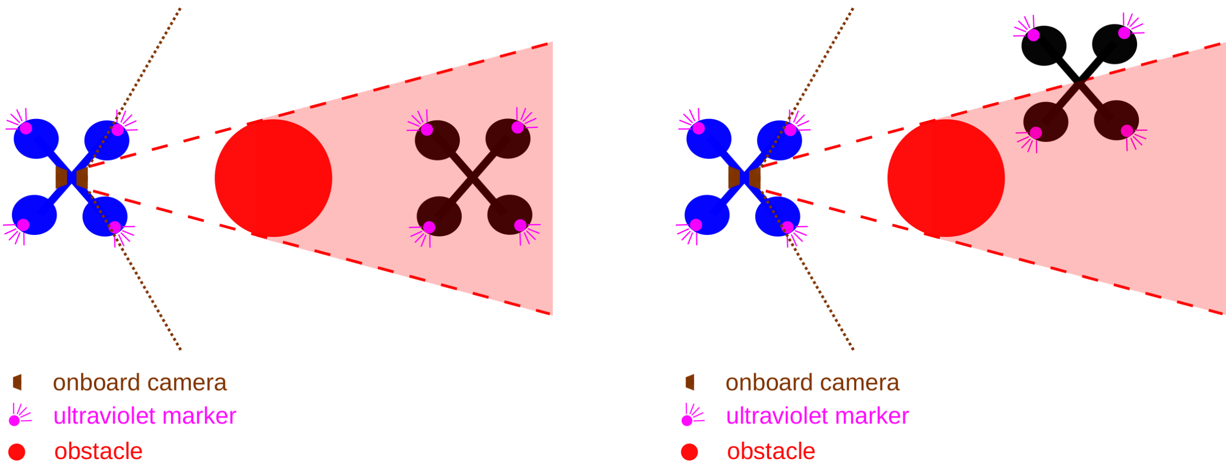

(a) MAV behind an obstacle (b) MAV partially behind an obstacle

Figure 3.3: UVDAR system - localization failure

Position estimation using the UVDAR system was verified in Gazebo simulator. There were two agents - MAV-1 and MAV-2. The MAV-1 was in a fixed position and measured the position of the moving MAV-2. The situation is shown in Figure 3.4. Errors of position estimation from the record of the simulation in Gazebo are shown in Figure 3.5. In the upper left corner there are ground truth (gt) coordinates (x_{gt}, y_{gt}, z_{gt}) with coordinates obtained from the UVDAR system (x_{uv}, y_{uv}, z_{uv}). In the upper right corner there is the absolute error of individual coordinates calculated as

$$x_{er} = x_{uv} - x_{gt}, \tag{3.1}$$
$$y_{er} = y_{uv} - y_{gt}, \tag{3.2}$$
$$z_{er} = z_{uv} - z_{gt}, \tag{3.3}$$

The last graph expresses the norm of error vector $||\vec{e}||$ which is defined as

$$\vec{e} = \begin{pmatrix} x_{er} \\ y_{er} \\ z_{er}, \end{pmatrix} \tag{3.4}$$

and its mean value. Results show that the mean value of position estimation error is 1.35 m. Therefore, the swarm control system must be robust to handle these inaccuracies which is done by appropriately setting the parameters for each force presented in Chapter 2.

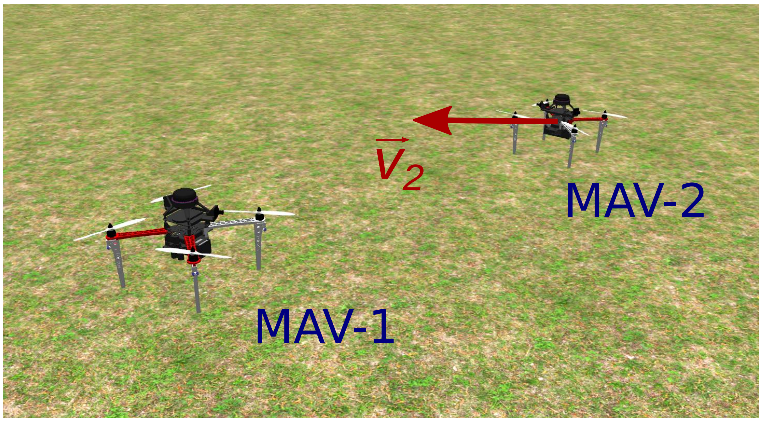

Figure 3.4: Situation in which MAV-1 is measuring position of moving MAV-2 using the UVDAR system in Gazebo simulator

The UVDAR system is not able to measure velocity $\vec{v}_{uv}$ of MAVs directly so the velocity is calculated as

$$\vec{v}_{uv} = \begin{pmatrix} x_{uv,t_i} - x_{uv,t_{i-1}} \\ y_{uv,t_i} - y_{uv,t_{i-1}} \\ z_{uv,t_i} - z_{uv,t_{i-1}} \end{pmatrix} \frac{1}{t_i - t_{i-1}}. \tag{3.5}$$

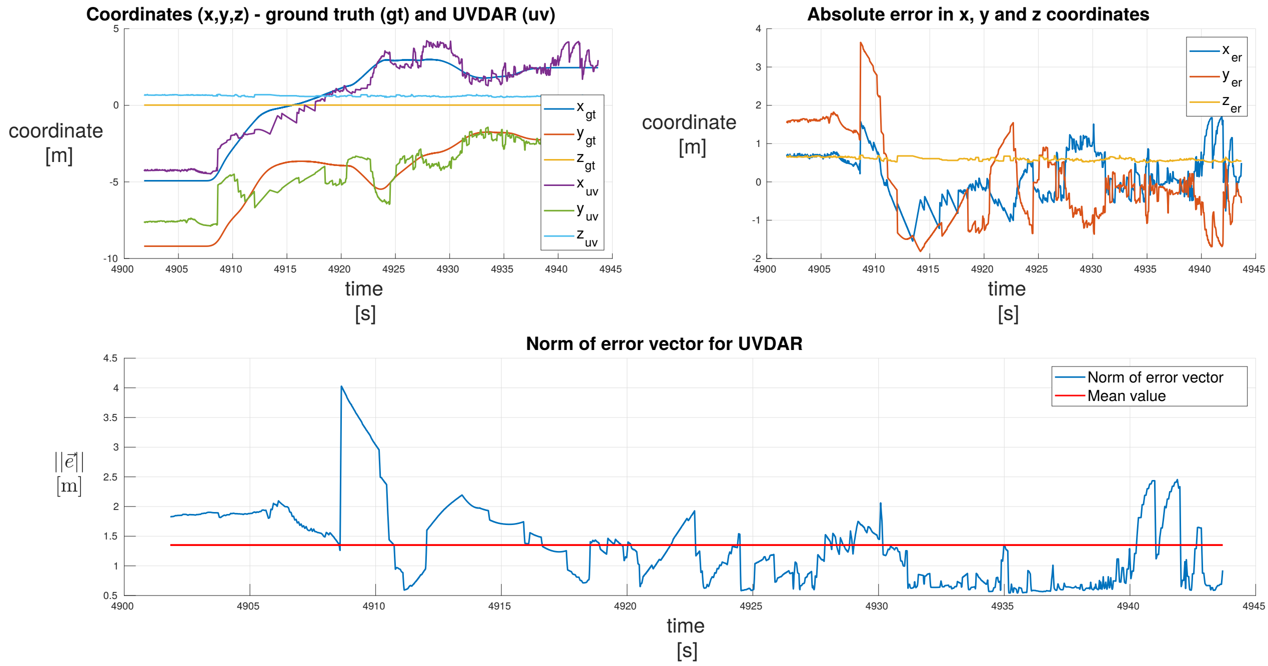

Figure 3.5: Errors of position estimation using UVDAR

3.3 Localization of a predator

In order to verify the Escape behaviour, the localization of the predator needs to be implemented. In the previous section, two methods were introduced - GPS with states sharing and UVDAR system. These two methods will also be used for localization of the predator. The method using GPS can substitute a better sensor for predator detection. The other method is based on the UVDAR system. In the experiments, the predator has a unique flicker frequency of ultraviolet markers that is known to the swarm members. The predator localization is the same as the swarm members localization, but due to the unique flicker frequency, swarm members recognize the predator as distinct from the swarm members.

However, in the real world, the predator will not cooperate by broadcasting its state (position) or carrying ultraviolet markers blinking on a unique frequency that is known to swarm members. Therefore, these localization methods are not applicable in real situations and neither are other methods that require artificial visual markers mounted on predator [17][18][19]. The usage of UVDAR in this thesis serves as a placeholder for a real detection of a non-cooperative moving object, and in terms of precision it exhibits characteristics typical of any vision-based object localization.

Next method is based on a combination of RADAR and LiDAR [20], which is meant to be used for long-range detection using ground sensors. There is no way to obtain onboard relative localization in short ranges. Other methods are markerless methods based on computer vision [21][22][23][24]. These methods do not require external markers on target and are based on processing images from an onboard camera. For this reason, these methods could be used for predator localization, but they need sufficient lighting when capturing the image, and have other requirements such as specialized processing units.

In [21], marker-less MAV detection is presented using onboard camera and a Convolutional Neural Network (CNN). Firstly, the onboard camera captures an image and then the image is processed by the CNN into an image with detected bounding boxes, class predictions and candidate confidences of the objects of interest. The relative position $\vec{p}_i$ to target i is according to [21] determined using vector $\vec{a}_1$ and $\vec{a}_2$ (see Figure 3.7) as

$$l = \frac{\sqrt{2}r}{\sqrt{1 - \frac{\vec{a}_1 \cdot \vec{a}_2}{||\vec{a}_1||\ ||\vec{a}_2||}}}, \tag{3.6}$$

$$\vec{a}_c = \frac{\vec{a}_1 + \vec{a}_2}{2}, \tag{3.7}$$

$$\vec{p}_i = l\frac{\vec{a}_c}{||\vec{a}_c||}, \tag{3.8}$$

where r is radius of bounding sphere (see Figure 3.7).

The system in [21] was successfully verified in real-world experiments and is applicable to Autonomous Aerial Intercepting Systems (AAIS) (Figure 3.6) that are aimed at preventing the potentially harmful behaviour of another vehicle. Due to these reasons, the system could be also used to detect a dynamic obstacle (predator).

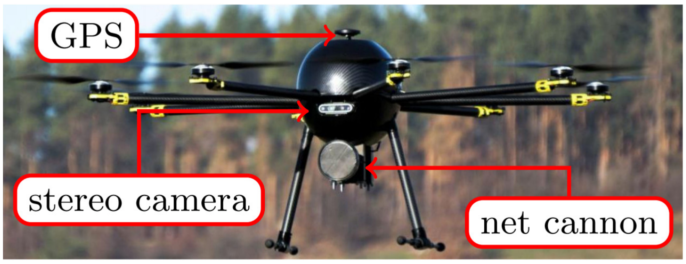

Figure 3.6: AAIS MAV platform, which was used in experiments with CNN-based MAV-detection [22, p. 3407]

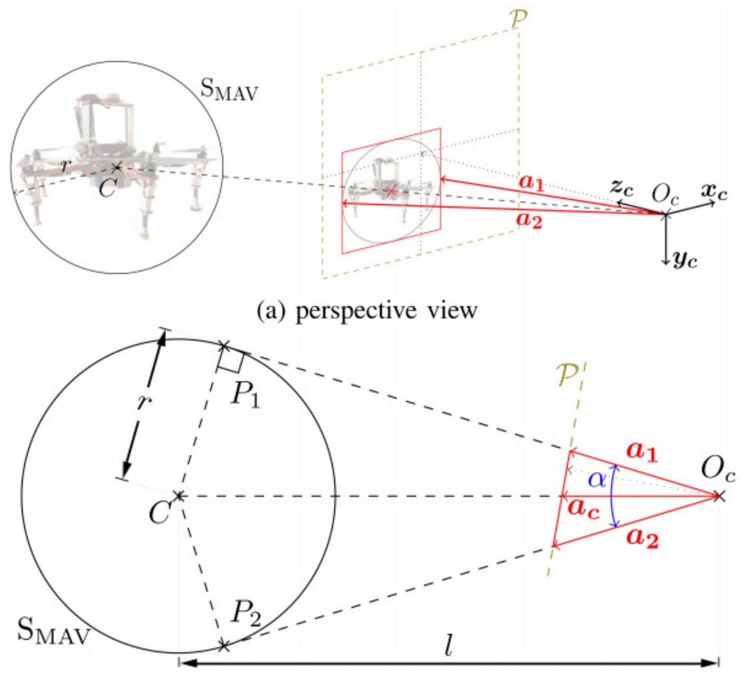

Figure 3.7: Diagram of the projection of a detected MAV and its bounding sphere S_{MAV} to camera projection plane P. A perspective view of the situation is shown in subfigure (a), and a top view (assuming that the camera is oriented horizontally) is shown in (b). The bounding sphere of the MAV (S_{MAV}) is specified by the center point C and radius r. The camera coordinate frame is defined by the camera origin O_c and vectors x_c, y_c and z_c. Vectors $\vec{a}_1$ and $\vec{a}_2$ (in figure denoted as $\mathbf{a}_1$ and $\mathbf{a}_2$) are directional vectors of lines originating in O_c and intersecting the centres of the vertical edges of the bounding rectangle of the MAV projection to P. These are assumed to be tangent to S_{MAV}. Points P_1 and P_2 are the respective intersections of these lines with S_{MAV}. [21, p. 2462]

Chapter 4

Escape behaviour

The Boids algorithm presented in Chapter 2 is used for basic swarm behaviour where agents can move together without collisions and work on a given task. A swarm can also move in an environment with obstacles. However, when the swarm is close to colliding with a dynamic obstacle, called here a predator, it is necessary to implement specific behaviour to protect members of the swarm. This behaviour is called the *Escape behaviour*. The implementation of this behaviour used in this thesis is an extension of the approach described in [1], where a similar system is designed for ground robots moving in two-dimensional space, into the three-dimensional space available to MAVs.

Adaptation of the system in [1] to three-dimensional space is presented in [11]. The escape algorithm designed in [11] was successfully verified in V-REP simulator, and its structure is used for the system developed in this thesis for real MAVs using localization methods presented in Chapter 3.

The Escape behaviour consists of three states (escape modes) - Normal mode, Active mode and Passive mode. In Normal mode, the agent does not detect a predator or unusual behaviour of other agents. In the Active mode the agent detects an approaching moving object (predator) and starts escaping. When the agent does not see a predator, but the behaviour of other agents indicates the presence of a predator, the state is switched to the Passive mode. Description of each mode will follow.

4.1 Normal mode

In Normal mode, sensors that the agent uses to observe the surroundings do not reveal any object considered a predator, or the distance $||\vec{p}_{i,p}||$ to a potential predator is greater than $d_{E1} = 10$ m (Figure 4.1). Additionally, the behaviour of other swarm members does not indicate the presence of a predator. In Normal mode, movement is controlled only by the Boids algorithm presented in Chapter 2 and the new desired position is calculated by equation (2.32).

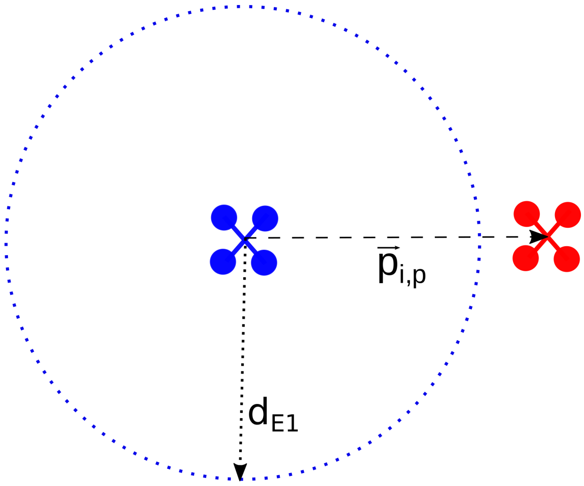

Figure 4.1: Diagram of the Normal mode - the agent in Normal mode is denoted in blue, the predator is red.

4.2 Active mode

When the agent detects a predator and the distance to the predator is less than $d_{E1} = 10$ m, its escape state is switched to Active mode to move the agent away from the predator to safety. Because the agent has information about the predator's position, this information can be used to modify its behaviour.

This is implemented by adding new force called Escape force $\vec{F}_E$. Its magnitude increases with decreasing distance between the agent and the predator. The direction of $\vec{F}_E$ is away from the predator (Figures 4.2).

The relative position between the agent i and the predator p will be denoted as $\vec{p}_{i,p}$. The Escape force $\vec{F}_E$ for n predators is obtained as

$$\vec{F}_E = -\frac{1}{n} \sum_{p=1}^{n} \epsilon_p \frac{\vec{p}_{i,p}}{||\vec{p}_{i,p}||}. \tag{4.1}$$

The parameter ϵ_p is defined as

$$\epsilon_p = \begin{cases} k_E \left(\dfrac{\sqrt{p_{2i}}}{p_{2i}} - \dfrac{\sqrt{d_{E2}}}{d_{E2}} \right), & p_{2i} < d_{E2} \\ 0, & \text{otherwise} \end{cases} \tag{4.2}$$

$$p_{2i} = \begin{cases} ||\vec{p}_{i,p}|| - l, & ||\vec{p}_{i,p}|| > l + l_{min} \\ l_{min}, & \text{otherwise} \end{cases} \tag{4.3}$$

where $l = 1$ m, $l_{min} = 0.0001$ m and parameters k_E, $d_{E2} \in \mathbb{R}^+$. Magnitude of Escape force with $k_E = 7$ m$^{\frac{1}{2}}$ and $d_{E2} = 15$ m is shown on the graph in Figure 4.3.

The Total force $\vec{F}_T$ is then obtained as

$$\vec{F}_T = \vec{F}_C + \vec{F}_S + \vec{F}_A + \vec{F}_O + \vec{F}_E. \tag{4.4}$$

The determination of the new desired position is based on equation (2.32).

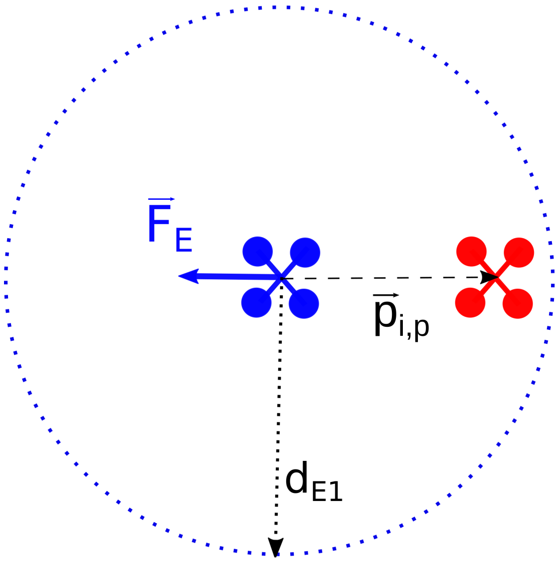

Figure 4.2: Diagram of the Active mode - the agent in Active mode is denoted in blue, the predator is red.

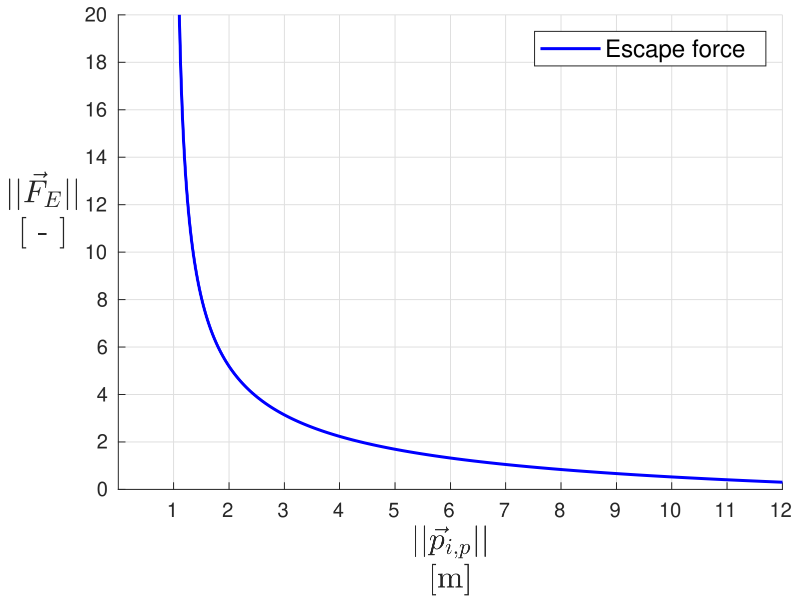

Figure 4.3: Graph of the Escape force $\vec{F}_E$ for $k_E = 7\ \mathrm{m}^{\frac{1}{2}}$ and $d_{E2} = 15$ m

4.3 Passive mode

Even if an agent does not detect a predator, it still does not mean that the predator is not nearby. Another member of the swarm can detect the predator and starts escaping due to Escape force $\vec{F}_E$, which causes rapid changes in its behaviour. If agent recognizes this unexpected behaviour of another member of the swarm, its escape state is changed to the Passive mode (Figure 4.4).

In the Passive mode, it is necessary to increase swarm interaction. Agent will react more dynamically to the movement of others. The result will be evasion of the swarm away from the predator. Forces presented in the Boids algorithm have a similar effect, but the reaction of the agent to the movement of swarm members is slow. A new force called Following force $\vec{F}_F$ will be introduced and the parameters of the Cohesion force $\vec{F}_C$ and of the Separation force $\vec{F}_S$ will be modified to decrease the reaction time.

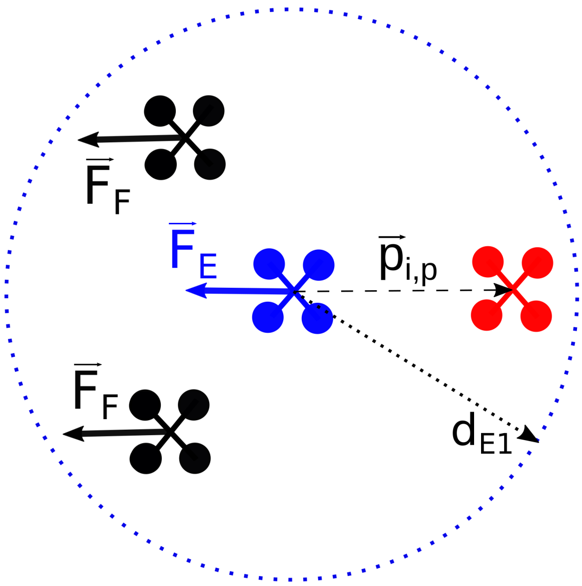

Figure 4.4: Diagram of the Passive mode - the blue agent is in Active mode, the black agents are in Passive mode and the predator is shown in red

The Following force $\vec{F}_F$ based on the velocity $\vec{v}_i$ of other swarm members is defined as

$$\vec{F}_F = \frac{1}{n}\sum_{i=1}^{n} \epsilon_i \frac{\vec{v}_i}{||\vec{v}_i||}. \tag{4.5}$$

The coefficient ϵ_i is defined as

$$\epsilon_i = k_F \log(k_V||\vec{v}_i|| + d_F), \tag{4.6}$$

where $k_V = 1$ s·m^{-1}, and parameters k_F, $d_F \in \mathbb{R}^+$. Graph of the magnitude $||\vec{F}_F||$ for parameters $k_F = 3$ and $d_F = 1$ is shown in Figure 4.5.

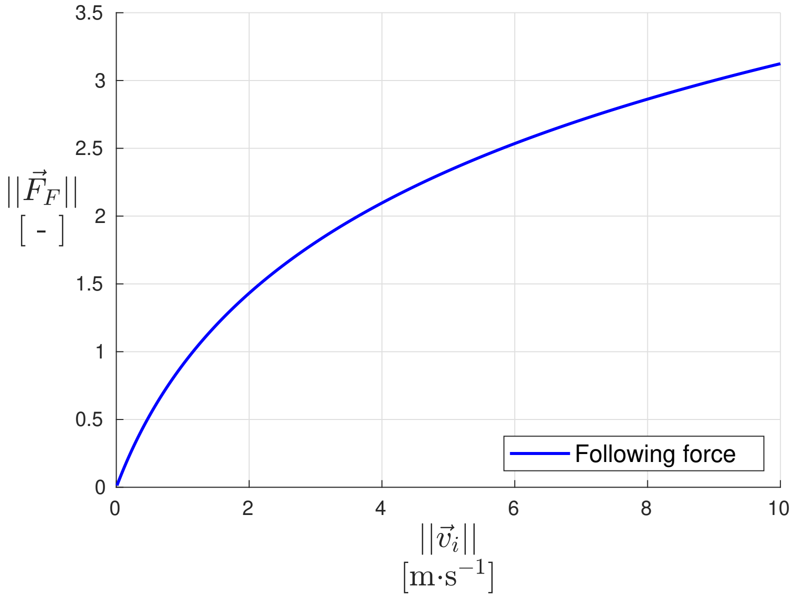

Figure 4.5: Graph of the Following force $\vec{F}_F$ for $k_F = 3$ and $d_F = 1$

The parameters for Cohesion force $\vec{F}_C$ and Separation force $\vec{F}_S$ are changed when agent switches to the Passive mode. Parameters in Passive mode are denoted by upper index P. Values of the parameters are provided in Table 4.1 and Table 4.2.

Parameters of the Cohesion force			
Normal mode		**Passive mode**	
d_{min}	4 m	d^P_{min}	3.5 m
d_C	6 m	d^P_C	5.5 m
k_{1C}	0.1 m^{-2}	k^P_{1C}	0.2 m^{-2}
k_{2C}	1	k^P_{2C}	1.5

Table 4.1: Values of parameters for Cohesion force in the Normal mode and in the Passive mode

The Total force acting on an agent is obtained as

$$\vec{F}_T = \vec{F}_C + \vec{F}_S + \vec{F}_A + \vec{F}_O + \vec{F}_F. \tag{4.7}$$

The new desired position of an agent from this Total force $\vec{F}_T$ is determined as in Normal mode based on equation (2.32).

Parameters of the Separation force

Normal mode		Passive mode	
d_{max}	4 m	d^P_{max}	3.5 m
d_S	2 m	d^P_S	1.5 m
k_{1S}	0.075 m^{-2}	k^P_{1S}	0.175 m^{-2}
k_{2S}	1.45 m$^{\frac{1}{2}}$	k^P_{2S}	1.95 m$^{\frac{1}{2}}$

Table 4.2: Values of parameters for Separation force in the Normal mode and in the Passive mode

4.4 Transition between modes without Communication

In this thesis, two methods of escape mode transitions are presented. Swarm members can broadcast their escape state (escape mode and position of the detected predator) similar to states sharing in localization (Chapter 3). Due to these similarities, escape state sharing is called *Communication* and states sharing for localization of other swarm members is called *States sharing*. The transition between modes without Communication is described in this section, the transition between modes with Communication is described in section 4.5.

4.4.1 Transition to Active mode

Transition to Active mode does not depend on the current escape mode of the agent. If an agent detects a predator within the distance of $d_{E1} = 10$ m, the escape state is changed to the Active mode and the agent starts escaping.

4.4.2 Transition to Passive mode

In [1], changing the state to the Passive mode depends on the heading of the other robots. This method is not suited for real MAVs (agents), because they can move in any direction without a change of their heading. Additionally, reliable control and state estimation of MAVs during rotation is difficult to achieve. Therefore, magnitude of the velocity of an agent is chosen as a variable to evaluate the behaviour of other swarm members. Evaluation of the behaviour of other agents depends on velocity in two subsequent time steps. In [11], the variance of velocity δ is equal to

$$\delta = \frac{||\vec{v}_{j,t_i} - \vec{v}_{j,t_{i-1}}||}{||\vec{v}_{j,t_i}|| + ||\vec{v}_{j,t_{i-1}}||}, \tag{4.8}$$

where $\vec{v}_{j,t_i}$ is velocity of agent j in current time and $\vec{v}_{j,t_{i-1}}$ is velocity of agent j in previous time. This variance δ is computed for each neighbouring agent and if its value is higher than a threshold value δ_{TH}, the escape state is changed to Passive mode and the agent starts a timer Tmr.

When the UVDAR system is used for localization, which is the main challenge in this thesis, the velocity determination of surrounding agents suffers from oscillations. For this reason, the escape state is often changed to Passive mode because of δ variance high value, even though it is not the correct decision. A new method based on flicker frequency change of the ultraviolet markers is introduced. A frequency f_{AM} known to all swarm members is selected. When an agent switches to the Active mode, the flicker frequency of its ultraviolet markers is changed to f_{AM}. If another agent notices the frequency f_{AM}, its state is switched to the Passive mode and the timer Tmr starts.

4.4.3 Transition to Normal mode

When a MAV (agent) starts flying, its escape state is in the Normal mode. During flight, the agent can change its escape state to the Active mode or to the Passive mode. If the agent is in the Active mode, the escape state returns to the Normal mode when it does not detect a predator in a specified time period t_{nd} or the distance to the predator is greater than the safe distance after escaping for $d_{E2} = 15$ m.

If the agent is in the Passive mode, the transition to Normal mode depends on the timer Tmr. As mentioned in subsection 4.4.2, the agent starts the timer Tmr during transition to the Passive mode. When Tmr is active for longer than a specified time t_{esc}, the escape state is set back to the Normal mode.

4.5 Transition between modes with Communication

If the agent detects a predator, it transitions to the Active mode in the same way as in section 4.4.1. When the predator is not detected, the agent evaluates received messages. If all received messages report Normal mode, the agent reverts to the Normal mode. On the other hand, if any of the received messages reports that another swarm particle is in the Active mode with detected position of a predator, the escape state of the agent is changed. If the distance to the received position of the predator is less than $d_{E2} = 15$ m, the escape state is switched to the Active mode. When the distance to position of the predator is greater than d_{E2}, the escape state is switched to the Passive mode.

4.6 Diagram

Diagram 4.6 shows the structure of the system designed in this thesis. The term Boids denotes the Total force $\vec{F}_T$ from the equation (2.26) retrieved by the algorithm from Chapter 2.

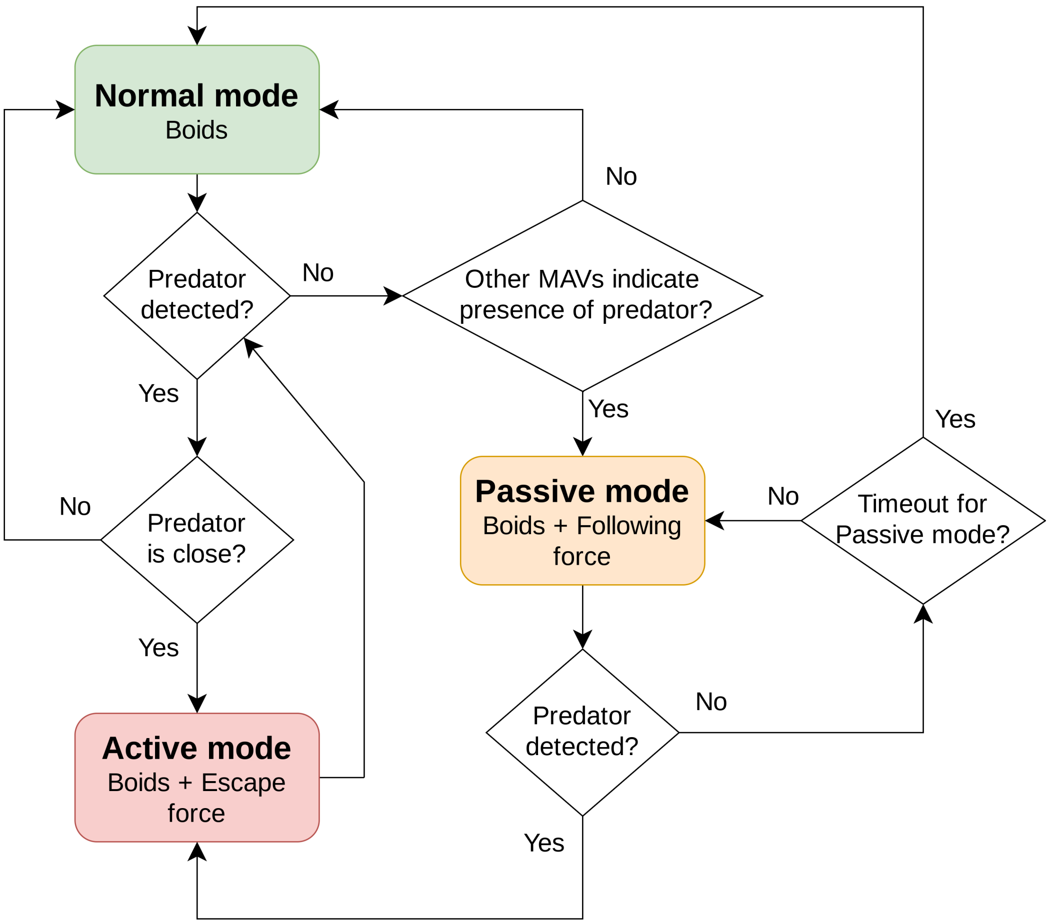

Figure 4.6: Diagram of Escape behaviour

Chapter 5

Simulations

The system described in this thesis was initially implemented in Matlab, where the system was evaluated on massless particles without dynamic properties. For this reason, the simulations do not correspond to experiments in the real world, but the demands on processing power are low. This meant that the behaviour of a swarm with a large number of members could be tested. Because the UVDAR system is not implemented in Matlab, the agents use only States sharing.

To imitate the real conditions, the system has been subsequently tested in the Gazebo simulator. This simulator allows for dynamic simulations with physics engines *ODE*, *Bullet*, *Simbody* and *DART*. Because the demands on computing power are significantly greater in this case, only a swarm with a limited number of members could be tested - the maximum of six MAVs without the UVDAR system and maximum of four MAVs with the UVDAR system. The values of parameters for all simulations are provided in tables in Appendix B. Videos from simulations in Gazebo simulator are stored on the enclosed CD.

The simulations are divided according to the following terms. *All see* means that all of the swarm members can detect a predator, *one see* means that only one swarm member can detect the predator. *Communication* is the designation for sharing information about escape mode and position of a detected the predator among the swarm members. If the MAVs do not use Communication, transitions between escape modes are made according to the section 4.4. In the graphs, the distance is denoted as d and the time as t. For evaluation of simulated systems in Gazebo simulator, these symbols are used:

- t_s - time when the predator is in the safe area (i.e. distance to predator is less than d_{E1}) of any MAV for the first time,
- t_d - time of the first detection of the predator by any MAV,
- t_e - time when all swarm members start escaping (switch their mode to Active or Passive),
- $t_r = t_e - t_d$ - reaction time of the whole swarm in the presence of a predator.

5.1 Matlab

In this section, a simulation with fifty swarm members is presented. In the simulation, agents stay in a swarm when a predator starts to approach. After predator detection, agents start escaping while avoiding static obstacles in their way. Agents use States sharing and Communication.

Agents are spawned 1 m apart (shown in green colour in Figure 5.1a). After starting the simulation, the agents form an approximate sphere that is shown in Figure 5.1b. Then the predator (shown in red) approaches and the agents begin to escape. During the escape, agents fly between obstacles, as shown in Figure 5.2a.

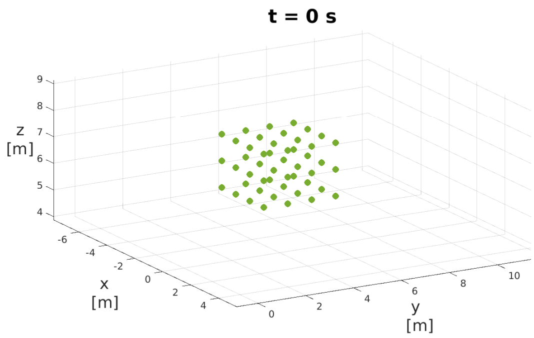

(a) Initial layout of fifty agents

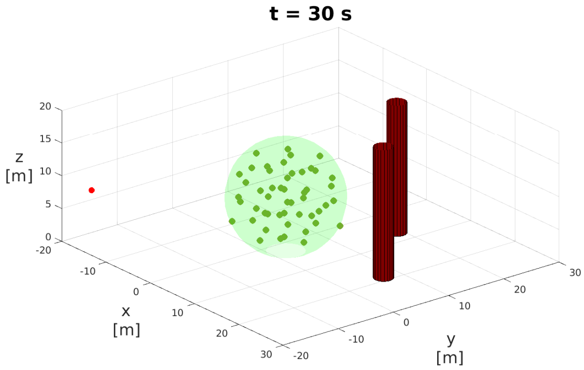

(b) The sphere that is formed by fifty agents.

Figure 5.1: Fifty agents in the simulation in Matlab

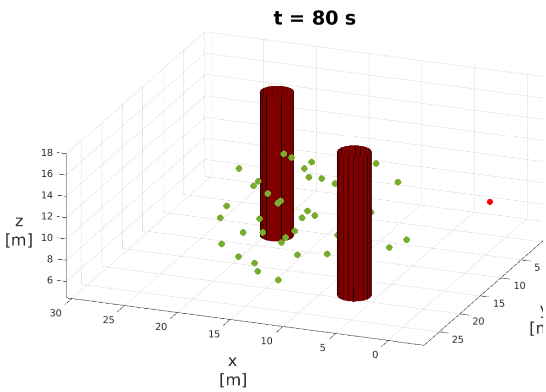

(a) Agents fly between obstacles.

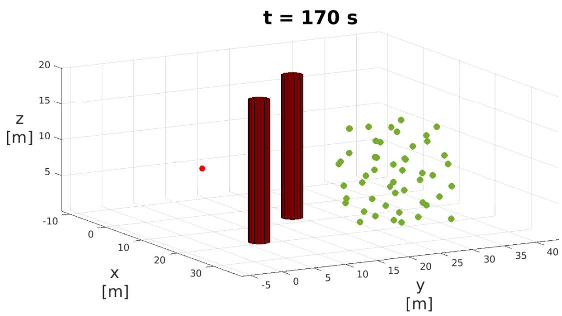

(b) Agents after escaping

Figure 5.2: Fifty agents in the simulation in Matlab

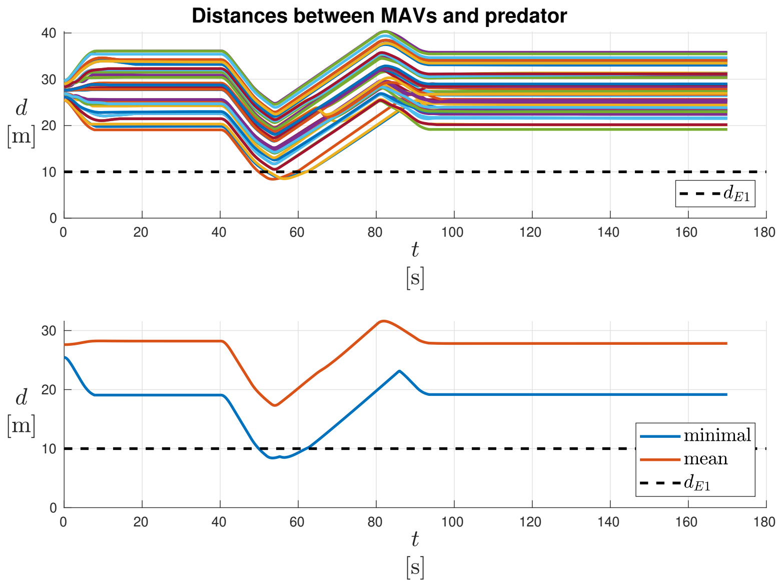

Figure 5.3: The upper figure is a graph of distances between fifty agents (MAVs) and the predator if all agents can detect the predator and use Communication and States sharing. The lower figure shows minimal and mean distance between agents and the predator.

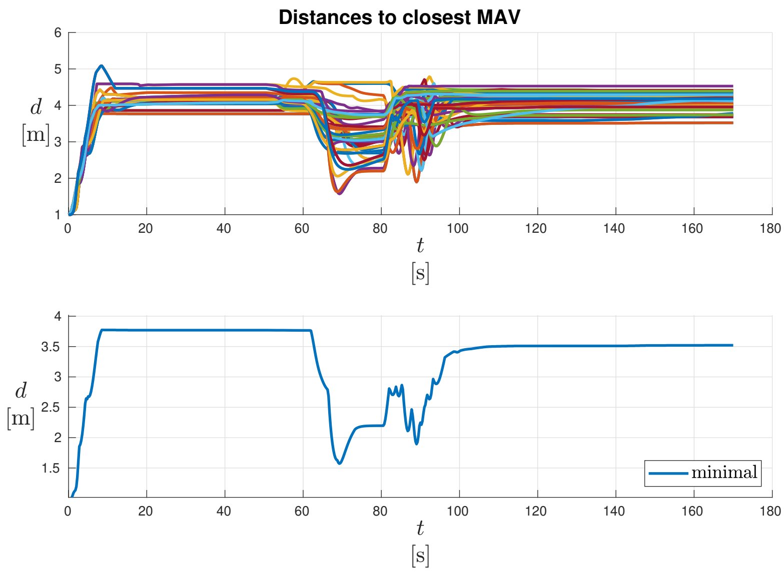

Figure 5.4: The absolute and minimal distance from each of agents (MAVs) to the closest agent if all agents can detect a predator and use Communication and States sharing.

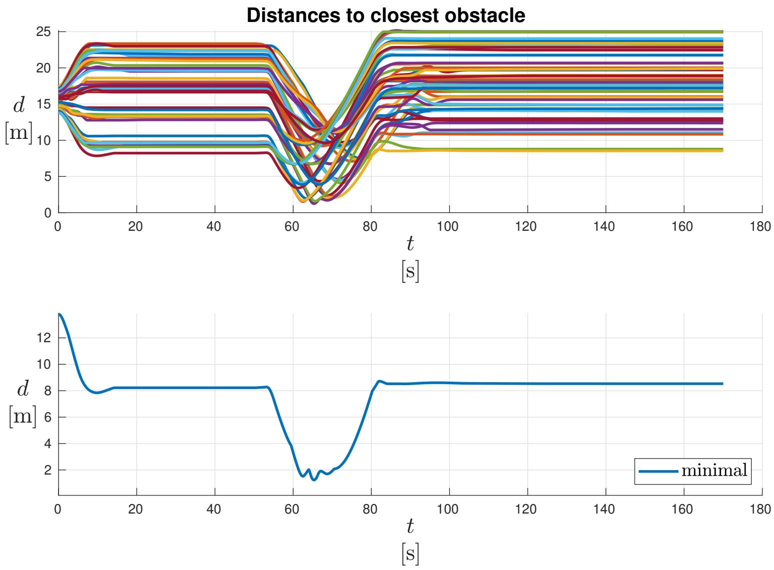

Figure 5.5: The upper figure is a graph of distances between agents (MAVs) and their closest obstacle if all agents can detect a predator, use Communication and States sharing. The lower figure shows the smallest of these distances.

5.1.1 Evaluation

In the presented Matlab simulation, the swarm consisting of fifty agents successfully escaped the predator. Graphs in Figures 5.3, 5.4 and 5.5 show that no collisions occurred. The minimal distance between agents was approximately 1.5 m when the agents fly between the obstacles. The minimal distance to an obstacle was approximately 2 m. The results of this simulation show that the system designed in this thesis is applicable on massless particles and thus further simulations made in realistic Gazebo simulator were warranted.

5.2 Gazebo - 6 MAVs - States sharing

Six MAVs are used for simulations for the first situation in the Gazebo simulator. Five of them are swarm MAVs and the last one is the predator. At the beginning of simulation, the five MAVs stay in the swarm. The predator then starts flying towards the swarm. When the predator is detected, the swarm starts escaping. After escaping, the swarm MAVs reform into the swarm again. The situation at the beginning of simulation is shown in Figure 5.6. All MAVs use States sharing for localization of other swarm members as well as for predator detection. The limitation of computing power prevents the use of UVDAR system on six MAVs.

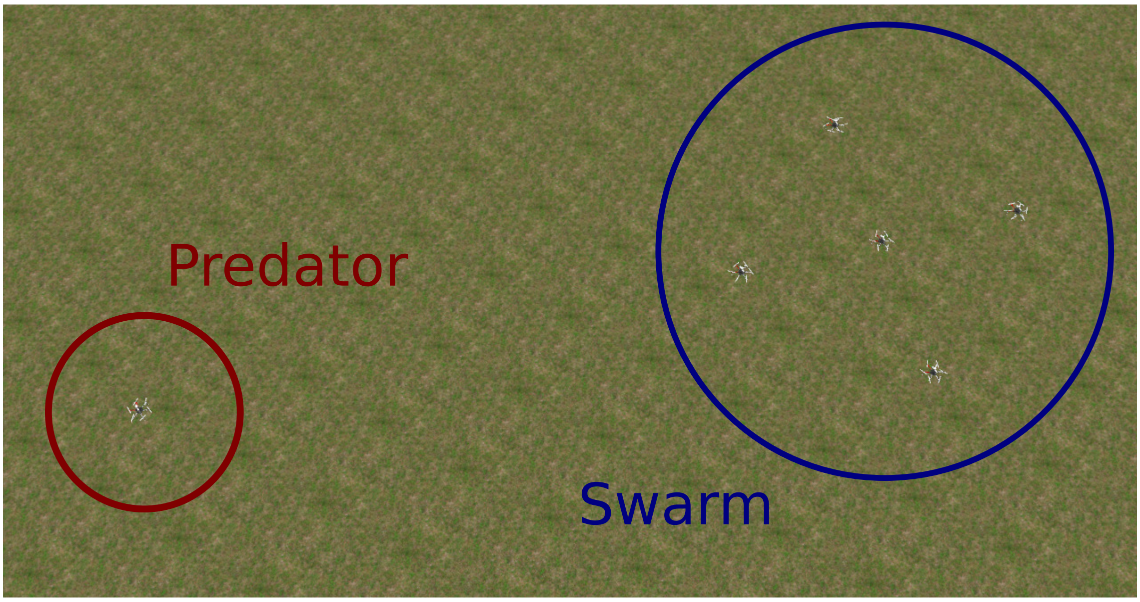

Figure 5.6: Situation of six MAVs in the Gazebo simulator

All see with Communication

t_s [s]	t_d [s]	t_e [s]	t_r [s]
13.308	13.352	13.652	0.300

Table 5.1: Quantities t_s, t_d, t_e and t_r measured in simulation in which all five MAVs can detect a predator and use Communication and States sharing.

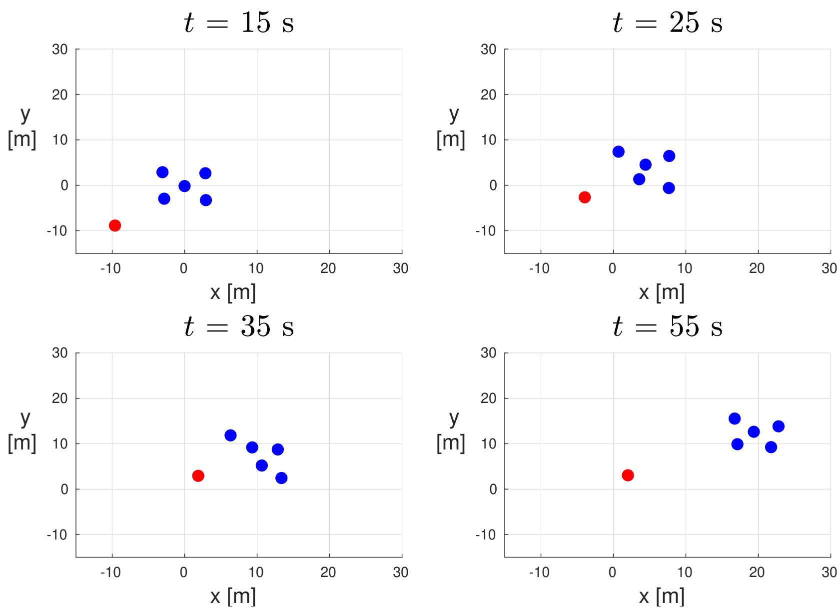

Figure 5.7: Sub-figures contain positions of blue swarm members and red predator in x, y coordinates in time t if all five MAVs can detect the predator and use Communication and States sharing.

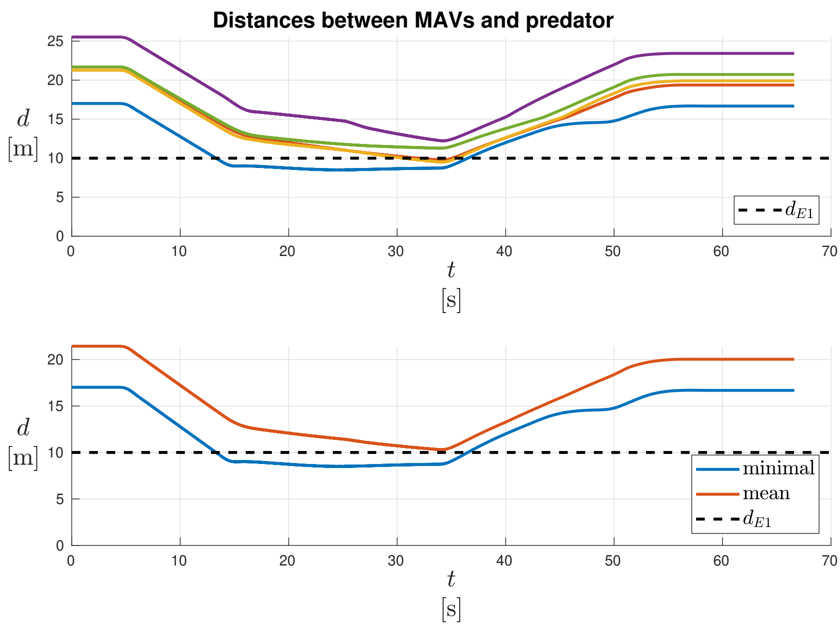

Figure 5.8: The upper figure is a graph of distances between the five MAVs and the predator if all MAVs can detect the predator and use Communication and States sharing. The lower figure shows minimal and mean distance between MAVs and the predator.

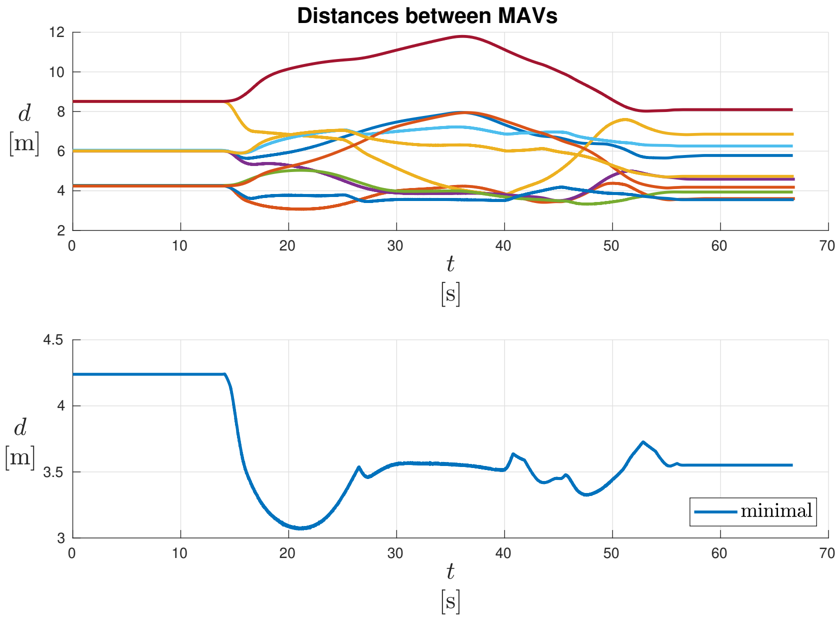

Figure 5.9: The absolute and minimal distances between the five MAVs if all MAVs can detect a predator and use Communication and States sharing.

All see without Communication

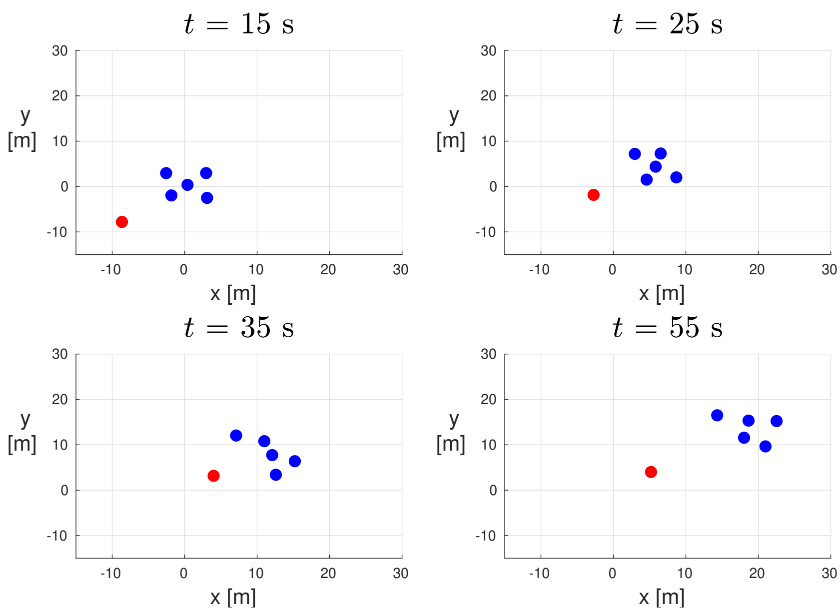

Figure 5.10: Sub-figures contain positions of blue swarm members and red predator in x, y coordinates in time t if all five MAVs can detect the predator, use States sharing and do not use Communication.

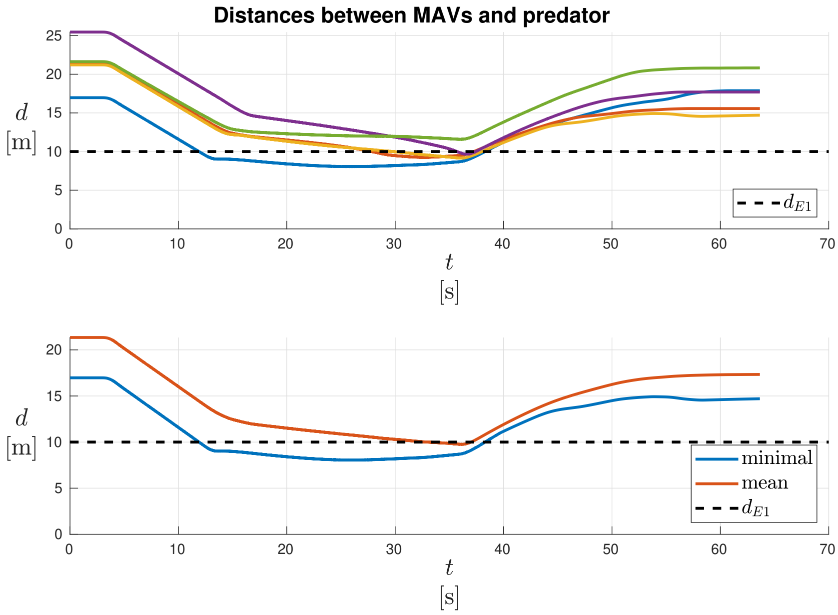

Figure 5.11: The upper figure is a graph of distances between the five MAVs and the predator if all MAVs can detect the predator, use States sharing and do not use Communication. The lower figure shows minimal and mean distance between MAVs and the predator.

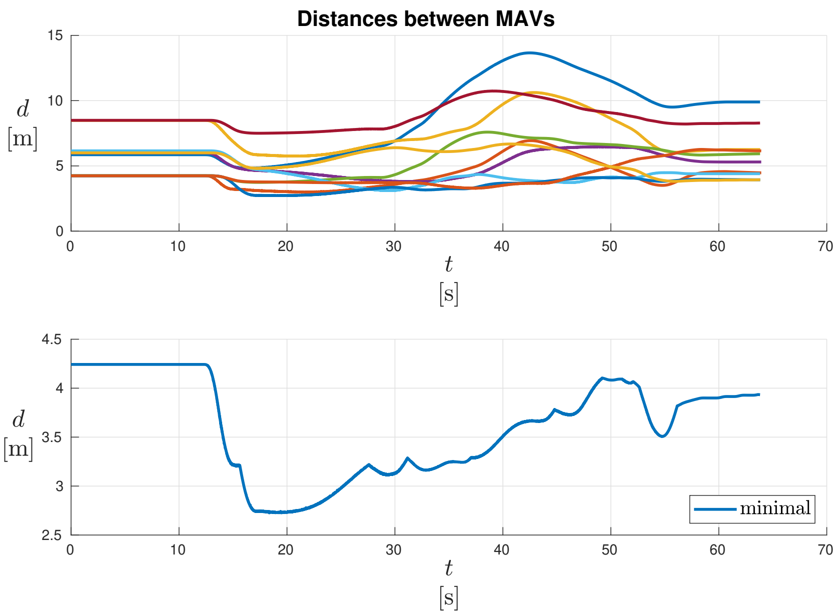

Figure 5.12: The absolute and minimal distances between the five MAVs if all MAVs can detect a predator, use States sharing and do not use Communication.

t_s [s]	t_d [s]	t_e [s]	t_r [s]
11.900	11.930	12.852	0.922

Table 5.2: Quantities t_s, t_d, t_e and t_r measured in simulation in which all five MAVs can detect a predator, use States sharing and do not use Communication.

One see with Communication

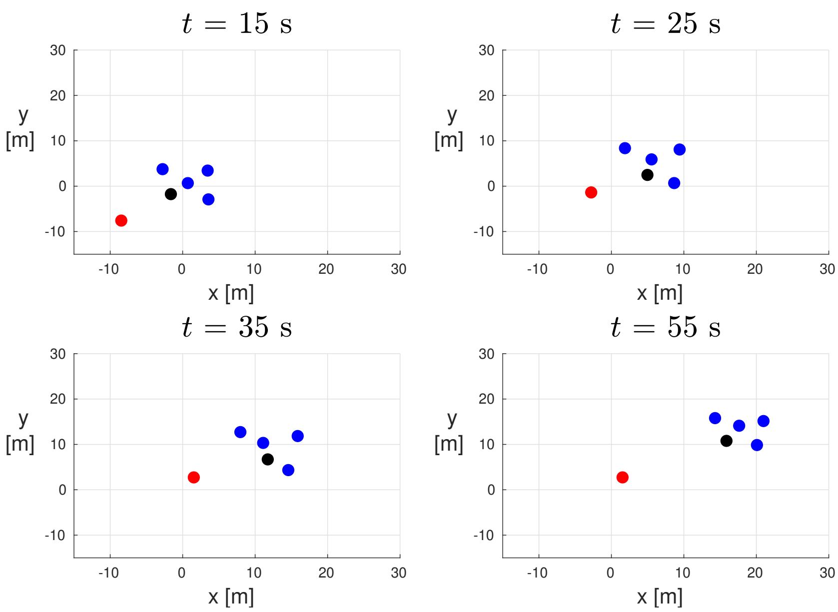

Figure 5.13: Sub-figures contain positions of blue and black swarm members and red predator in x, y coordinates in time t if one of five MAVs (black) can detect the predator and all MAVs use Communication and States sharing.

t_s [s]	t_d [s]	t_e [s]	t_r [s]
11.585	11.700	11.900	0.200

Table 5.3: Quantities t_s, t_d, t_e and t_r measured in simulation in which one of five MAVs can detect a predator and all MAVs use Communication and States sharing.

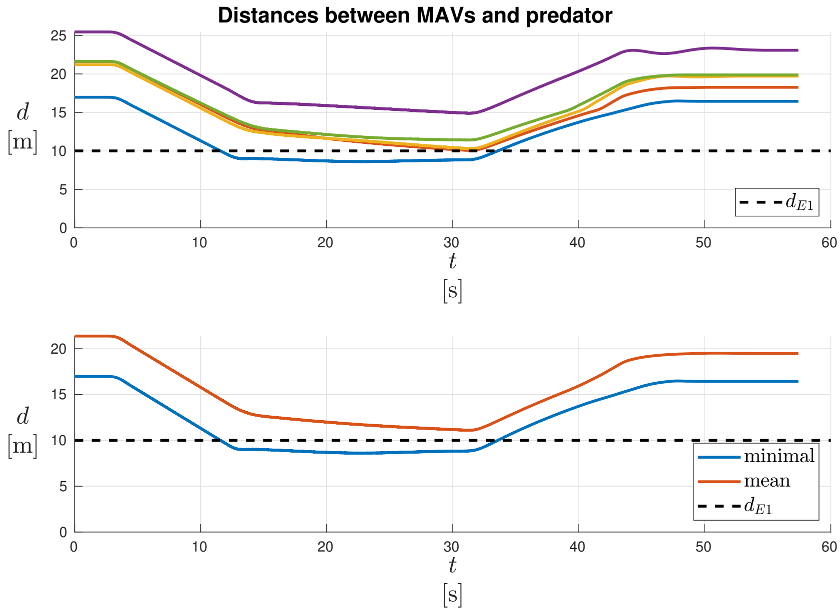

Figure 5.14: The upper figure is a graph of distances between the five MAVs and the predator if one MAV can detect the predator and all MAVs use Communication and States sharing. The lower figure shows minimal and mean distance between the MAVs and the predator.

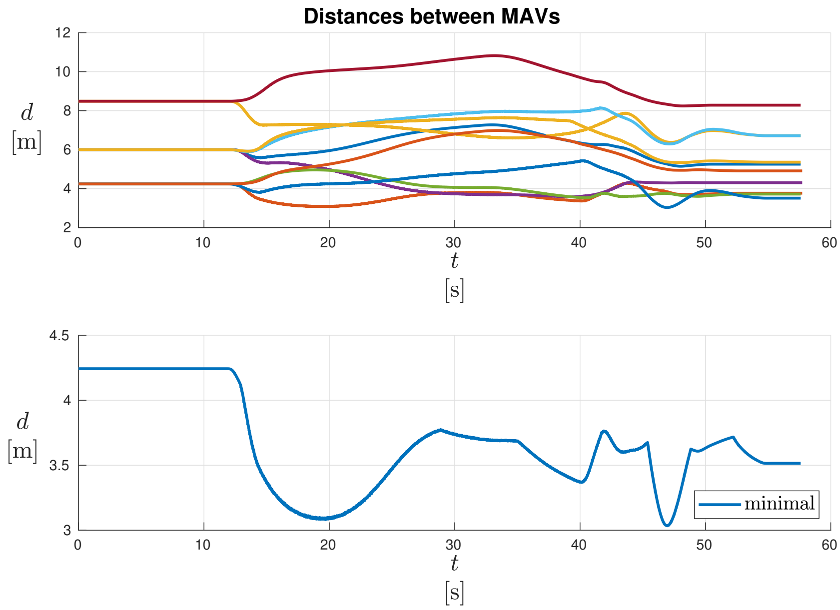

Figure 5.15: The absolute and minimal distances between the five MAVs if one MAV can detect a predator and all MAVs use Communication and States sharing.

One see without Communication

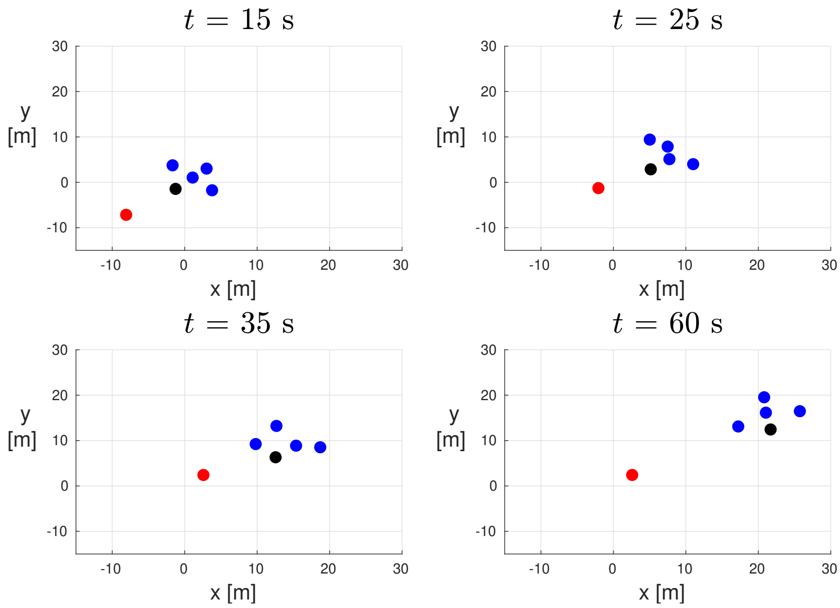

Figure 5.16: Sub-figures contain positions of blue and black swarm members and red predator in x, y coordinates in time t if one of five MAVs (black) can detect the predator and all MAVs use States sharing and do not use Communication.

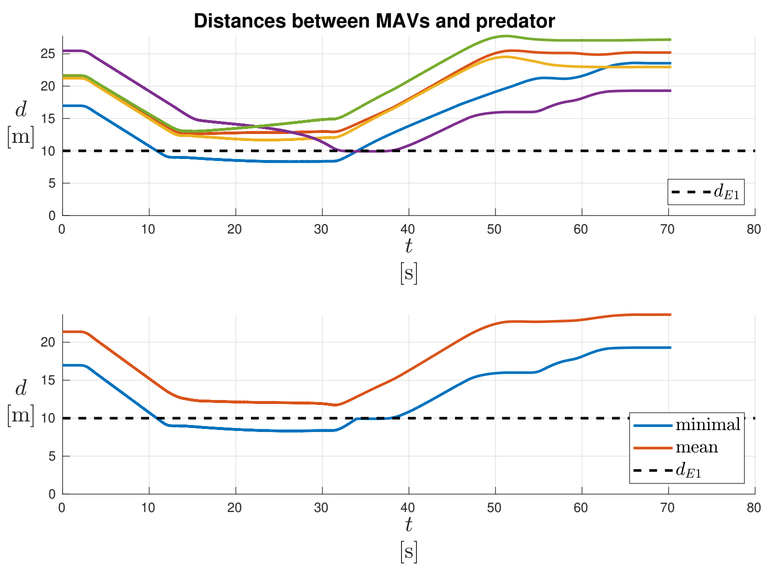

Figure 5.17: The upper figure is a graph of distances between the five MAVs and the predator if one MAV can detect the predator and all MAVs use States sharing and do not use Communication. The lower figure shows minimal and mean distance between the MAVs and the predator.

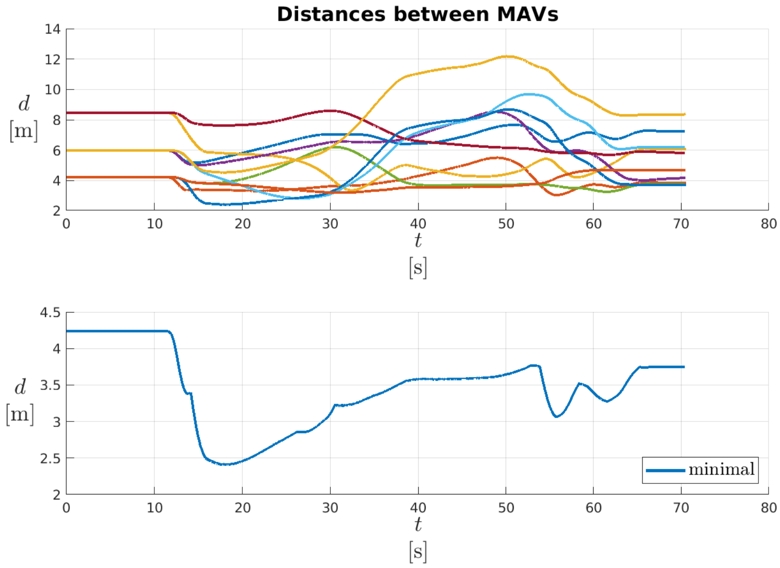

Figure 5.18: The absolute and minimal distances between the five MAVs if one MAV can detect a predator and all MAVs use States sharing and do not use Communication.

t_s [s]	t_d [s]	t_e [s]	t_r [s]
10.888	10.918	11.852	0.934

Table 5.4: Quantities t_s, t_d, t_e and t_r measured in simulation in which one of five MAVs can detect a predator and all MAVs use States sharing and do not use Communication.

5.2.1 Evaluation

The swarm of five MAVs successfully escaped the predator in all simulations presented in this section. Measured distances between the MAVs show that collisions did not occur and after the escape, the swarm was restored. There is a difference between simulations in which swarm members use Communication and in which they do not. If swarm MAVs use Communication, the minimal distance between them is about 3 m as shown in Figure 5.9 and 5.15. However, if swarm MAVs do not use Communication, minimal distance between them drops to 2.5 m as shown in Figure 5.12 and 5.18.

Another difference is in the measured times. If MAVs use Communication, their reaction to the approaching predator was fast - $t_r = 0.3$ s if all MAVs can detect a predator (Table 5.1) and $t_r = 0.2$ s if only one MAV can detect the predator (Table 5.3). When MAVs did not use Communication - time $t_r = 0.922$ s (Table 5.2) and $t_r = 0.934$ s (Table 5.4). The difference between time t_d and time t_s shows that the predator was detected as soon as its distance to any MAV was less than d_{E1}. This is thanks to the use of States sharing for predator detection.

5.3 Gazebo - 4 MAVs - UVDAR system

In the situation in Gazebo simulator presented in this section, the swarm is made up of three MAVs. The fourth MAV serves as the predator. The situation is shown in Figure 5.19. When the simulation starts, the predator moves towards the swarm. After detecting the predator, the swarm starts escaping.

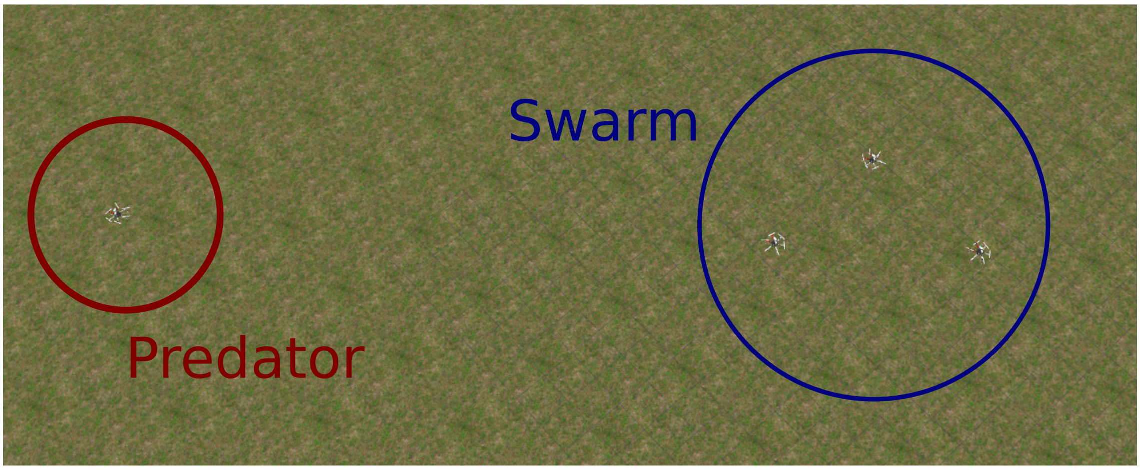

Figure 5.19: Situation of four MAVs in the Gazebo simulator

In these simulations, the MAVs use the UVDAR system for localizing other swarm members. For predator localization, the MAVs also use the UVDAR system in all simulations. The next two simulations are presented in Appendix A.1 in which one of the swarm members uses States sharing for predator localization and the other swarm members can not detect a predator. These two simulations are called *One see (States sharing) with Communication* and *One see (States sharing) without Communication*. Predator detection using States sharing simulates the use of a high-precision sensor attached on one of the swarm members for predator detection.

All see with Communication

t_s [s]	t_d [s]	t_e [s]	t_r [s]
20.700	21.600	21.752	0.152

Table 5.5: Quantities t_s, t_d, t_e and t_r measured in simulation in which all three MAVs can detect a predator and use Communication and the UVDAR system.

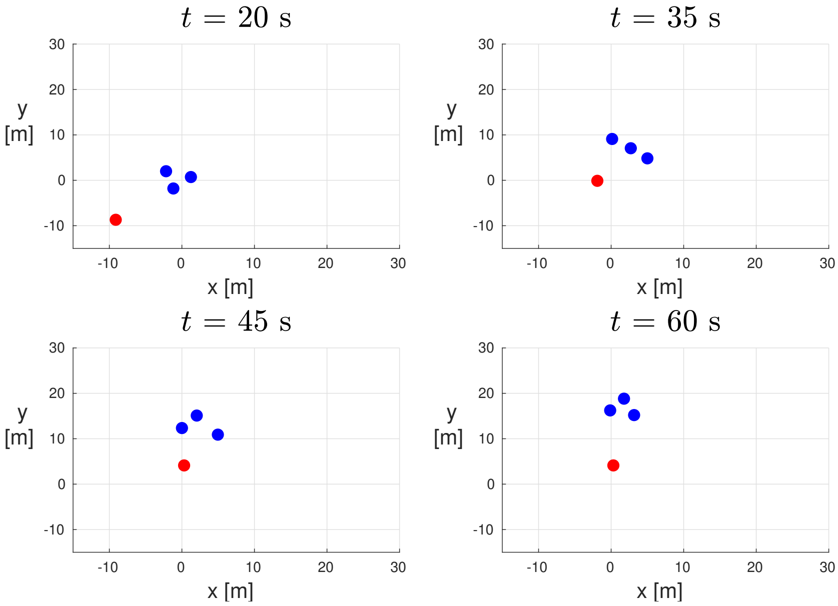

Figure 5.20: Sub-figures contain positions of blue swarm members and red predator in x, y coordinates in time t if all three MAVs can detect the predator and use Communication and the UVDAR system.

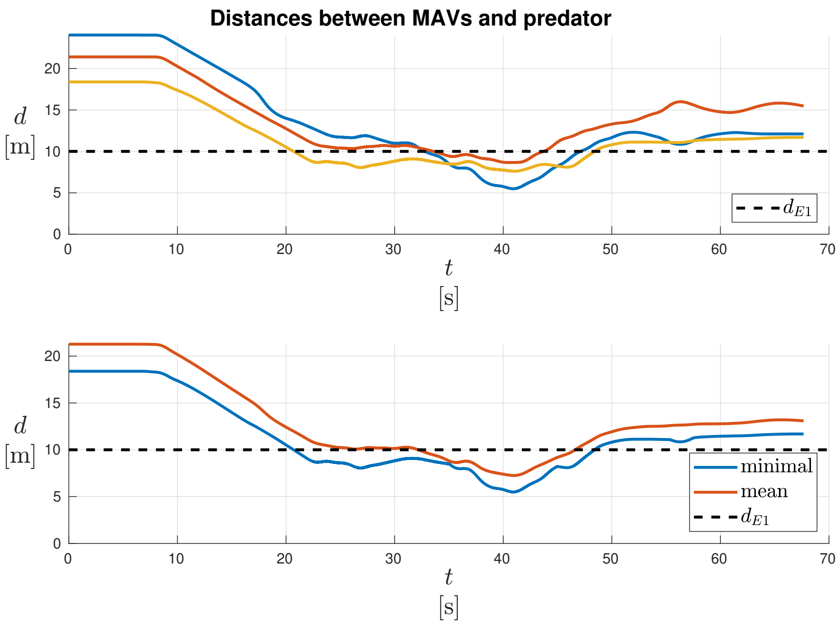

Figure 5.21: The upper figure is a graph of distances between three MAVs and the predator if all MAVs can detect the predator and use Communication and the UVDAR system. The lower figure shows the minimal and mean distance between MAVs and the predator.

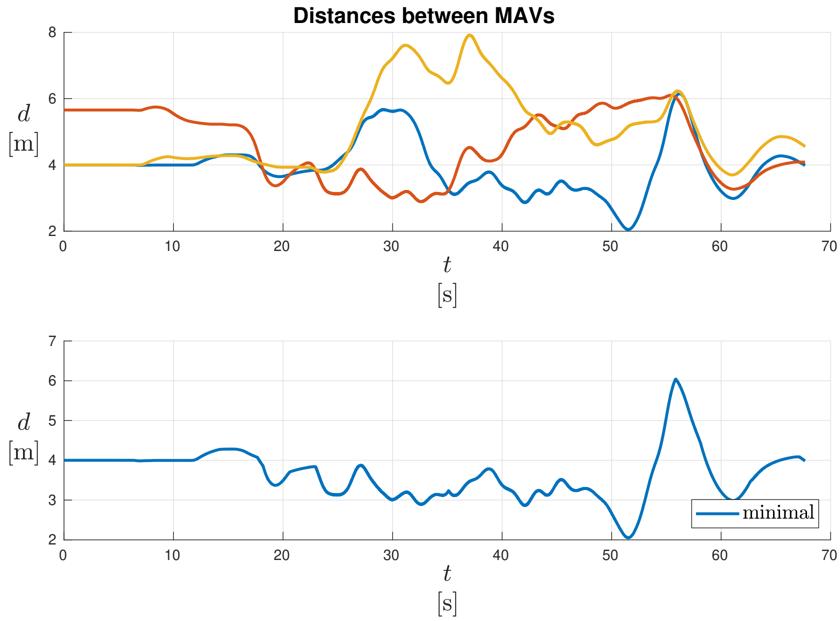

Figure 5.22: The absolute and minimal distances between three MAVs if all MAVs can detect a predator and use Communication and the UVDAR system.

All see without Communication

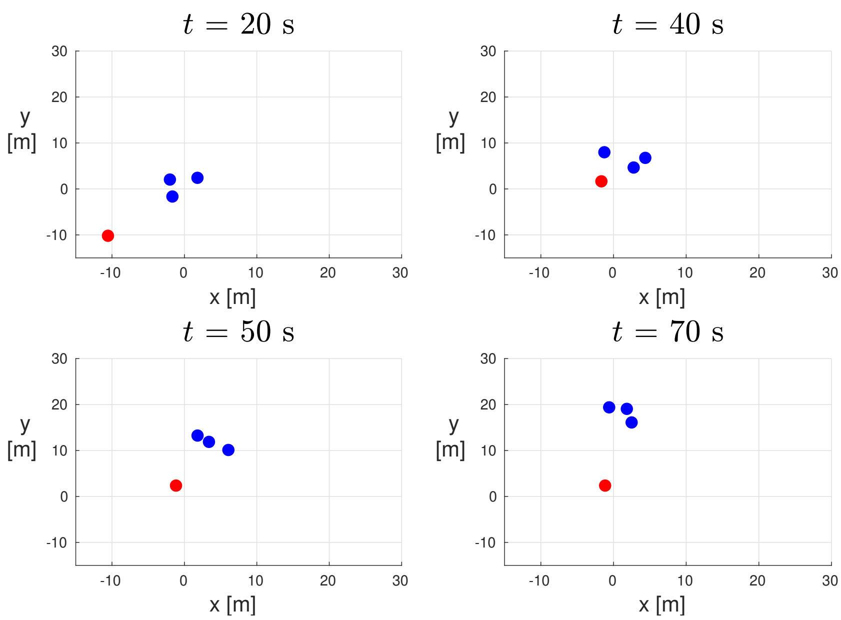

Figure 5.23: Sub-figures contain positions of blue swarm members and red predator in x, y coordinates in time t if all three MAVs can detect the predator, use the UVDAR system and do not use Communication.

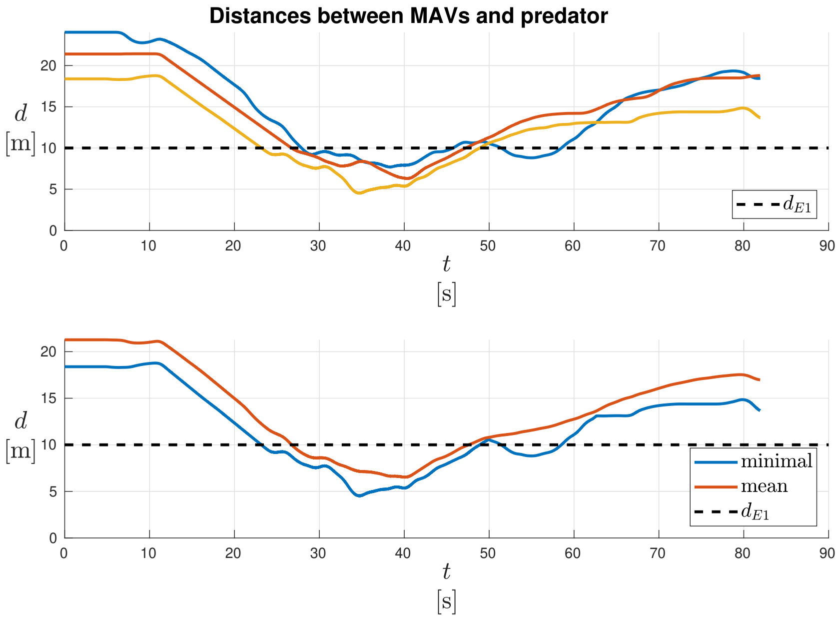

Figure 5.24: The upper figure is a graph of distances between three MAVs and the predator if all MAVs can detect the predator, use the UVDAR system and do not use Communication. The lower figure shows the minimal and mean distance between MAVs and the predator.

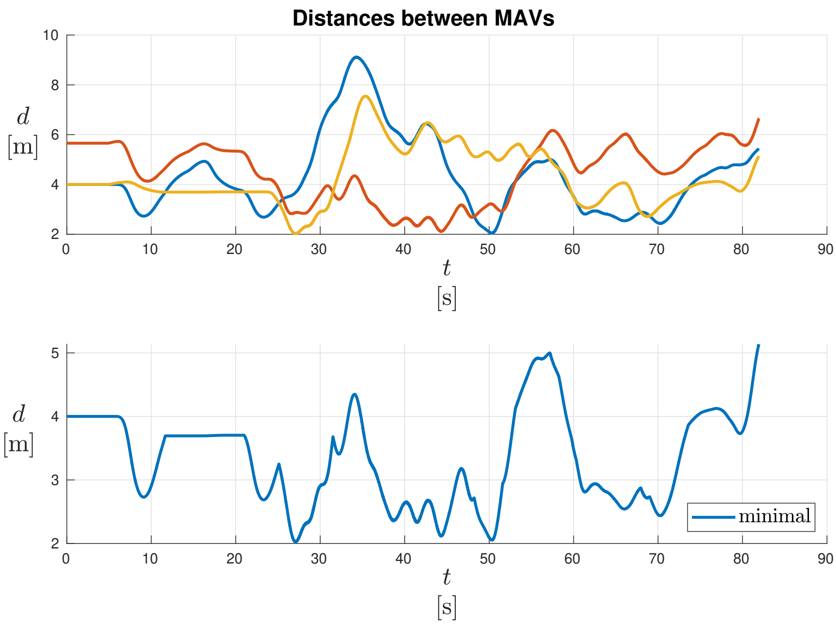

Figure 5.25: The absolute and minimal distances between three MAVs if all MAVs can detect a predator, use the UVDAR system and do not use Communication

t_s [s]	t_d [s]	t_e [s]	t_r [s]
23.168	23.416	24.400	0.984

Table 5.6: Quantities t_s, t_d, t_e and t_r measured in simulation in which all three MAVs can detect a predator, use the UVDAR system and do not use Communication.

One see with Communication

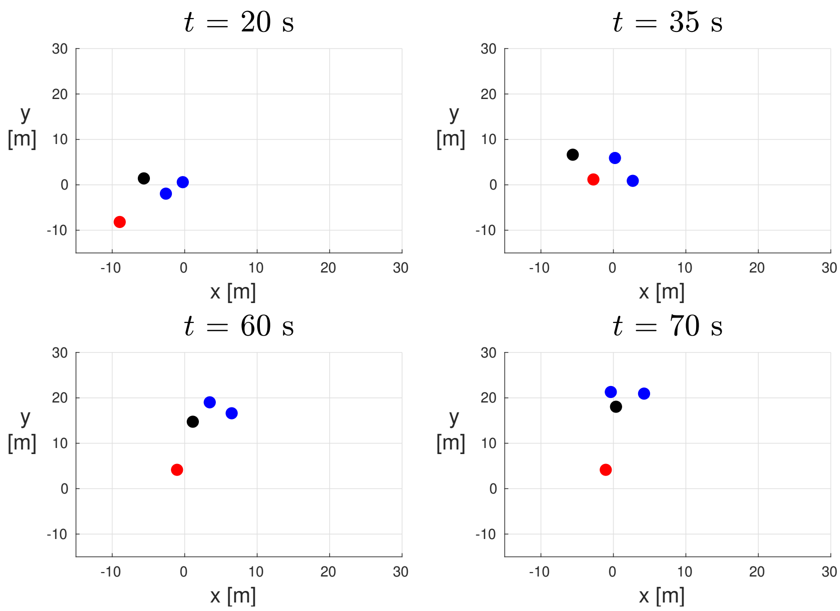

Figure 5.26: Sub-figures contain positions of blue and black swarm members and red predator in x, y coordinates in time t if one MAV (black) can detect the predator and all MAVs use Communication and the UVDAR system.

t_s [s]	t_d [s]	t_e [s]	t_r [s]
18.522	26.400	26.500	0.100

Table 5.7: Quantities t_s, t_d, t_e and t_r measured in simulation in which one of three MAVs can detect a predator and all MAVs use Communication and the UVDAR system.

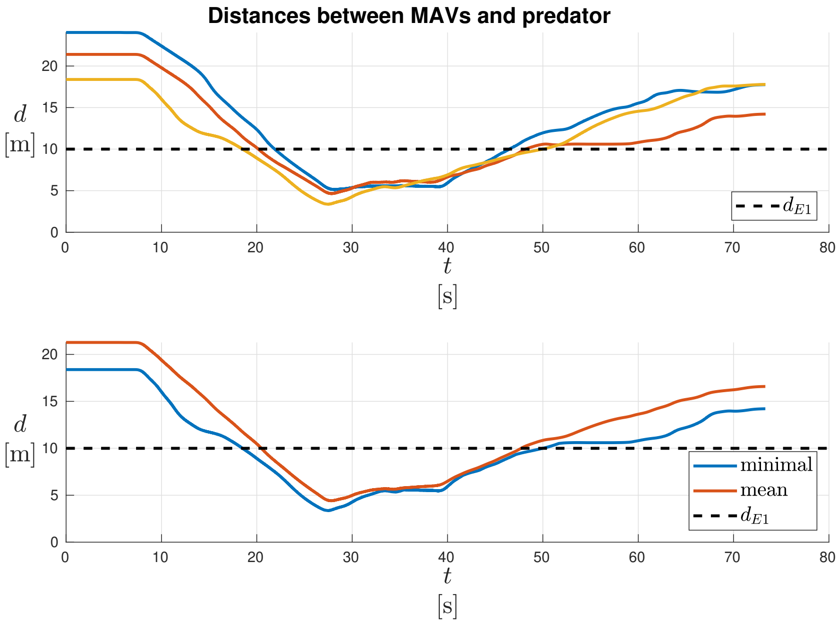

Figure 5.27: The upper figure is a graph of distances between three MAVs and the predator if one MAV can detect the predator and all MAVs use Communication and the UVDAR system. The lower figure shows the minimal and mean distance between MAVs and the predator.

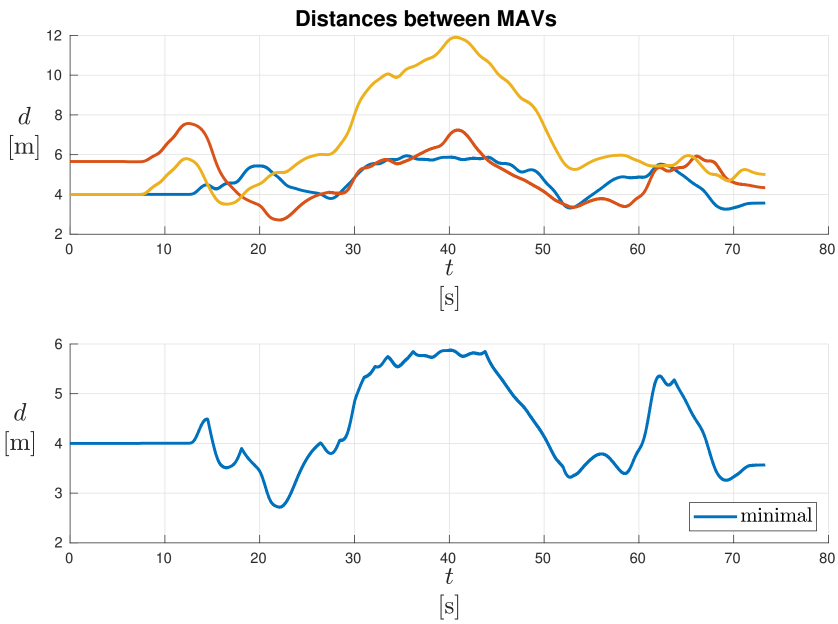

Figure 5.28: The absolute and minimal distances between three MAVs if one MAV can detect a predator and all MAVs use Communication and the UVDAR system.

One see without Communication

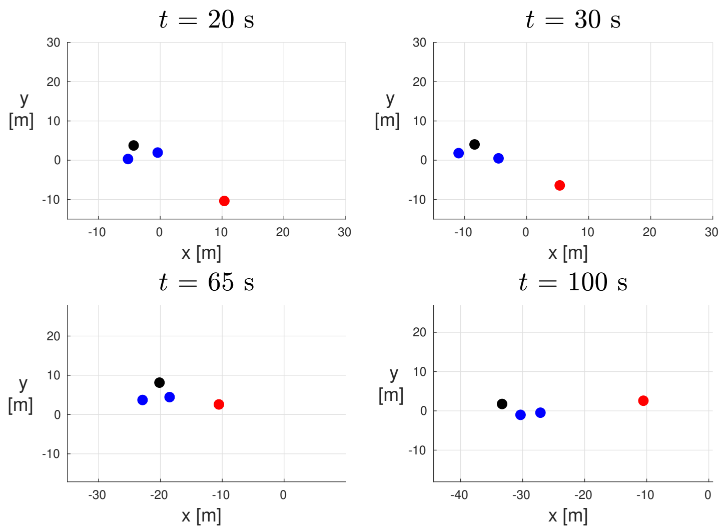

Figure 5.29: Sub-figures contain positions of blue and black swarm members and red predator in x, y coordinates in time t if one MAV (black) can detect the predator and all MAVs use the UVDAR system and do not use Communication.

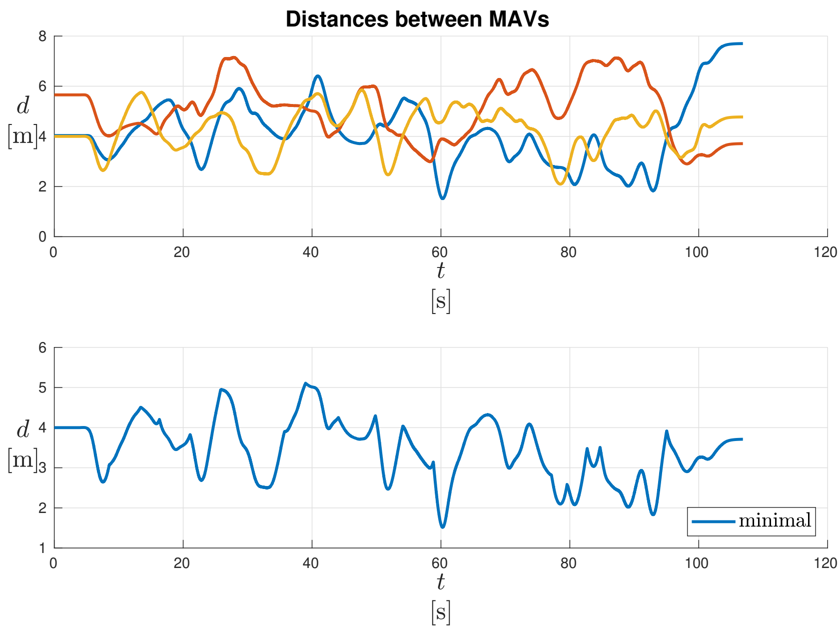

Figure 5.30: The absolute and minimal distances between three MAVs if one MAV can detect a predator and all MAVs use the UVDAR system and do not use Communication.

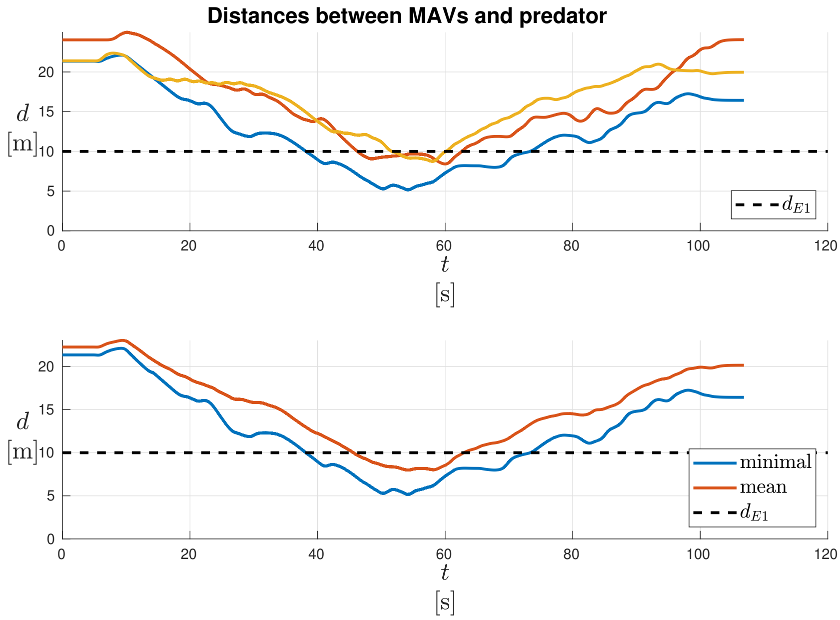

Figure 5.31: The upper figure is a graph of distances between three MAVs and the predator if one MAV can detect the predator and all MAVs use the UVDAR system and do not use Communication. The lower figure shows the minimal and mean distance between MAVs and the predator.

t_s [s]	t_d [s]	t_e [s]	t_r [s]
38.180	48.316	49.248	0.932

Table 5.8: Quantities t_s, t_d, t_e and t_r measured in simulation in which one of three MAVs can detect a predator and all MAVs use the UVDAR system and do not use Communication.

5.3.1 Evaluation

In all presented simulations the swarm of MAVs successfully escapes the predator without colliding with it. However, the minimal distance to the predator in presented simulations decreases to 5 m as shown in Figures 5.21, 5.24, 5.27 and 5.31. Compared to the minimal distance to the predator in the section 5.2 where MAVs use States sharing, the values where MAVs use the UVDAR system are smaller. As a result, using States sharing for localization of other swarm members and the predator is more secure in terms of the requirement to maintain a safe distance from the predator.

If MAVs use States sharing for localization of other swarm members (section 5.2), there is a difference in the minimal distance between MAVs in simulations in which swarm members use Communication and in which they do not. As listed in section 5.2 the minimal distance is 3 m for MAVs with Communication and 2.5 m for MAVs without Communication. However, when MAVs use the UVDAR system for localizing other swarm members, the minimal distance between MAVs decreases to 2 m in all presented simulations except one (Figure 5.28) in which the value drops just below 3 m. Such results show that using States sharing is safer for MAVs swarm movement.

In simulations presented in this section, there is the same difference in the measured time quantities between simulations where swarm MAVs use and do not use Communication as in the previous section 5.2. Time t_r in simulations in which swarm MAVs use Communication are smaller than time t_r in simulations in which swarm MAVs do not use Communication. This result confirms the claim that the use of communication reduces the time required for starting the escape of the entire swarm from the predator compared to other methods presented in this thesis in section 4.4. Comparing the measured time t_s and t_d in individual simulations shows that the predator is detected significantly faster when all MAVs can detect it than if only one MAV can.

In summary, the UVDAR system can be used for localization in the swarm of MAVs which has been verified in many simulations. However, the safest way is to use States sharing with Communication if the distance to a predator is taken into account as well as the distance between the individual members of the swarm. If the focus is on the distance between swarm members and a predator, it is better to use Communication and allow as many swarm MAVs as possible to detect the predator. In terms of the distance between individual swarm MAVs it is better to use State Sharing than the UVDAR system.

The previous paragraph may suggest that States sharing is an ideal method for localization of the other swarm members. Nevertheless, States sharing requires a very reliable communication network, which is difficult to establish. Additionally, for this method to work, each member of the swarm needs to know its absolute position in the world very precisely. The exact position is viable only under a precise localization system where all agents share the same coordinate frame, e.g. Real Time Kinematics (RTK)-GPS [25] that requires at least the presence of pre-calibrated base station. Unlike in simulation, States sharing does not work well in real world. That is why the UVDAR localization system is being developed for real world applications.

5.4 Gazebo - only Boids without Escape behaviour

In order to compare a swarm with implemented Escape behaviour and a swarm without Escape behaviour using only the Boids algorithm, the following simulations in Gazebo were made. In this section the swarm members do not use Escape behaviour. A predator can be detected only as a static obstacle by an onboard sensor RPLIDAR A3 placed on every MAV in the swarm (section 2.2). In the first two simulations the MAVs use States sharing to localize other swarm members. In the other two simulations, the MAVs use the UVDAR system to localize other swarm members.

Two situations for each localization method (UVDAR system and Sharing position) are presented. In the first one, the predator is moving into the centre of the swarm. In the second one, the goal of the predator is to hit one of the swarm members. If the predator succeeds, an impact occurs. This is called a *collision*.

In these simulations, only three time quantities are measured, t_s, t_d and t_r, where t_s is same as in previous simulations, t_d is the predator detection time by any MAV for the first time as a static obstacle and $t_r = t_d - t_s$.

5.4.1 States sharing - 6 MAVs

Using the States sharing localization method, six MAVs can be simulated in the Gazebo simulator. The initial situation is the same as in Figure 5.6. Swarm is made up of five MAVs and the last one acts as a predator. When the simulation starts, the predator moves towards the swarm with a the task to reach the centre of the swarm or hit one of the swarm members.

Predator moves into the centre of the swarm

t_s [s]	t_d [s]	t_r [s]
9.496	14.324	4.828

Table 5.9: Quantities t_s, t_d and t_r measured in simulation in which all five MAVs use States sharing, do not use Escape behaviour and the predator moves into the centre of the swarm.

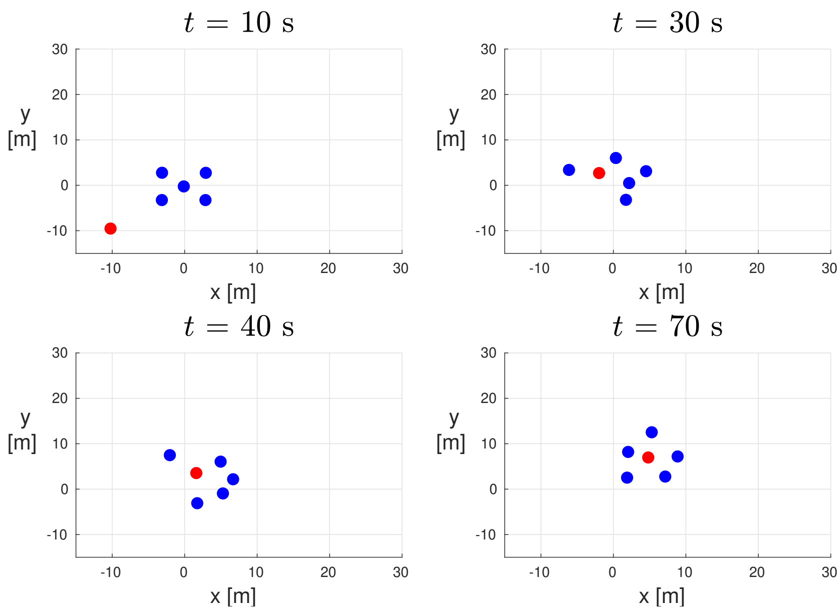

Figure 5.32: Sub-figures contain positions of blue swarm members and red predator in x, y coordinates in time t if all five swarm MAVs do not use Escape behaviour, use States sharing and the predator moves into the centre of the swarm.

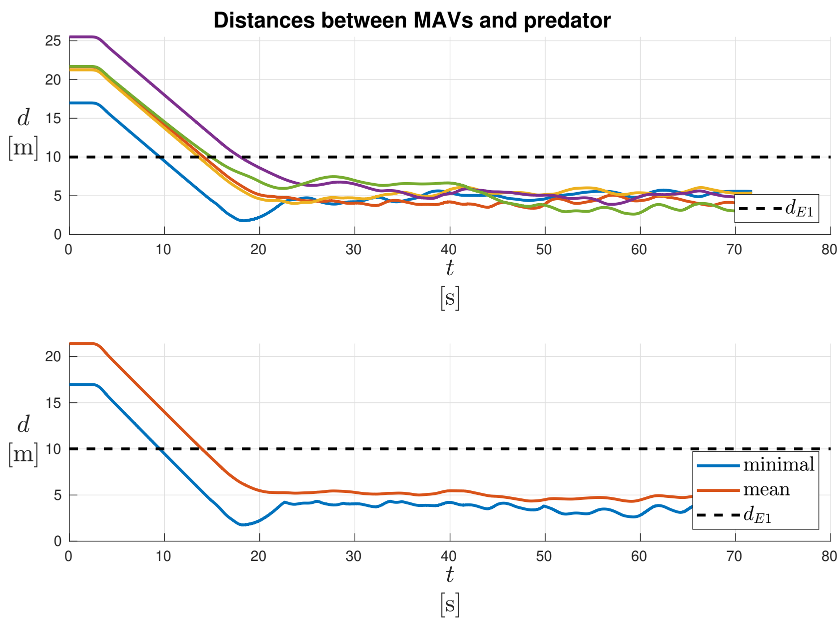

Figure 5.33: The upper figure is a graph of distances between five MAVs and the predator if all swarm MAVs do not use Escape behaviour, use States sharing and the predator moves into the centre of the swarm. The lower figure shows minimal and mean distance between MAVs and the predator.

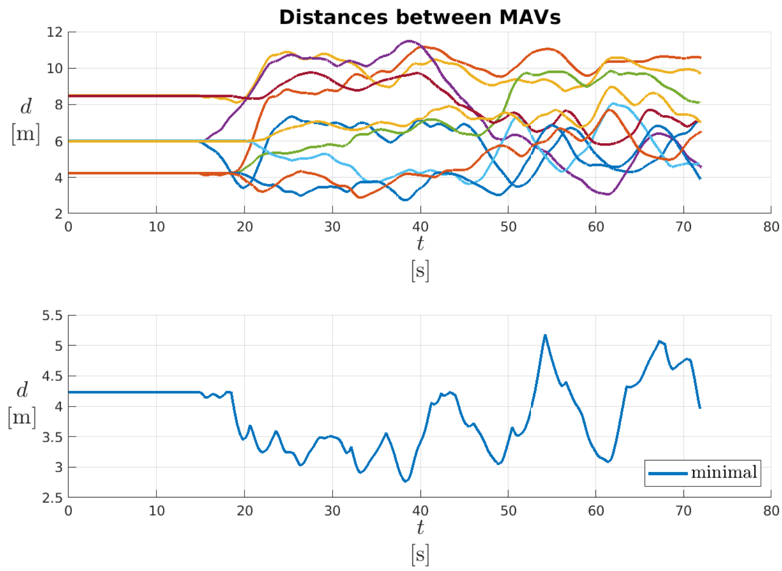

Figure 5.34: The absolute and minimal distances between five MAVs if all swarm MAVs do not use Escape behaviour, use States sharing and the predator moves into the centre of the swarm.

Predator attempts to hit one of the swarm members

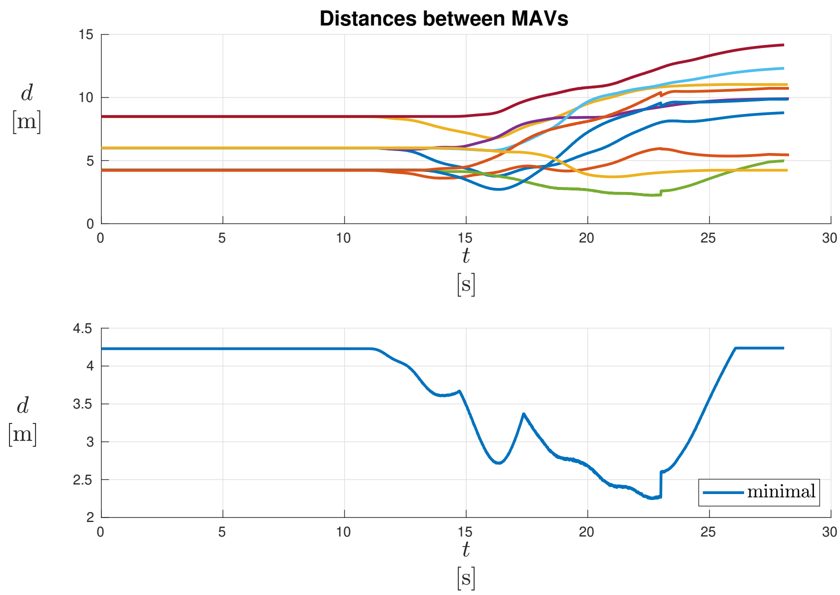

Figure 5.35: The absolute and minimal distances between five MAVs if all swarm MAVs do not use Escape behaviour, use States sharing and the predator attempts to hit one of the swarm members.

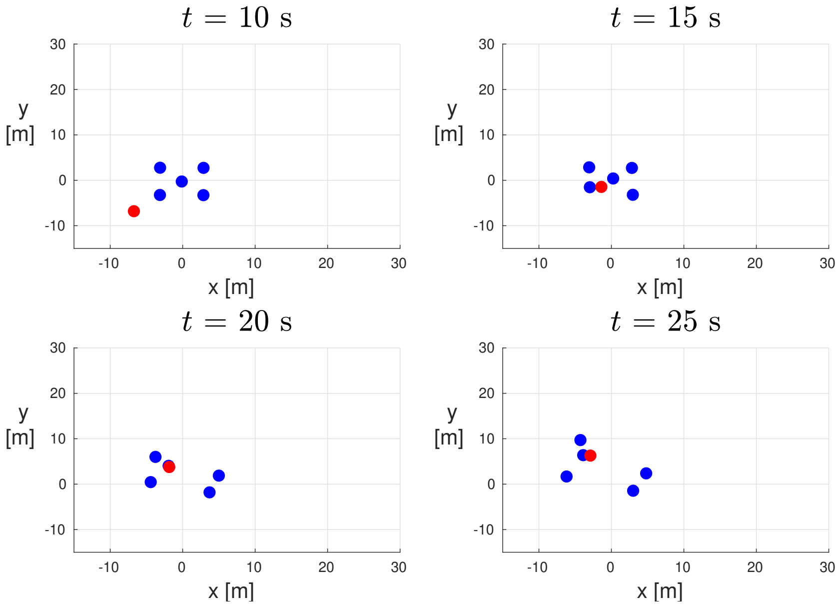

Figure 5.36: Sub-figures contain positions of blue swarm members and red predator in x, y coordinates in time t if all five swarm MAVs do not use Escape behaviour, use States sharing and the predator attempts to hit one of the swarm members.

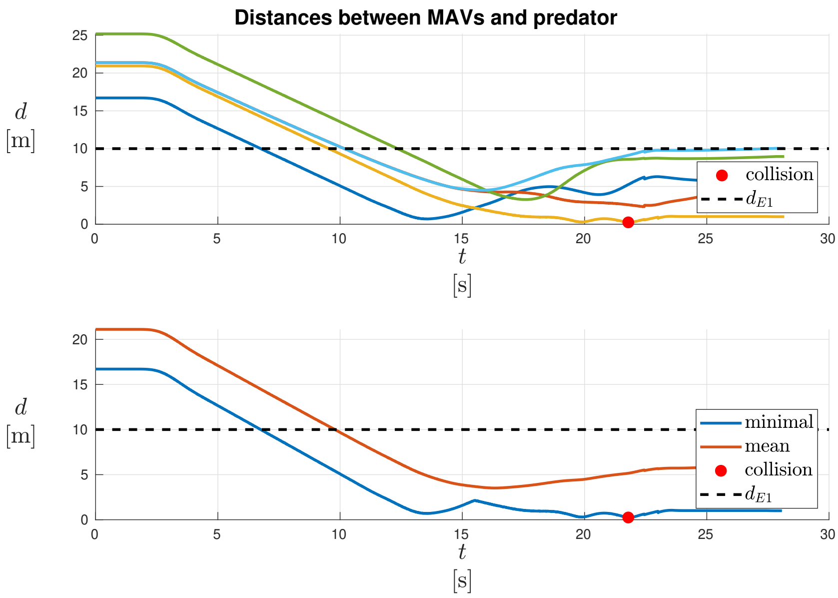

Figure 5.37: The upper figure is a graph of distances between five MAVs and the predator if all swarm MAVs do not use Escape behaviour, use States sharing and the predator attempts to hit one of the swarm members. The lower figure shows minimal and mean distance between MAVs and the predator.

t_s [s]	t_d [s]	t_r [s]
6.760	10.048	3.288

Table 5.10: Quantities t_s, t_d and t_r measured in simulation in which all five MAVs do not use Escape behaviour, use States sharing and the predator attempts to hit one of the swarm members.

5.4.2 UVDAR system - 4 MAVs

If MAVs use the UVDAR system for localization of the other MAVs in Gazebo simulator, only four MAVs can be simulated. Three of them create a swarm, the fourth is a predator with the same task as in subsection States sharing 5.4.1. The initial situation is the same as in Figure 5.19.

Predator moves into the centre of the swarm

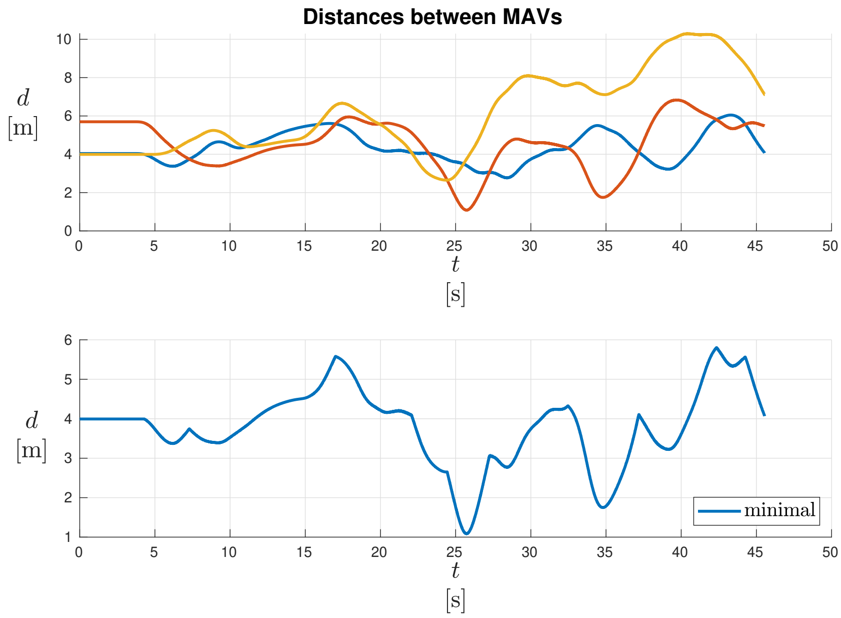

Figure 5.38: The absolute and minimal distances between three MAVs if all swarm MAVs do not use Escape behaviour, use the UVDAR system and the predator moves into the centre of the swarm.

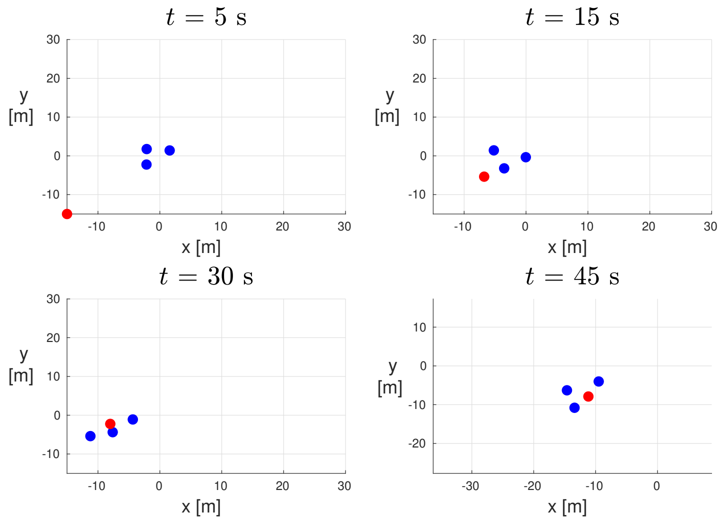

Figure 5.39: Sub-figures contain positions of blue swarm members and red predator in x, y coordinates in time t if three swarm MAVs do not use Escape behaviour, use the UVDAR system and the predator moves into the centre of the swarm.

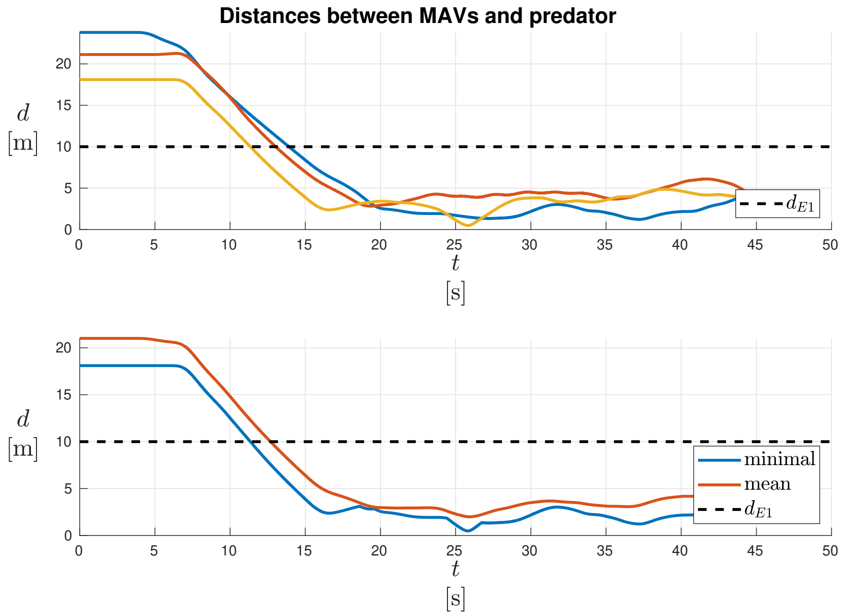

Figure 5.40: The upper figure is a graph of distances between three MAVs and the predator if all swarm MAVs do not use Escape behaviour, use the UVDAR system and the predator moves into the centre of the swarm. The lower figure shows minimal and mean distance between MAVs and the predator.

t_s [s]	t_d [s]	t_r [s]
11.352	14.268	2.916

Table 5.11: Quantities t_s, t_d and t_r measured in simulation in which all three MAVs do not use Escape behaviour, use the UVDAR system and the predator moves into the centre of the swarm.

Predator attempts to hit one of the swarm members

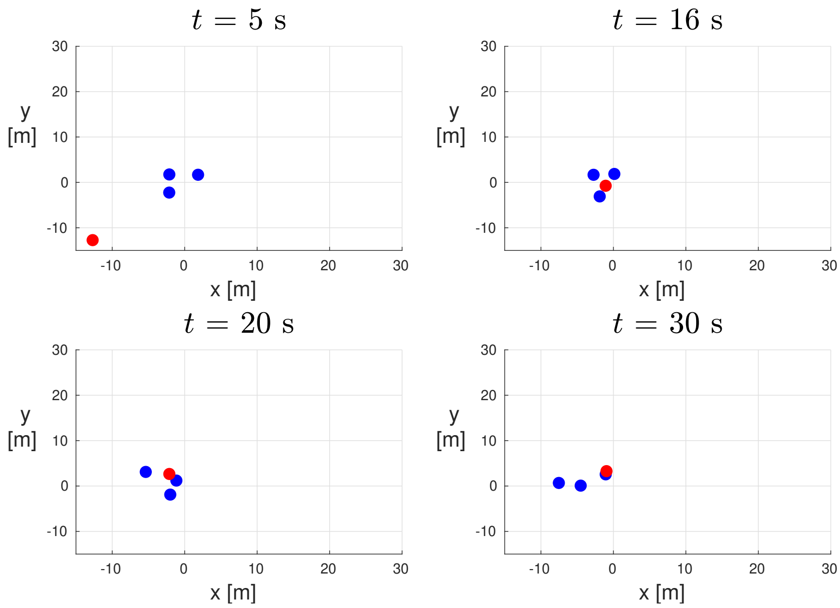

Figure 5.41: Sub-figures contain positions of blue swarm members and red predator in x, y coordinates in time t if three swarm MAVs do not use Escape behaviour, use the UVDAR system and the predator attempts to hit one of the swarm members.

t_s [s]	t_d [s]	t_r [s]
8.640	12.688	4.048

Table 5.12: Quantities t_s, t_d and t_r measured in simulation in which all three MAVs do not use Escape behaviour, use the UVDAR system and the predator attempts to hit one of the swarm members.

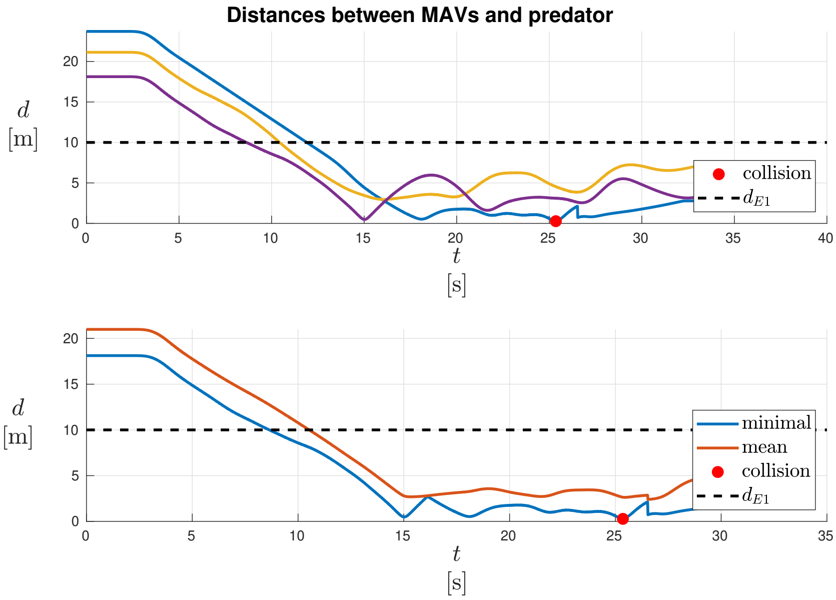

Figure 5.42: The upper figure is a graph of distances between three MAVs and the predator if all swarm MAVs do not use Escape behaviour, use the UVDAR system and the predator attempts to hit one of the swarm members. The lower figure shows minimal and mean distance between MAVs and the predator.

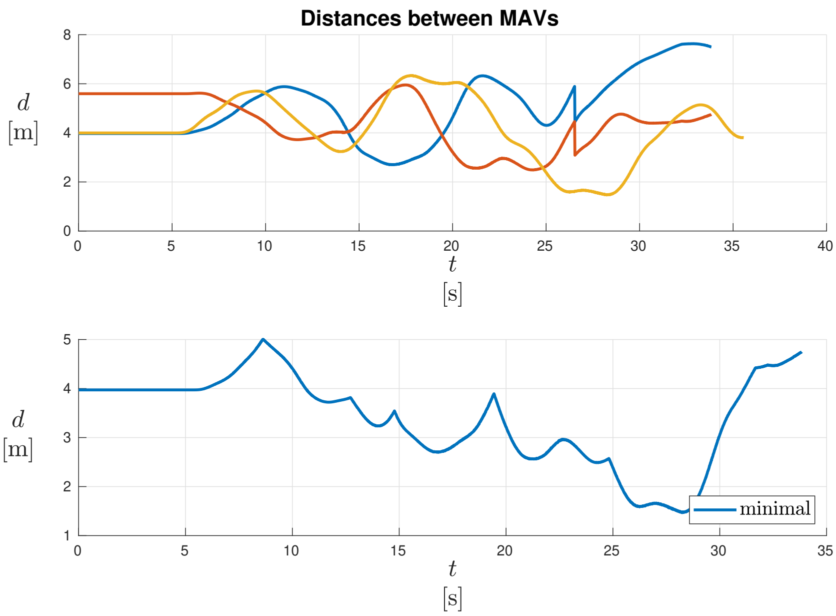

Figure 5.43: The absolute and minimal distances between three MAVs if all swarm MAVs do not use Escape behaviour, use the UVDAR system and the predator attempts to hit one of the swarm members.

5.4.3 Evaluation

The results show that when the predator moves to the centre of the swarm, MAVs create a swarm around the predator. The behaviour of the predator and the swarm members becomes similar to a situation where the predator was merely another swarm member. Thanks to the Obstacle and Separation forces, collision does not occur. However, if a predator attempts to hit one of the swarm members, a collision occurs and other members of the swarm stay close to this collision. Time t_r shows, how long it takes the swarm members to react to the presence of the predator that has entered their safe zone (i.e. the distance from any swarm MAV to the predator is less than d_{E1}).

The main difference between the swarm using Escape behaviour and the swarm without it is in the distance to the predator. If the swarm of MAVs uses Escape behaviour (section 5.2 and 5.3), the distance to the predator first diminishes and then stabilizes. As soon as the predator stops, the swarm's distance from the predator grows again and stabilizes at a distance greater than d_{E1}. On the other hand, if Escape behaviour is not used, the distance to the predator first diminishes and then stabilizes at a distance less than d_{E1}. As a result, the swarm stays close to the predator and does not escape.

Another difference is in the minimal distance between the individual swarm members when they use States sharing or the UVDAR system. The minimal distance between swarm MAVs decreases to 2.5 m if they use States sharing. However, if swarm MAVs use the UVDAR system, the minimal distance between individual swarm members drops down to 1 m. The results of these simulations show that it is necessary to implement Escape behaviour for avoiding a dynamic obstacle.

5.5 Gazebo - obstacles

In this section, a swarm of MAVs moves in an environment with obstacles in the Gazebo simulator. Two simulated worlds were created that represent different types of obstacles. The first one is shown in Figure 5.44a where a house with a car is placed next to a road bordered with trees. The Matlab representation of this world is plotted in Figure 5.44b. Orange rectangles represent the house and the car. Orange circles are a representation of the trees. The second world is shown in Figure 5.45a. The obstacles in this world are trees that correspond to a forest in the real world. Matlab representation of this world is shown in 5.45b. Each orange circle represents one tree. The initial situations for all presented simulations in this section are in Appendix A.2. Simulations in this section demonstrate the functionality of the system designed for the swarm of MAVs in an environment with static obstacles without any collisions. Data about static obstacles are obtained only from the sensor RPLIDAR A3 presented in section 2.2.

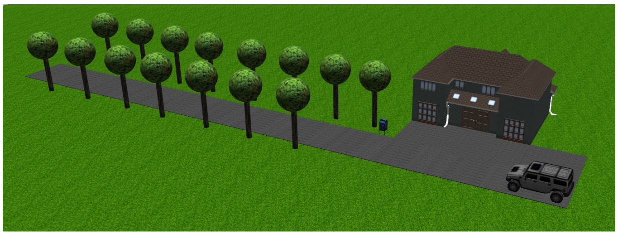

(a) Gazebo simulator

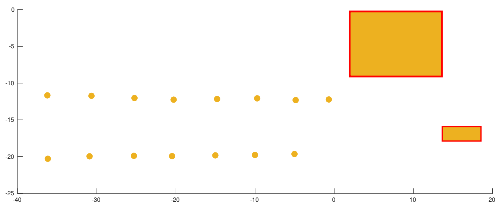

(b) Matlab representation

Figure 5.44: A simulated world with a house, a car and trees

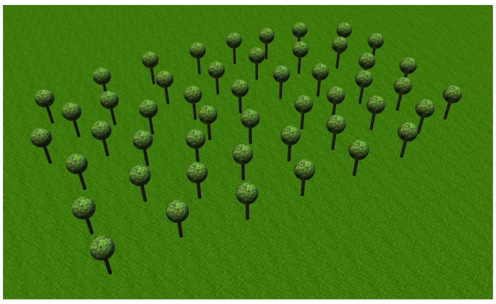

(a) Gazebo simulator

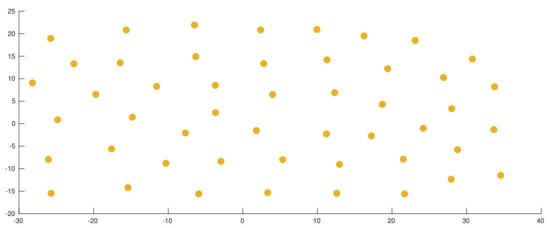

(b) Matlab representation

Figure 5.45: A simulated world with a forest

5.5.1 States sharing - 6 MAVs

Using States sharing, six MAVs are used for these simulations. The swarm consists of five MAVs and the last MAV is the predator. Swarm MAVs do not use Communication and they use States sharing for localization of other swarm members and the predator.

World with a house

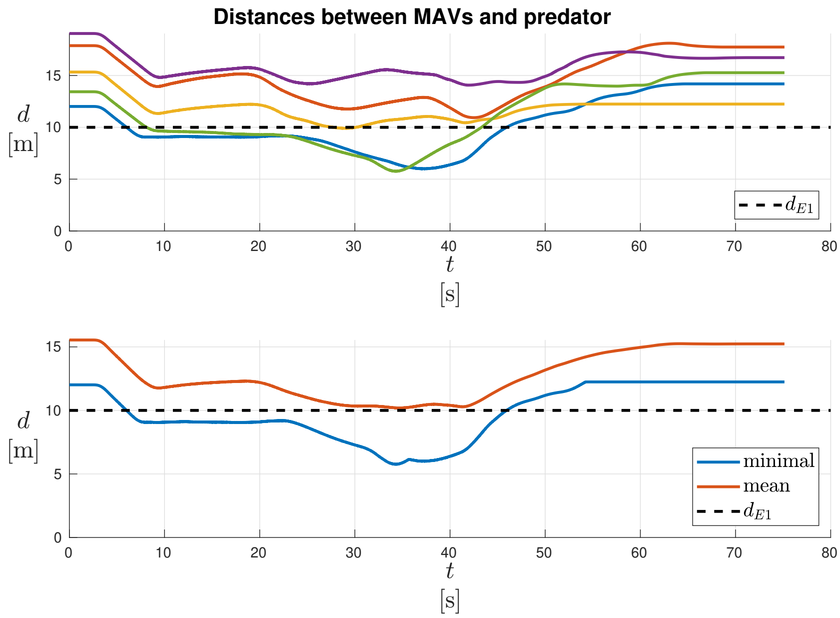

Figure 5.46: The upper figure is a graph of distances between five MAVs and the predator in world with a house if all MAVs can detect the predator, use States sharing and do not use Communication. The lower figure shows the minimal and the mean distance between the MAVs and the predator.

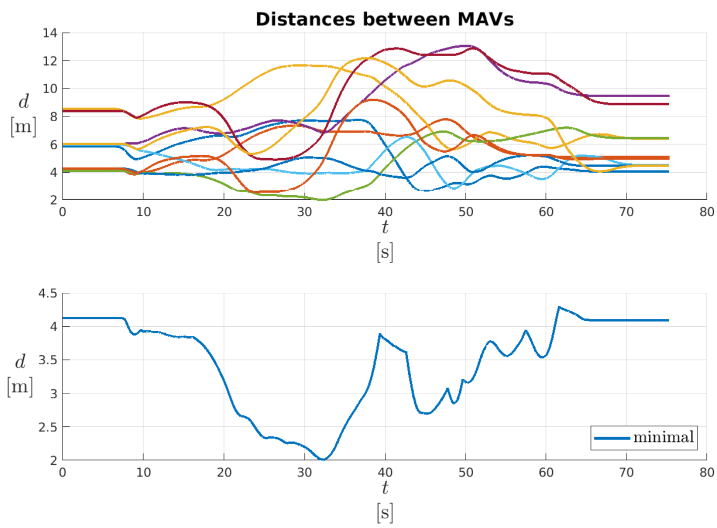

Figure 5.47: The absolute and the minimal distances between five MAVs in world with a house if all MAVs can detect a predator, use States sharing and do not use Communication.

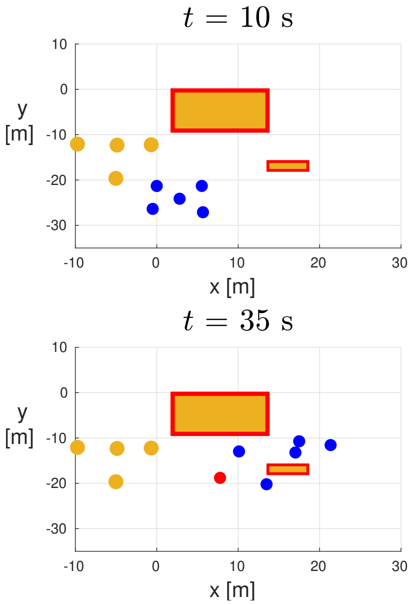

Figure 5.48: Sub-figures contain positions of blue swarm members and red predator in x, y coordinates of world with a house in time t if all five MAVs can detect the predator, use States sharing and do not use Communication.

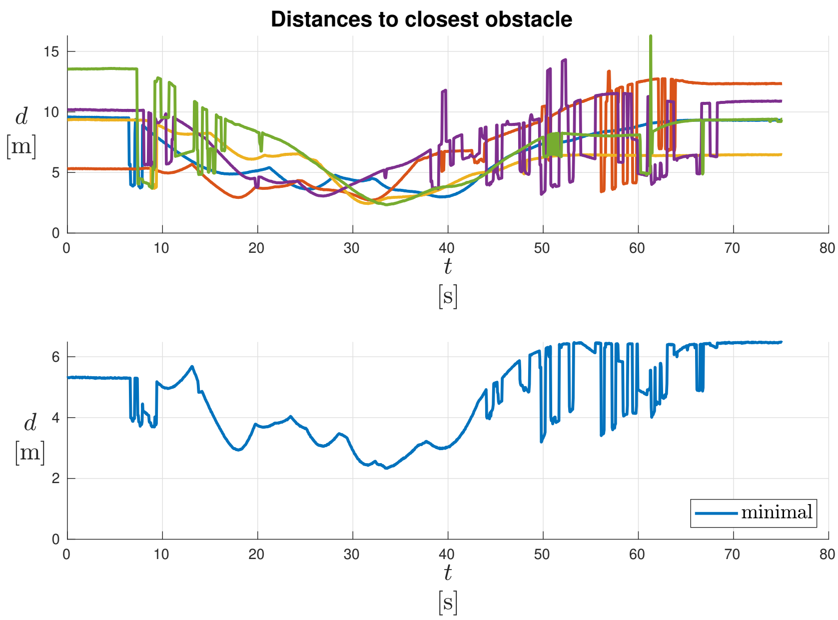

Figure 5.49: The upper figure is a graph of distances measured by RPLIDAR A3 between the MAVs and their closest obstacle in world with a house if all MAVs can detect a predator, use States sharing and do not use Communication. The lower figure shows the minimal distance from these distances.

Forest

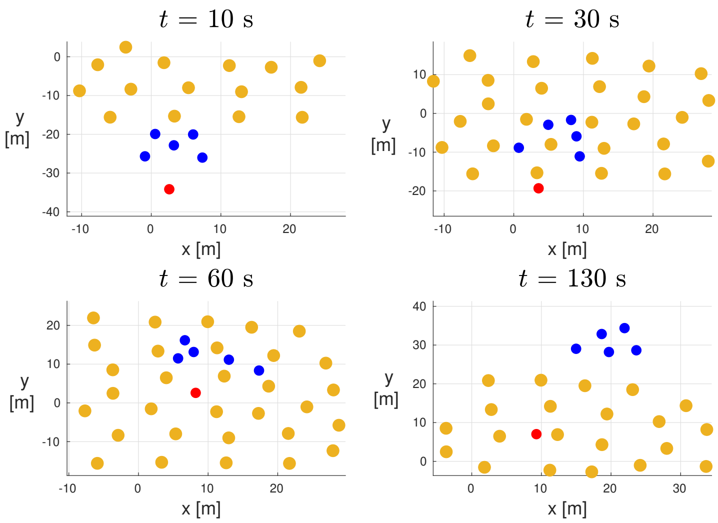

Figure 5.50: Sub-figures contain positions of blue swarm members and red predator in x, y coordinates of forest world in time t if all five MAVs can detect the predator, use States sharing and do not use Communication.

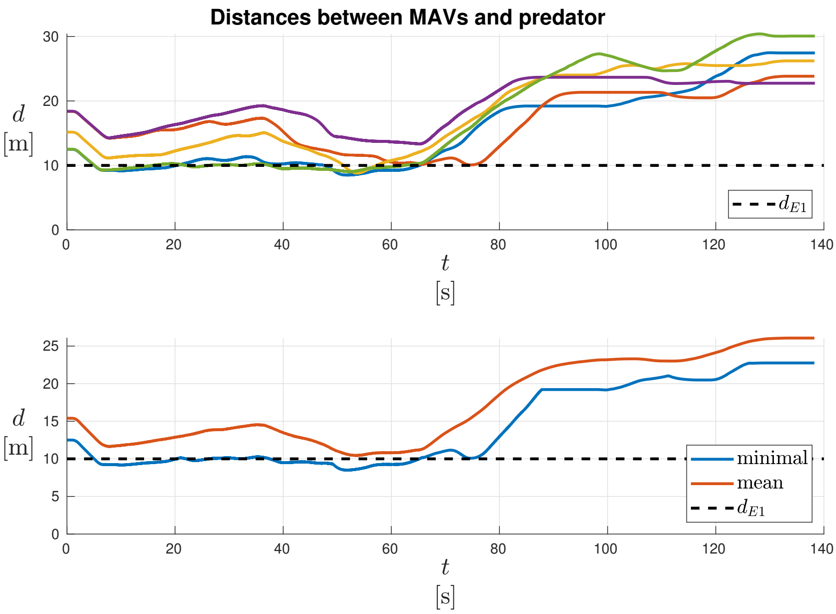

Figure 5.51: The upper figure is a graph of distances between five MAVs and the predator in a forest if all MAVs can detect the predator, use States sharing and do not use Communication. The lower figure shows the minimal and the mean distance between the MAVs and the predator.

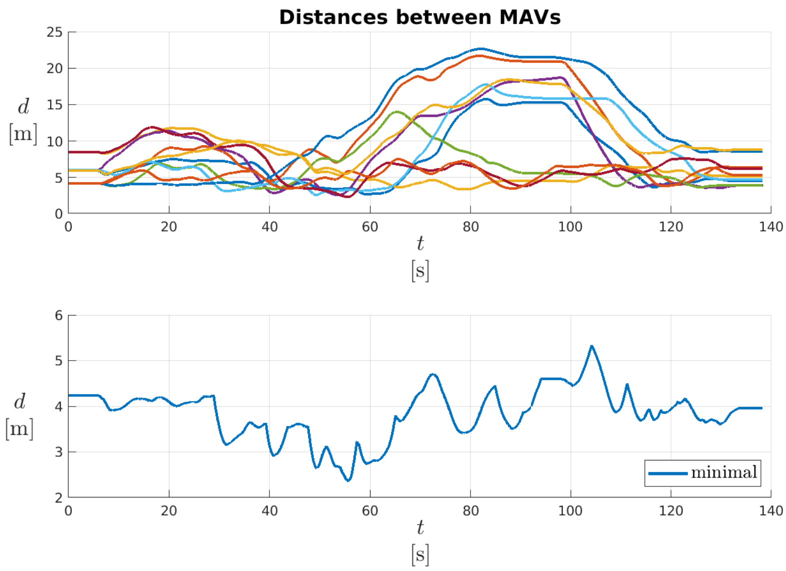

Figure 5.52: The absolute and the minimal distances between five MAVs in a forest if all MAVs can detect a predator, use States sharing and do not use Communication.

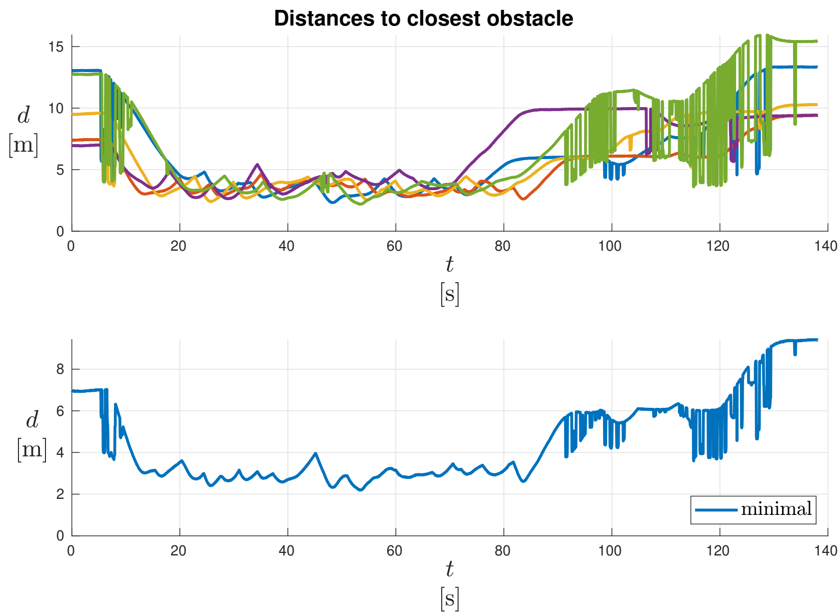

Figure 5.53: The upper figure is a graph of distances measured by RPLIDAR A3 between the MAVs and their closest obstacle in a forest if all MAVs can detect a predator, use States sharing and do not use Communication. The lower figure shows the minimal distance from these distances.

Evaluation

As shown in the graphs of both simulations, collisions do not occur. The swarm of MAVs successfully escapes from the predator and flies through the forest or around the house and the car. The distance to the closest obstacle in both simulations is higher than 2 m which is the distance for safe movement around obstacles.

During the flight through the forest the swarm divides into two groups and after passing the forest the MAVs merge back into one group. This is shown in Figure 5.52 at time 60 - 120 s.

5.5.2 UVDAR system - 4 MAVs

Four MAVs are used for a simulation if the UVDAR system is used. Three of them create a swarm and the last MAV is a predator. Swarm MAVs do not use Communication. State sharing is used for localization of a predator and the UVDAR system is applied for locating other swarm members.

World with a house

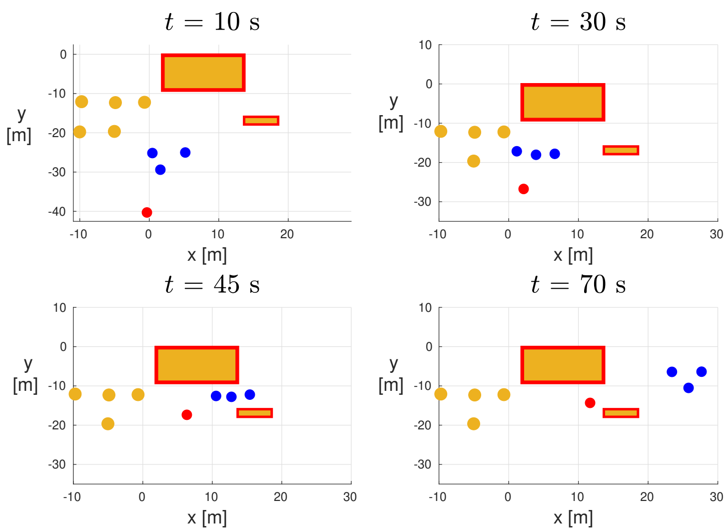

Figure 5.54: Sub-figures contain positions of blue swarm members and red predator in x, y coordinates of world with a house in time t if all three MAVs can detect a predator, use the UVDAR system and do not use Communication.

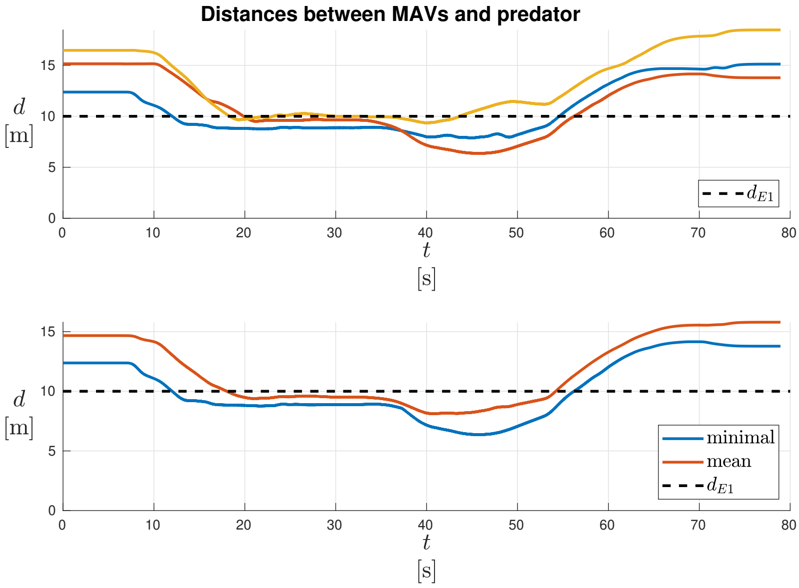

Figure 5.55: The upper figure is a graph of distances between three MAVs and the predator in world with a house if all MAVs can detect the predator, use the UVDAR system and do not use Communication. The lower figure shows the minimal and the mean distance between the MAVs and the predator.

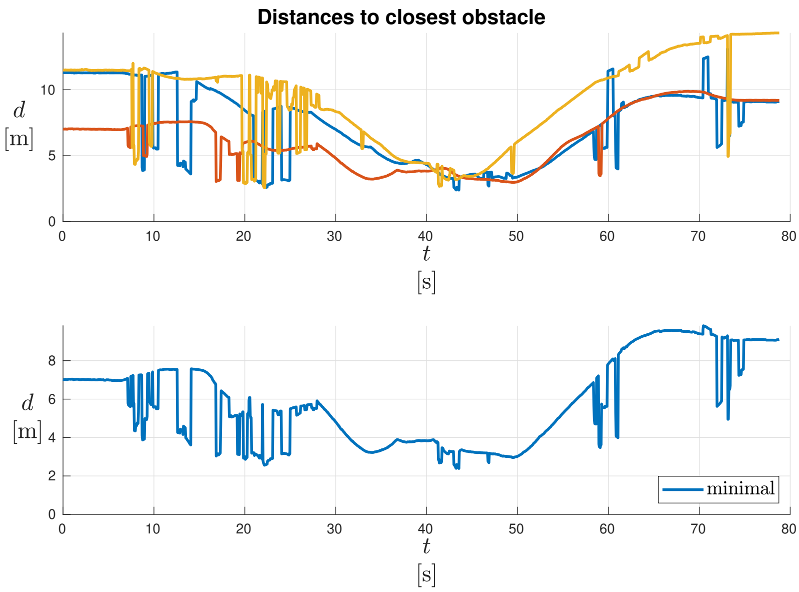

Figure 5.56: The upper figure is a graph of distances measured by RPLIDAR A3 between the MAVs and their closest obstacle in world with a house if all MAVs can detect a predator, use the UVDAR system and do not use Communication. The lower figure shows the minimal distance from these distances.

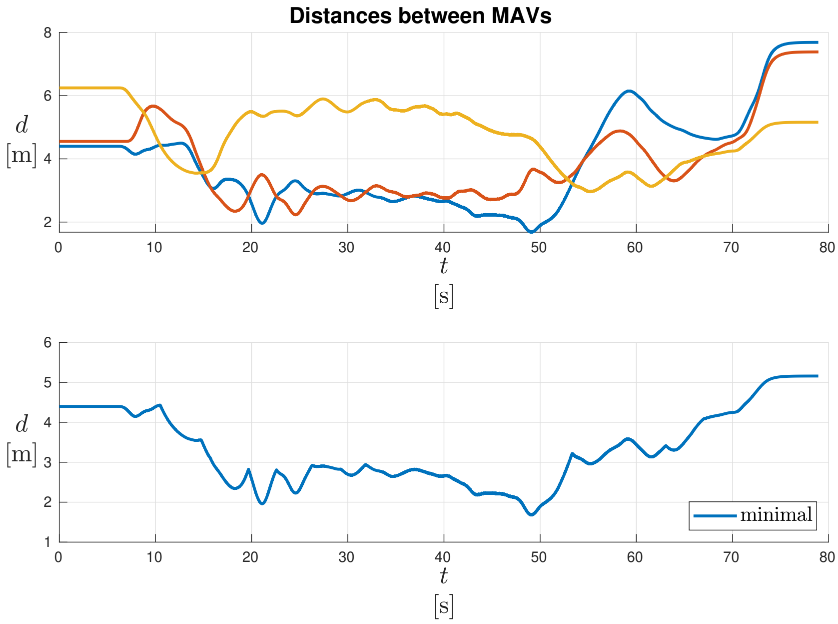

Figure 5.57: The absolute and the minimal distances between three MAVs in world with a house if all MAVs can detect a predator, use the UVDAR system and do not use Communication.

Forest

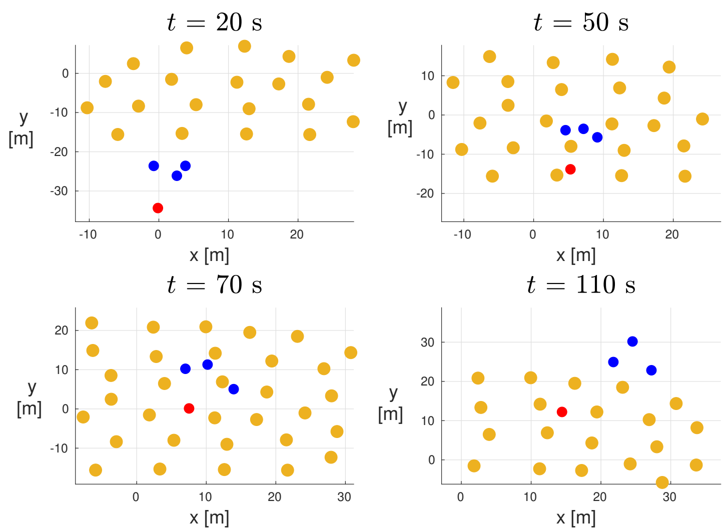

Figure 5.58: Sub-figures contain positions of blue swarm members and red predator in x, y coordinates of forest world in time t if all three MAVs can detect a predator, use the UVDAR system and do not use Communication.

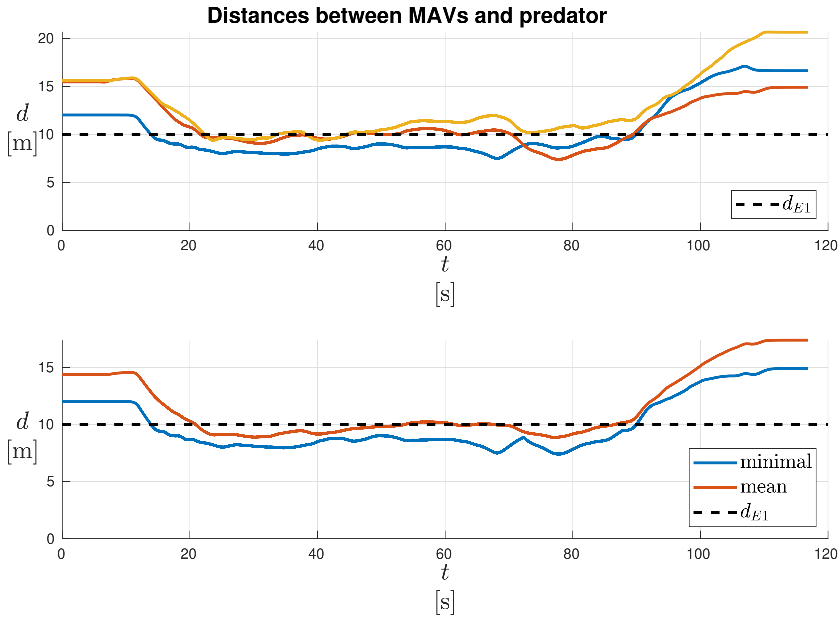

Figure 5.59: The upper figure is a graph of distances between three MAVs and the predator in a forest if all MAVs can detect the predator, use the UVDAR system and do not use Communication. The lower figure shows the minimal and the mean distance between the MAVs and the predator.

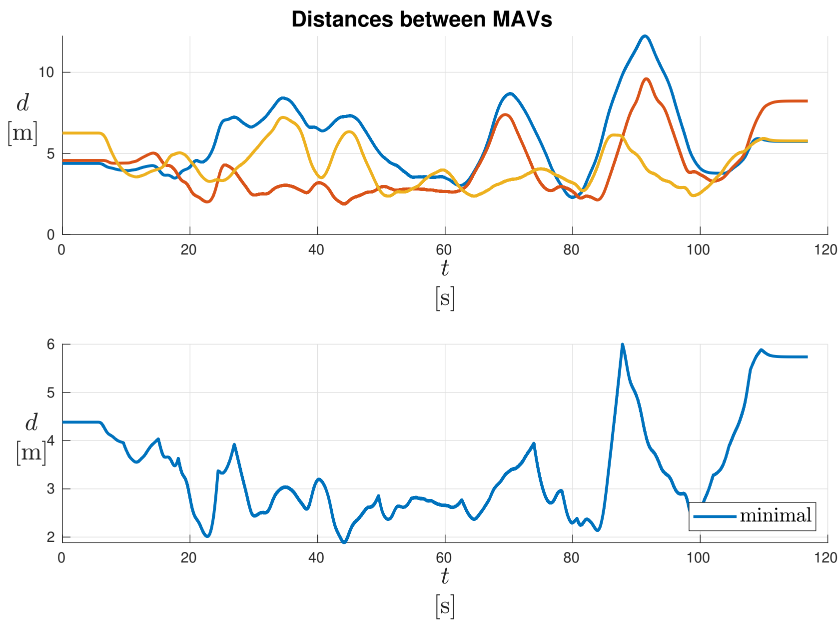

Figure 5.60: The absolute and the minimal distances between three MAVs in a forest if all MAVs can detect a predator, use the UVDAR system and do not use Communication.

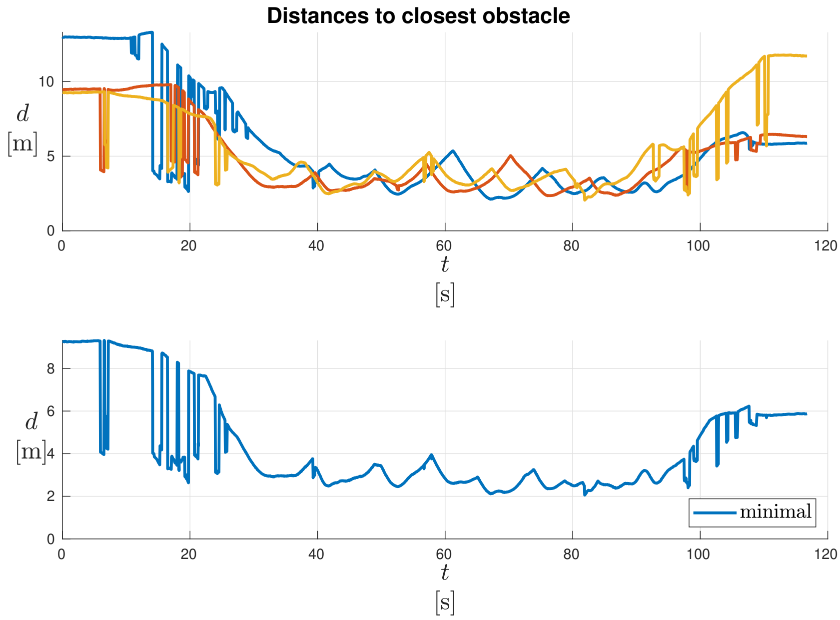

Figure 5.61: The upper figure is a graph of distances measured by RPLIDAR A3 between the MAVs and their closest obstacle in a forest if all MAVs can detect a predator, use the UVDAR system and do not use Communication. The lower figure shows the minimal distance from these distances.

Evaluation

As in the previous section 5.5.1, the swarm of MAVs successfully escapes from the predator in both environments with obstacles. Collisions do not occur in the two presented simulations as show the resulting graphs where the minimal distance between the MAVs is approximately 2 m which is similar to section 5.5.1 where MAVs use States sharing. The minimal distance to obstacles is greater than or equal to 2 m in both simulations which is a safe distance between the MAVs and obstacles.

During the flight through the forest, it is once again possible to see a division of the swarm. This is shown in Figure 5.60 in time 80 - 100 s. Outside of the forest, the swarm MAVs merge back into a single group.

Chapter 6

Experiments

After successful testing in the Gazebo simulator, the system designed in this thesis has been verified by conducting real-world experiments. These experiments took place in a meadow covering an area of 100 m by 200 m. Four MAVs were used to carry out the experiments that are pictured in Figure 6.1. Three of them made up the swarm. The last one represented the predator and was controlled manually.

At the beginning of the experiments, the swarm MAVs stayed together and the predator moved towards them. After predator detection, the swarm of MAVs started escaping and was chased by the predator for 176 s when swarm MAVs used Communication and for 254 s when swarm MAVs did not use Communication. For mutual MAVs localization, the UVDAR system was used in both experiments. All swarm MAVs could detect the predator. The predator detection was performed using only the UVDAR system. To evaluate the distances between MAVs, the GPS module Holybro Pixhawk 4 Neo-M8N GPS [26] was used. Videos from real-world experiments are stored on the enclosed CD and can also be found on YouTube[1].

Figure 6.1: MAVs used for real-world experiments

[1] https://www.youtube.com/playlist?list=PLulwAeIg-Kc3mi3_rl4kUhb2eOjeq_x22

6.1 UVDAR system - Communication

In this section, swarm MAVs used Communication to share information about the detected predator. If one of the swarm MAVs detected predator, it sent the position of detected predator via WiFi network to other MAVs. To share the position of the detected predator, swarm MAVs need a common global frame, which was provided by the GPS module [26]. The snapshots from this experiment are displayed in Figure 6.2 and show the position of the swarm and the predator at different times.

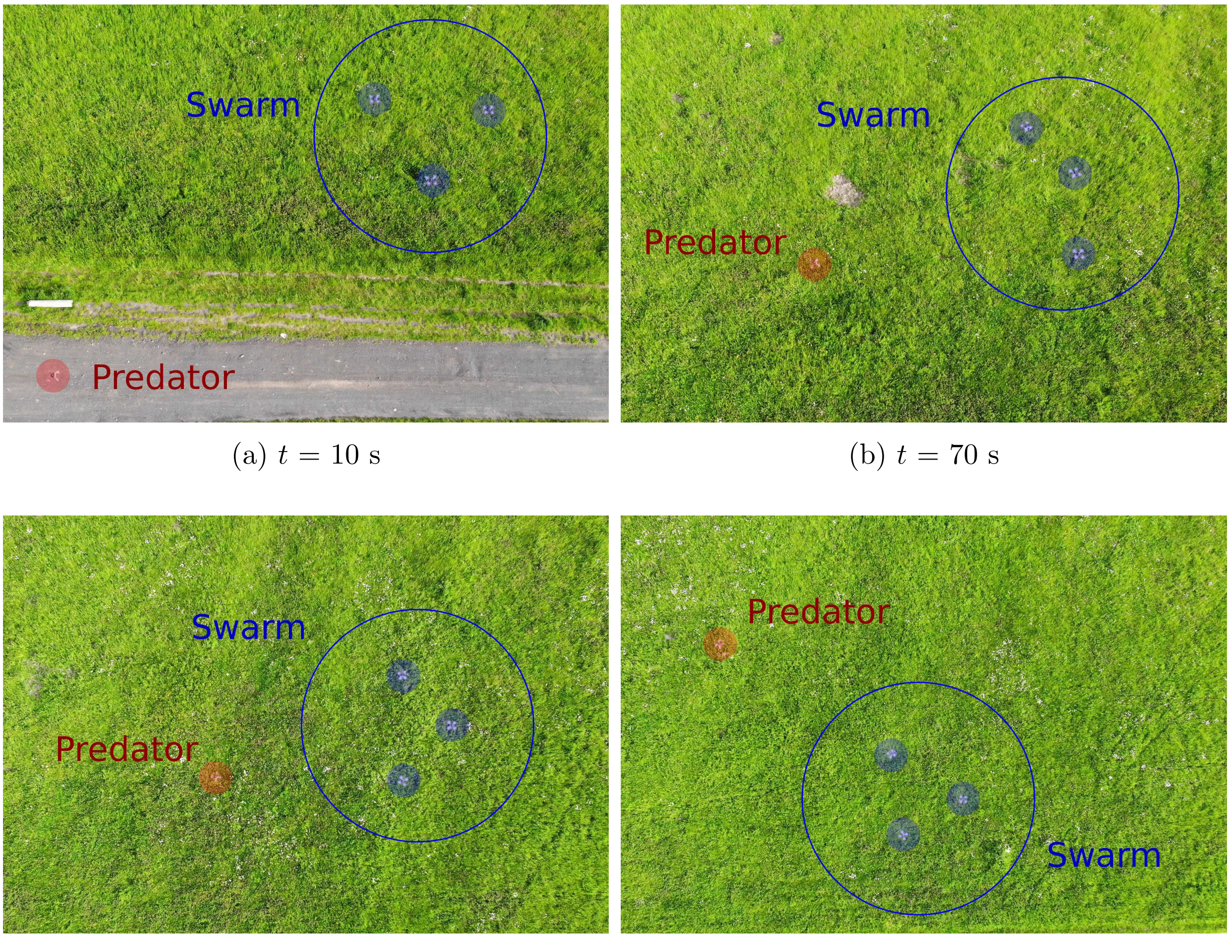

(a) $t = 10$ s (b) $t = 70$ s

(c) $t = 100$ s (d) $t = 175$ s

Figure 6.2: Snapshots from the real-world experiment in which MAVs used the UVDAR system and Communication.

The quantities measured in this experiment are plotted in Figure 6.3. The upper left graph shows the distances between swarm MAVs and the predator. The upper right graph shows the distances between swarm MAVs. Velocities of swarm MAVs and the predator are shown in the bottom left graph. Lastly the graph at the bottom right expresses the distances obtained from the UVDAR system of one swarm member (MAV-1). The distances from the UVDAR system are compared with distances from the GPS module between MAV-1 and other swarm MAVs and between MAV-1 and the predator.

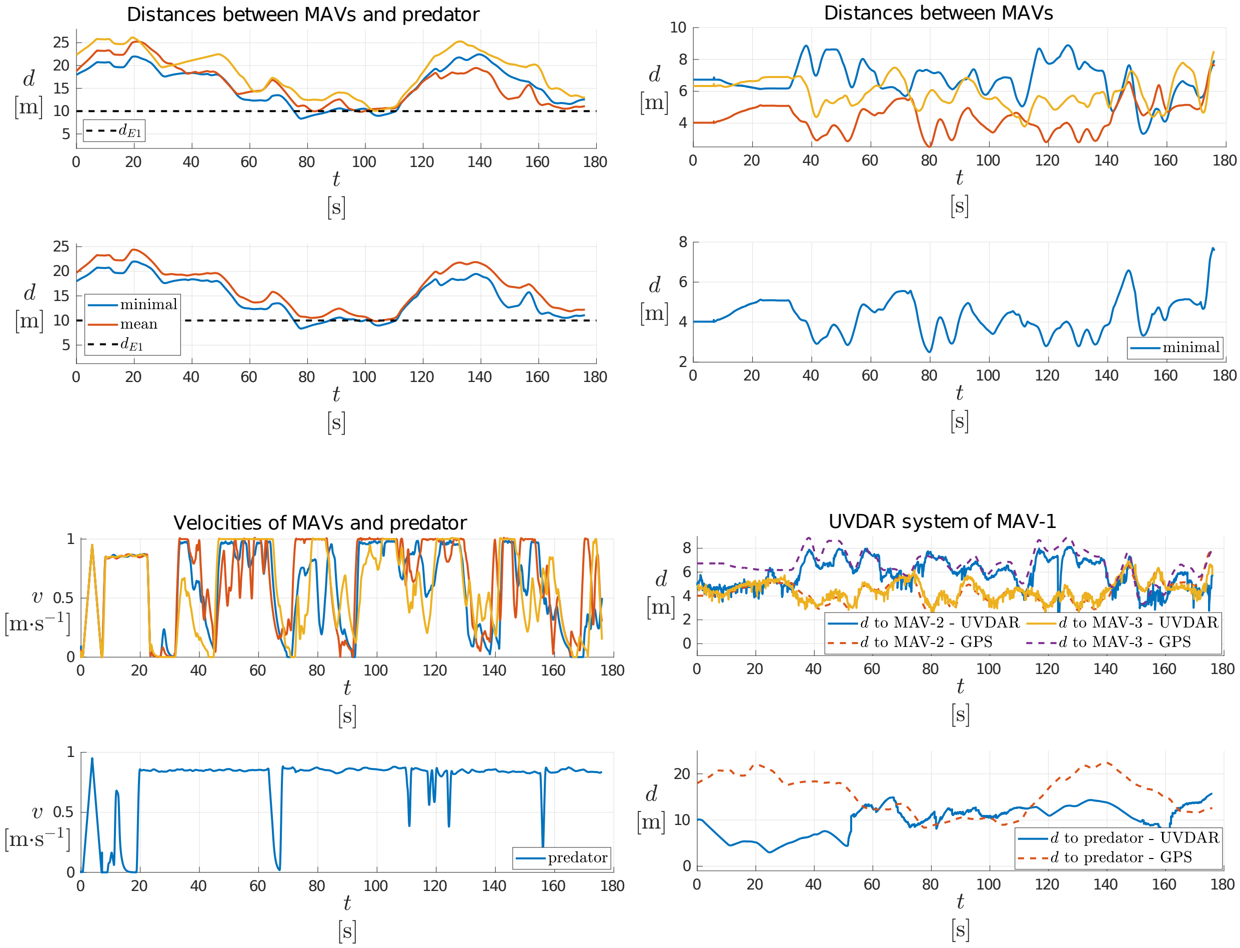

Figure 6.3: Distances between MAVs and the predator, distances between MAVs, velocities of MAVs and the predator, distances obtained from the UVDAR system of MAV-1 between MAV-1 and other swarm MAVs and between MAV-1 and the predator - measured in real-world experiment in which MAVs used the UVDAR system and Communication

6.2 UVDAR system - without Communication

In this section, the swarm MAVs did not send any messages via network. The transition between escape modes of MAVs was in accordance with section 4.4. Thanks to this approach, the swarm of MAVs was fully decentralised, thus communication or external infrastructures such as GNSS were not required. Swarm MAVs used only sensors carried onboard.

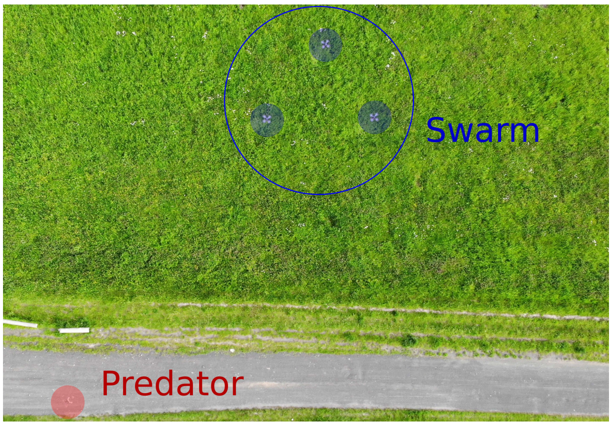

(a) $t = 20$ s

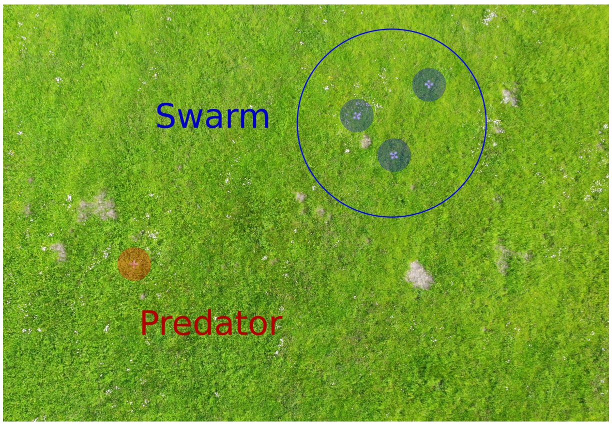

(b) $t = 70$ s

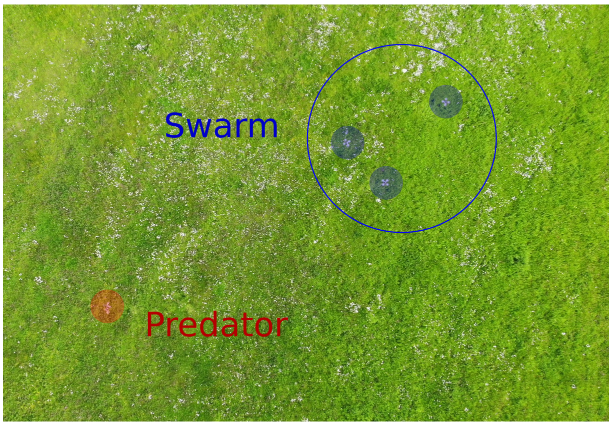

(c) $t = 170$ s

(d) $t = 253$ s

Figure 6.4: Snapshots from the real-world experiment in which MAVs used the UVDAR system and did not use Communication.

The quantities measured in this experiment are the same as in the previous one and are plotted in Figure 6.5:

- Upper left corner - distances between MAVs and the predator,
- Upper right corner - distances between swarm MAVs,
- Bottom left corner - velocities of swarm MAVs and the predator,
- Bottom right corner - distances obtained from the UVDAR system of MAV-1 between MAV-1 and other swarm MAVs and between MAV-1 and the predator.

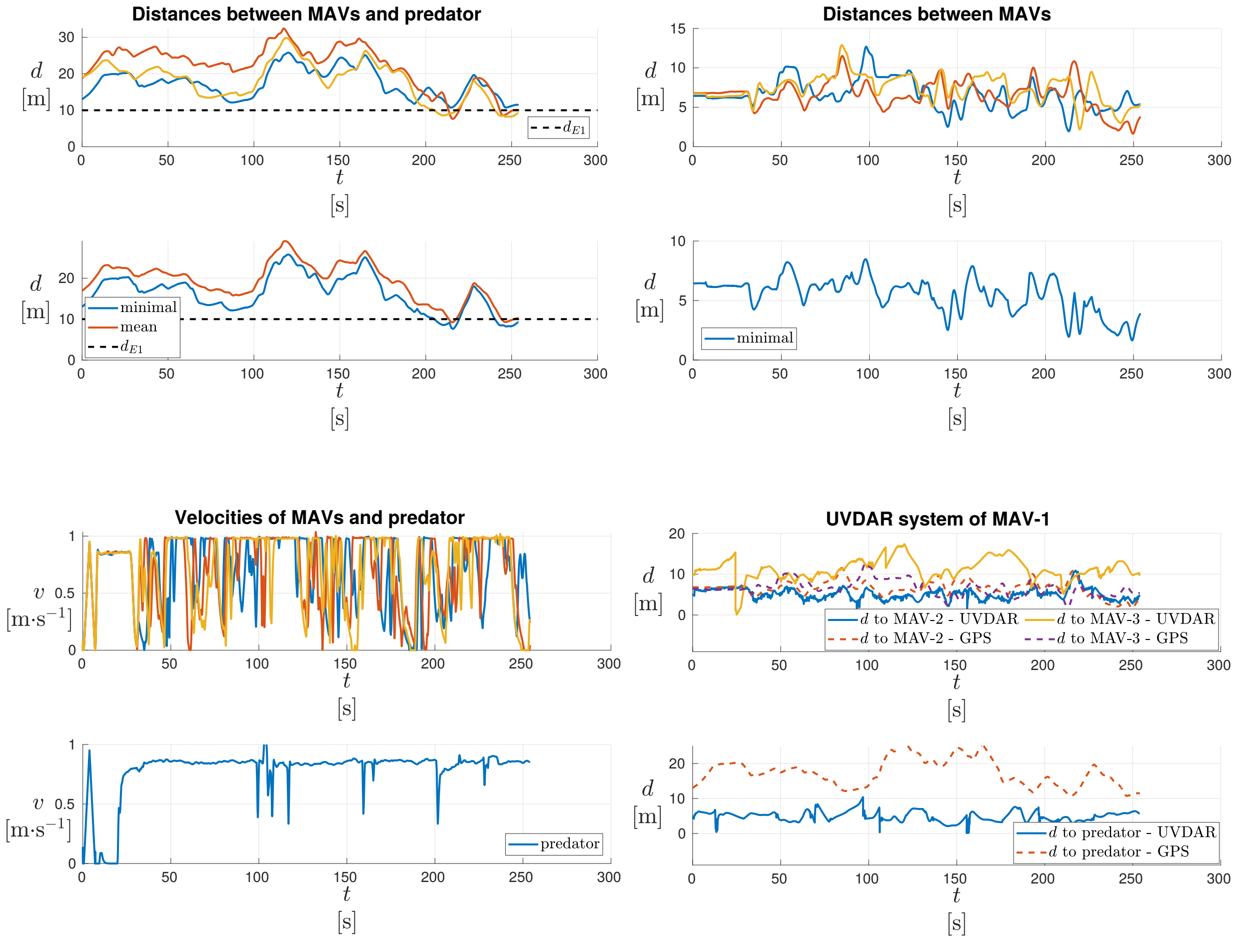

Figure 6.5: Distances between MAVs and the predator, distances between MAVs, velocities of MAVs and the predator, distances obtained from the UVDAR system of MAV-1 between MAV-1 and other swarm MAVs and between MAV-1 and the predator - measured in real-world experiment in which MAVs used the UVDAR system and did not use Communication

6.3 Evaluation

In the two presented experiments, the swarm of MAVs reliably exhibited its escape behaviour for the whole duration of both experiments - 176 s if swarm MAVs used Communication and 254 s if swarm MAVs did not use Communication. The graph of distances in Figures 6.3 and 6.5 shows that no collision had occurred. The minimal distance between MAVs in both experiments was greater than 2 m.

The data obtained from the UVDAR system implies that the UVDAR system works very well for short distances, i.e. the distance is lower than 10 m. But if the distance is greater than 10 m, the UVDAR system measured smaller distance than the calibrated GPS module, as shown by the graph of distances between the MAV-1 and the predator in Figure 6.3 and 6.5. Therefore, the UVDAR system is applicable for short-range detection, but long-range detection is problematic due to incorrect distance measurements.

The results of these experiments show that the system designed in this thesis is fully usable on the real MAVs that use onboard relative localization system. In the first experiment, swarm MAVs shared information about the position of a detected predator, but in the second one, the MAVs did not use any means sharing information via network and each member of the swarm made decisions only based on the data obtained from onboard sensors.

Chapter 7

Conclusion

In this thesis a decentralised system with implemented Escape behaviour algorithm has been developed for the swarm of real MAVs. The system has been tested in the realistic simulator Gazebo and verified by conducting real-world experiments. The designed system is able to use the method of relative localization of MAVs developed by MRS group at CTU in Prague called the UVDAR system. The proposed system can avoid static obstacles, which is presented in section 5.5. Thanks to the implemented Escape behaviour algorithm this system can also avoid dynamic obstacles and thus decrease the possibility of collisions with such obstacles. To summarise, the following tasks have been accomplished:

- The boids model for stabilization of a group of MAVs has been implemented in Chapter 2.
- Escape behaviour with shock propagation for a swarm of MAVs has been designed in Chapter 4.
- The proposed system has been adapted for use of the method of relative localization of MAVs developed by MRS group at CTU in Prague that is presented in section 3.2.
- The achieved behaviour has been compared with and without possibility of communication between particular MAVs in section 5.2 and 5.3.
- The designed system with implemented Escape behaviour algorithm has been compared with system using only classical Boids model without Escape behaviour algorithm in section 5.4.
- The designed system has been verified by conducting real-world experiments - Chapter 6.

The future research could focus on:

- Design and implementation of the method of recognition and localization of a predator onboard of a MAV.
- Considering cluster of points obtained from RPLIDAR as a single obstacle instead of each point being a new obstacle.
- Implementation of the method for navigation in environment with obstacles using Simultaneous Localization And Mapping (SLAM).
- Verify functionality of the proposed system on real MAVs with larger number of swarm members.

Bibliography

[1] H. Min and Z. Wang, "Design and analysis of group escape behavior for distributed autonomous mobile robots," *IEEE International Conference on Robotics and Automation*, May 2011, doi: 10.1109/ICRA.2011.5980123.

[2] C. W. Reynolds, "Flocks, herds, and schools: A distributed behavioral model," *Computer Graphics*, vol. 21, no. 4, July 1987.

[3] V. Trianni, *Evolutionary Swarm Robotics.* Springer, Berlin, Heidelberg, 2008, vol. 108, doi: 10.1007/978-3-540-77612-3.

[4] A. Tahir, J. Böling, M.-H. Haghbayan, H. T. Toivonen, and J. Plosila, "Swarms of unmanned aerial vehicles — a survey," *Journal of Industrial Information Integration*, vol. 16, December 2019, doi: 10.1016/j.jii.2019.100106.

[5] M. Campion, P. Ranganathan, and S. Faruque, "A review and future directions of uav swarm communication architectures," *IEEE International Conference on Electro/Information Technology*, May 2018, doi: 10.1109/EIT.2018.8500274.

[6] A. Bürkle, F. Segor, and M. Kollmann, "Towards autonomous micro uav swarms," *Journal of Intelligent & Robotic Systems volume*, vol. 61, 2011, doi: 10.1007/s10846-010-9492-x.

[7] R. Olfati-Saber, "Flocking for multi-agent dynamic systems: Algorithms and theory," *IEEE Transactions on Automatic Control*, vol. 51, no. 3, pp. 401–420, March 2006, doi: 10.1109/TAC.2005.864190.

[8] P. Petracek, "Decentralized model of a swarm behavior boids in ros," Bachelor's Thesis, Czech Technical University in Prague, May 2017, url: http://mrs.felk.cvut.cz/data/students/petracekBP.pdf.

[9] Gazebo, *Official site of Gazebo*, Accessed: March 20, 2020. [Online]. Available: http://gazebosim.org/

[10] J. Vakula, "Escape behavior in swarms of unmanned helicopters," Bachelor's Thesis, Czech Technical University in Prague, May 2012, url: http://mrs.felk.cvut.cz/data/students/bulusekBP.pdf.

[11] J. Bulusek, "Active and passive escape behavior designed for groups of autonomous helicopters in dynamic environment," Bachelor's Thesis, Czech Technical University in Prague, May 2014, url: http://mrs.felk.cvut.cz/data/students/bulusekBP.pdf.

[12] V. Walter, N. Staub, A. Franchi, and M. Saska, "Uvdar system for visual relative localization with application to leader–follower formations of multirotor uavs," *IEEE Robotics and Automation Letters*, vol. 4, no. 3, July 2019, doi: 10.1109/LRA.2019.2901683.

[13] V. Walter, N. Staub, A. Franchi, and M. Saska, "Mutual localization of uavs based on blinking ultraviolet markers and 3d time-position hough transform," *IEEE 14th International Conference on Automation Science and Engineering*, August 2018, doi: 10.1109/COASE.2018.8560384.

[14] G. Gellinger, *Image from Pixabay*, Accessed: March 29, 2020. [Online]. Available: https://cdn.pixabay.com/photo/2018/05/16/18/24/emotions-3406667_960_720.jpg

[15] SLAMTEC, *RPLIDAR A3*, Accessed: March 15, 2020. [Online]. Available: http://www.slamtec.com/en/Lidar/A3

[16] Robot Operating System, *Official site of Robot Operating System*, Accessed: March 10, 2020. [Online]. Available: https://www.ros.org/

[17] T. Krajnik, M. Nitsche, J. Faigl, P. Vanek, M. Saska, L. Preucil, T. Duckett, and M. Mejail, "A practical multirobot localization system," *Journal of Intelligent & Robotic Systems*, vol. 76, 2014, doi: 10.1007/s10846-014-0041-x.

[18] M. Krogius, A. Haggenmiller, and E. Olson, "Flexible layouts for fiducial tags," *IEEE/RSJ International Conference on Intelligent Robots and Systems*, November 2019, doi: 10.1109/IROS40897.2019.8967787.

[19] K. Boudjit and C. Larbes, "Detection and target tracking with a quadrotor using fuzzy logic," *International Conference on Modelling, Identification and Control*, November 2016, doi: 10.1109/ICMIC.2016.7804285.

[20] J. Ochodnicky, Z. Matousek, M. Babjak, and J. Kurty, "Drone detection by ku-band battlefield radar," *International Conference on Military Technologies*, June 2017, doi: 10.1109/MILTECHS.2017.7988830.

[21] M. Vrba and M. Saska, "Marker-less micro aerial vehicle detection and localization using convolutional neural networks," *IEEE Robotics and Automation Letters*, vol. 5, no. 2, April 2020, doi: 10.1109/LRA.2020.2972819.

[22] M. Vrba, D. Hert, and M. Saska, "Onboard marker-less detection and localization of non-cooperating drones for their safe interception by an autonomous aerial system," *IEEE Robotics and Automation Letters*, vol. 4, no. 4, October 2019, doi: 10.1109/LRA.2019.2927130.

[23] A. Rozantsev, V. Lepetit, and P. Fua, "Flying objects detection from a single moving camera," *IEEE Conference on Computer Vision and Pattern Recognition*, June 2015, doi: 10.1109/CVPR.2015.7299040.

[24] R. Opromolla, G. Fasano, and D. Accardo, "A vision-based approach to uav detection and tracking in cooperative applications," *Sensors*, vol. 18, no. 10, October 2018, doi: 10.3390/s18103391.

[25] K. M. Ng, J. Johari, S. A. C. Abdullah, A. Ahmad, and B. N. Laja, "Performance evaluation of the rtk-gnss navigating under different landscape," *2018 18th International Conference on Control, Automation and Systems*, October 2018.

[26] Holybro, *Holybro Pixhawk 4 Neo-M8N GPS*, Accessed: May 15, 2020. [Online]. Available: http://www.holybro.com/manual/Pixhawk4-GPS-Quick-Start-Guide.pdf

Appendices

Appendix A

Simulations

A.1 Gazebo - 4 MAVs - UVDAR system

One see (States sharing) with Communication

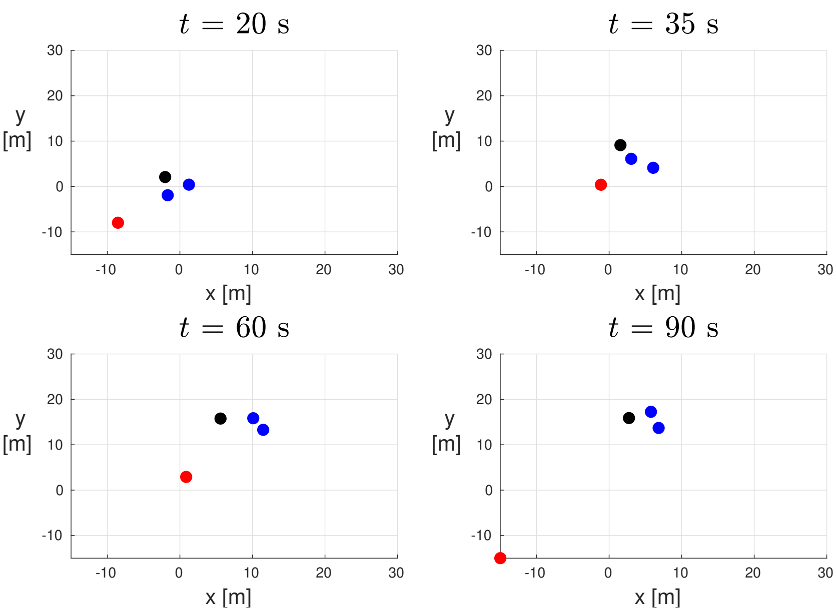

Figure A.1: Sub-figures contain positions of blue and black swarm members and red predator in x, y coordinates in time t if one of three MAVs (black) can detect a predator using States sharing and all MAVs use Communication and the UVDAR system.

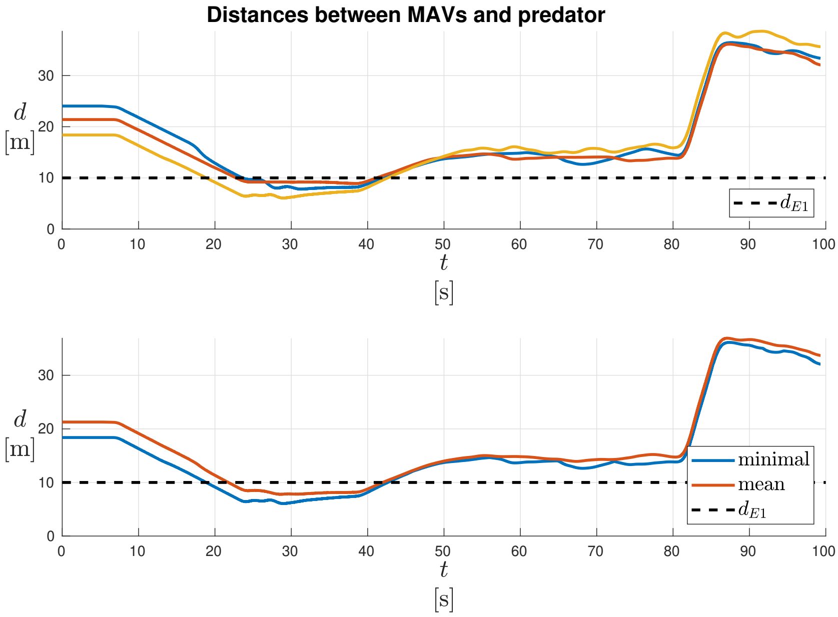

Figure A.2: The upper figure is a graph of distances between three MAVs and the predator if one MAV can detect the predator using States sharing and all MAVs use Communication and the UVDAR system. The lower figure shows minimal and mean distance between MAVs and the predator.

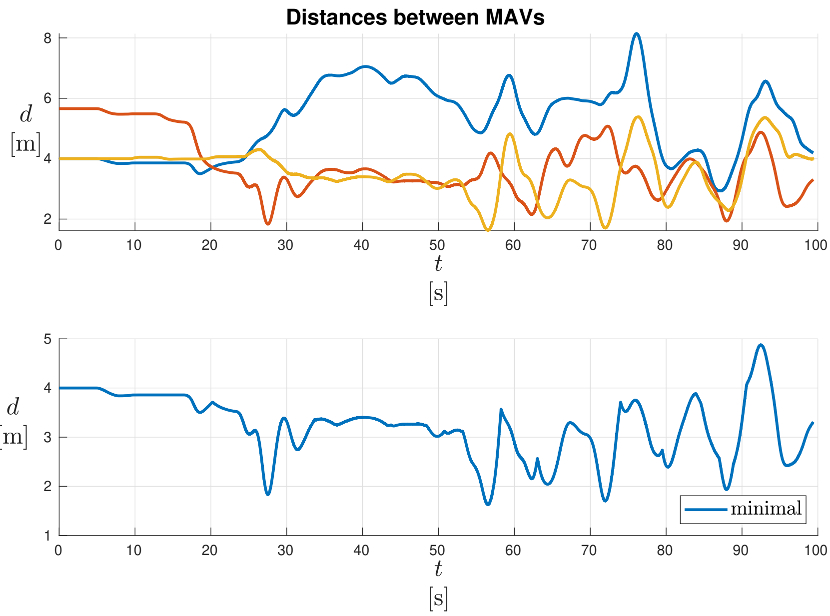

Figure A.3: The absolute and minimal distances between three MAVs if one MAV can detect a predator using States sharing and all MAVs use Communication and the UVDAR system.

t_s [s]	t_d [s]	t_e [s]	t_r [s]
18.860	22.800	22.948	0.148

Table A.1: Quantities t_s, t_d, t_e and t_r measured in simulation in which one of three MAVs can detect a predator using States sharing and all MAVs use Communication and the UVDAR system.

One see (States sharing) without Communication

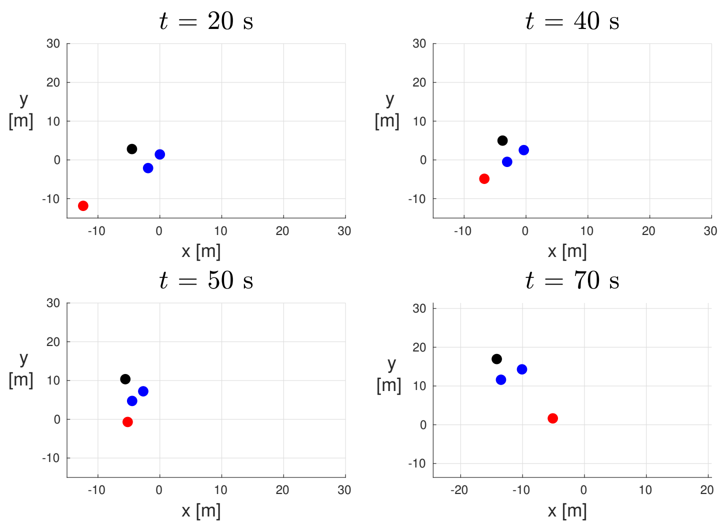

Figure A.4: Sub-figures contain positions of blue and black swarm members and red predator in x, y coordinates in time t if one of three MAVs (black) can detect a predator using States sharing and all MAVs use the UVDAR system and do not use Communication.

t_s [s]	t_d [s]	t_e [s]	t_r [s]
29.828	35.316	36.352	1.036

Table A.2: Quantities t_s, t_d, t_e and t_r measured in simulation in which one of three MAVs can detect a predator using States sharing and all MAVs use the UVDAR system and do not use Communication.

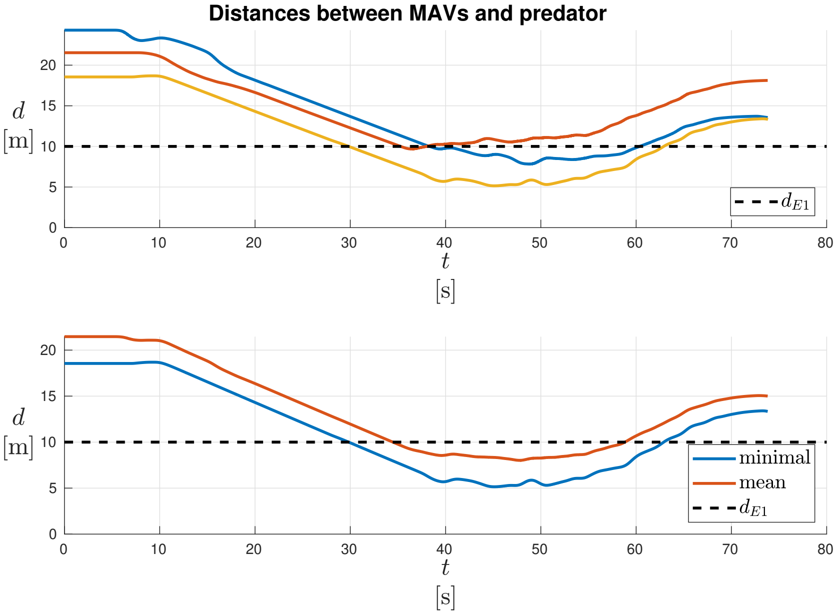

Figure A.5: The upper figure is a graph of distances between three MAVs and the predator if one MAV can detect the predator using States sharing and all MAVs use the UVDAR system and do not use Communication. The lower figure shows minimal and mean distance between MAVs and the predator.

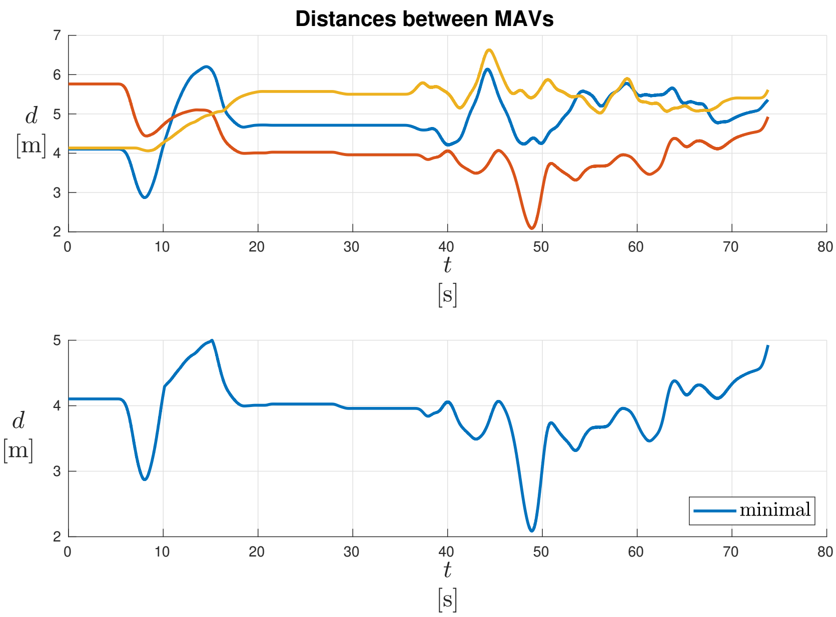

Figure A.6: The absolute and minimal distances between three MAVs if one MAV can detect a predator using States sharing and all MAVs use the UVDAR system and do not use Communication.

A.2 Gazebo - obstacles

6 MAVs

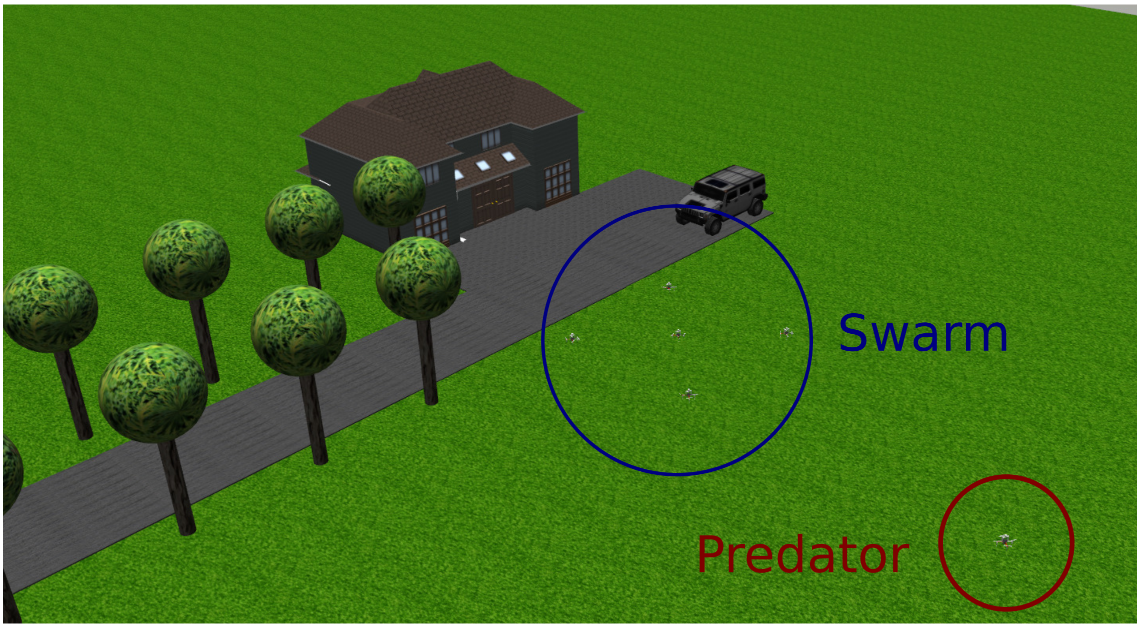

Figure A.7: Situation of six MAVs in the Gazebo simulator in world with a house, a car and trees

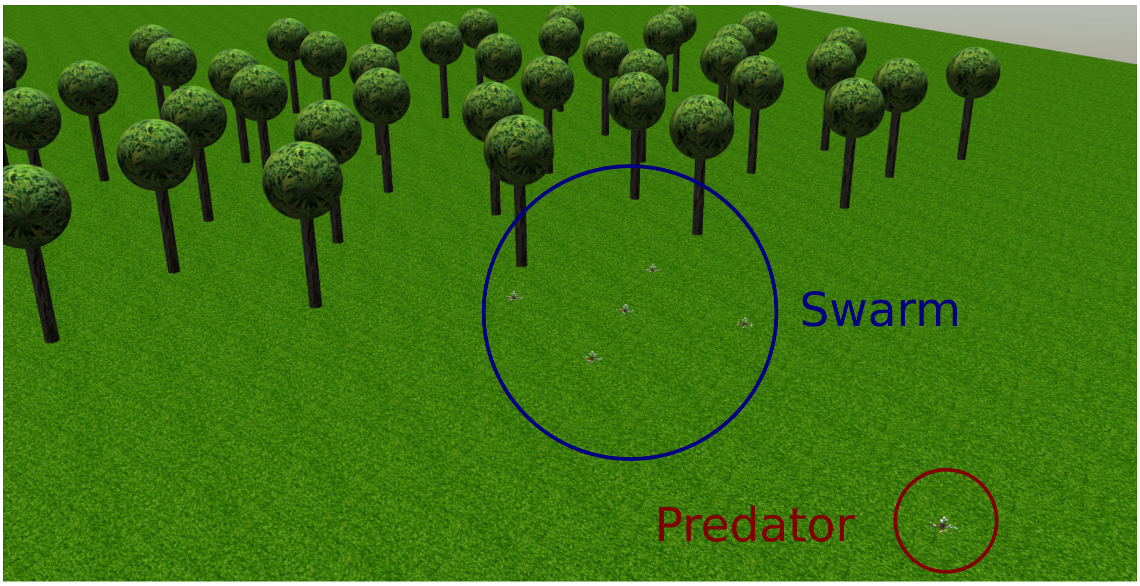

Figure A.8: Situation of six MAVs in the Gazebo simulator in world with a forest

4 MAVs

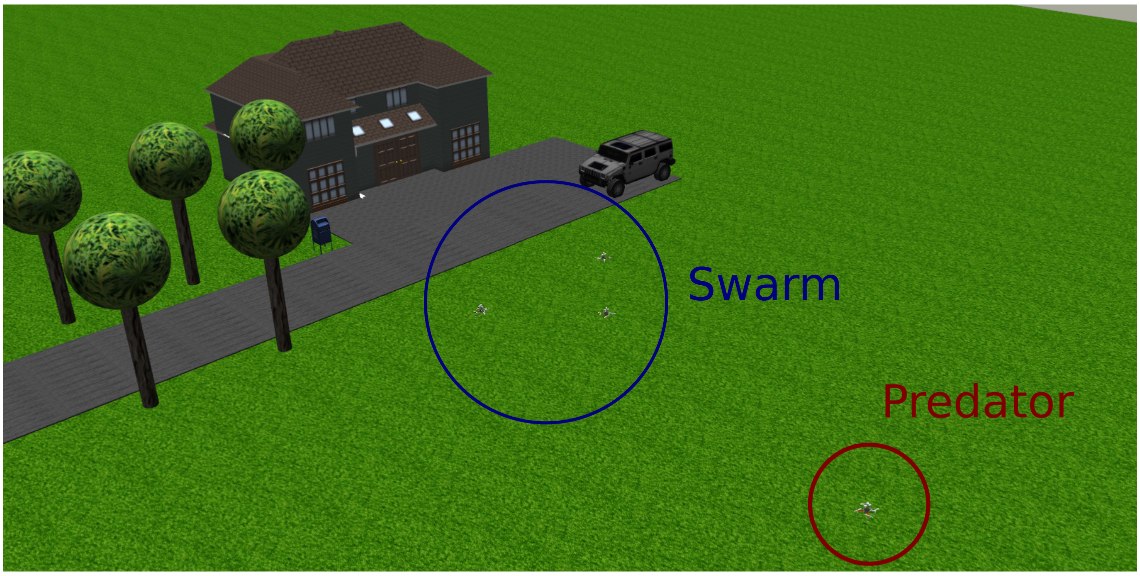

Figure A.9: Situation of four MAVs in the Gazebo simulator in world with a house, a car and trees

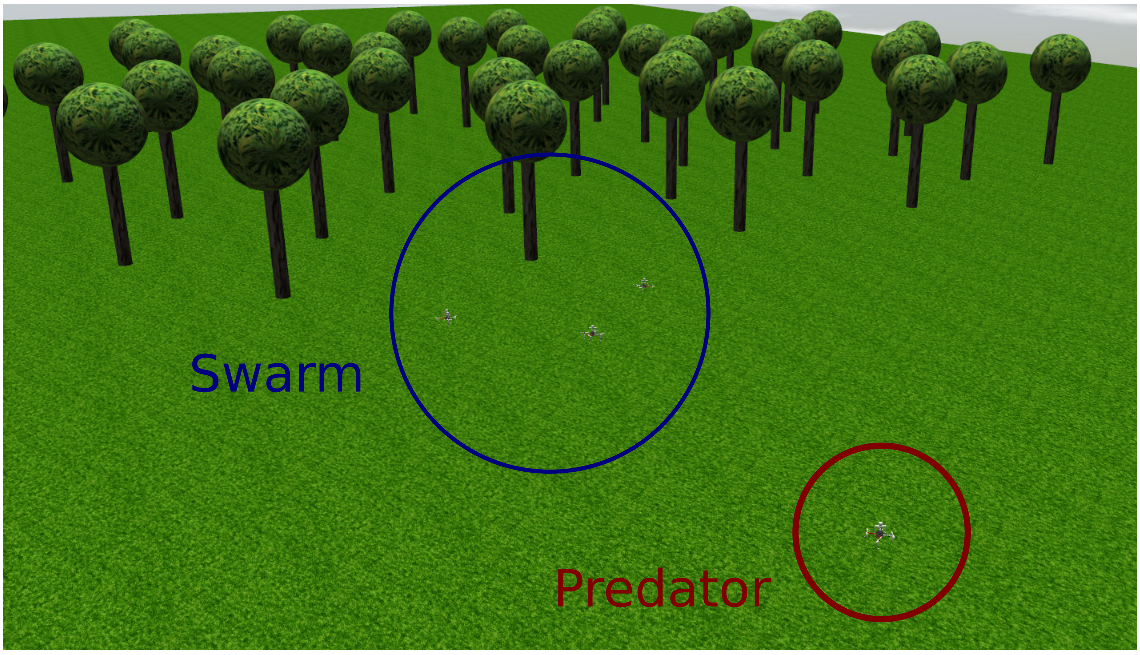

Figure A.10: Situation of four MAVs in the Gazebo simulator in world with a forest

Appendix B

Parameters for simulations

Matlab

r_B	d_{min}	d_C	k_{1C}	k_{2C}	d_{max}	d_S	k_{1S}	k_{2S}	k_A
15 m	4 m	6 m	0.1 m^{-2}	1	4 m	2 m	0.075 m^{-2}	1.45 $\mathrm{m}^{\frac{1}{2}}$	0.1 $\mathrm{s{\cdot}m}^{-1}$

k_E	d_{E1}	d_{E2}	k_F	d_F	d^P_{min}	d^P_C	k^P_{1C}	k^P_{2C}	d^P_{max}	d^P_S
7 $\mathrm{m}^{\frac{1}{2}}$	10 m	10 m	1	1	4 m	6 m	0.1 m^{-2}	1	4 m	2 m

k^P_{1S}	k^P_{2S}	t_{ESC}	t_{nd}	r_O	$d_{O,max}$	k_{O1}	k_{O2}
0.075 m^{-2}	1.45 $\mathrm{m}^{\frac{1}{2}}$	30 s	3 s	1.5 m	6 m	4 $\mathrm{m}^{\frac{1}{2}}$	4 $\mathrm{m}^{\frac{1}{2}}$

Table B.1: Parameters for simulation in section Matlab

Gazebo - 6 MAVs - States sharing

r_B	d_{min}	d_C	k_{1C}	k_{2C}	d_{max}	d_S	k_{1S}	k_{2S}	k_A
8 m	4 m	6 m	0.1 m^{-2}	1	4 m	2 m	0.075 m^{-2}	1.45 $\mathrm{m}^{\frac{1}{2}}$	0.1 $\mathrm{s{\cdot}m}^{-1}$

k_E	d_{E1}	d_{E2}	k_F	d_F	d^P_{min}	d^P_C	k^P_{1C}	k^P_{2C}	d^P_{max}	d^P_S
7 $\mathrm{m}^{\frac{1}{2}}$	10 m	15 m	3	1	4 m	6 m	0.1 m^{-2}	0.42	4 m	2 m

k^P_{1S}	k^P_{2S}	δ_{TH}	t_{ESC}	t_{nd}	r_O	$d_{O,max}$	k_{O1}	k_{O2}
0.075 m^{-2}	1.45 $\mathrm{m}^{\frac{1}{2}}$	0.75	30 s	3 s	1.5 m	6 m	4 $\mathrm{m}^{\frac{1}{2}}$	4 $\mathrm{m}^{\frac{1}{2}}$

Table B.2: Parameters for simulations in section Gazebo - 6 MAVs - States sharing

Gazebo - 4 MAVs - UVDAR system

r_B	d_{min}	d_C	k_{1C}	k_{2C}	d_{max}	d_S	k_{1S}	k_{2S}	k_A
10 m	4 m	6 m	0.1 m^{-2}	1	4 m	2 m	0.075 m^{-2}	1.45 $m^{\frac{1}{2}}$	0.1 s·m^{-1}

k_E	d_{E1}	d_{E2}	k_F	d_F	d^P_{min}	d^P_C	k^P_{1C}	k^P_{2C}	d^P_{max}	d^P_S
5 $m^{\frac{1}{2}}$	10 m	15 m	0.1	1	3.5 m	5.5 m	0.2 m^{-2}	1.5	3.5 m	1.5 m

k^P_{1S}	k^P_{2S}	t_{ESC}	t_{nd}	r_O	$d_{O,max}$	k_{O1}	k_{O2}
0.175 m^{-2}	1.95 $m^{\frac{1}{2}}$	30 s	2 s	1.5 m	6 m	4 $m^{\frac{1}{2}}$	4 $m^{\frac{1}{2}}$

Table B.3: Parameters for simulations in section Gazebo - 4 MAVs - UVDAR system

Gazebo - only Boids without Escape behaviour

States sharing - 6 MAVs

r_B	d_{min}	d_C	k_{1C}	k_{2C}	d_{max}	d_S	k_{1S}
8 m	4 m	6 m	0.1 m^{-2}	1	4 m	2 m	0.075 m^{-2}

k_{2S}	k_A	r_O	$d_{O,max}$	k_{O1}	k_{O2}
1.45 $m^{\frac{1}{2}}$	0.1 s·m^{-1}	1.6 m	5 m	3 $m^{\frac{1}{2}}$	3 $m^{\frac{1}{2}}$

Table B.4: Parameters for simulations in section Gazebo - only Boids without Escape behaviour: States sharing - 6 MAVs

UVDAR system - 4 MAVs

r_B	d_{min}	d_C	k_{1C}	k_{2C}	d_{max}	d_S	k_{1S}
8 m	4 m	6 m	0.1 m^{-2}	1	4 m	2 m	0.075 m^{-2}

k_{2S}	k_A	r_O	$d_{O,max}$	k_{O1}	k_{O2}
1.45 $m^{\frac{1}{2}}$	0.1 s·m^{-1}	1.6 m	5 m	3 $m^{\frac{1}{2}}$	3 $m^{\frac{1}{2}}$

Table B.5: Parameters for simulations in section Gazebo - only Boids without Escape behaviour: UVDAR system - 4 MAVs

Gazebo - obstacles

States sharing - 6 MAVs

r_B	d_{min}	d_C	k_{1C}	k_{2C}	d_{max}	d_S	k_{1S}	k_{2S}	k_A
8 m	4 m	6 m	0.1 m^{-2}	1	4 m	2 m	0.075 m^{-2}	1.45 m$^{\frac{1}{2}}$	0.1 s·m^{-1}

k_E	d_{E1}	d_{E2}	k_F	d_F	d^P_{min}	d^P_C	k^P_{1C}	k^P_{2C}	d^P_{max}	d^P_S
5 m$^{\frac{1}{2}}$	10 m	15 m	3	1	4 m	6 m	0.1 m^{-2}	0.42	4 m	2 m

k^P_{1S}	k^P_{2S}	δ_{TH}	t_{ESC}	t_{nd}	r_O	$d_{O,max}$	k_{O1}	k_{O2}
0.075 m^{-2}	1.45 m$^{\frac{1}{2}}$	0.75	30 s	3 s	1.6 m	6 m	6 m$^{\frac{1}{2}}$	6 m$^{\frac{1}{2}}$

Table B.6: Parameters for simulations in section Gazebo - obstacles: States sharing - 6 MAVs

UVDAR system - 4 MAVs

r_B	d_{min}	d_C	k_{1C}	k_{2C}	d_{max}	d_S	k_{1S}	k_{2S}	k_A
10 m	4 m	6 m	0.1 m^{-2}	1	4 m	2 m	0.075 m^{-2}	1.45 m$^{\frac{1}{2}}$	0.1 s·m^{-1}

k_E	d_{E1}	d_{E2}	k_F	d_F	d^P_{min}	d^P_C	k^P_{1C}	k^P_{2C}	d^P_{max}	d^P_S
5 m$^{\frac{1}{2}}$	10 m	15 m	0.1	1	3.5 m	5.5 m	0.2 m^{-2}	1.5	3.5 m	1.5 m

k^P_{1S}	k^P_{2S}	t_{ESC}	t_{nd}	r_O	$d_{O,max}$	k_{O1}	k_{O2}
0.175 m^{-2}	1.95 m$^{\frac{1}{2}}$	30 s	2 s	1.6 m	6 m	6 m$^{\frac{1}{2}}$	6 m$^{\frac{1}{2}}$

Table B.7: Parameters for simulations in section Gazebo - obstacles: UVDAR system - 4 MAVs

Appendix C

Parameters for experiments

UVDAR system - Communication

r_B	d_{min}	d_C	k_{1C}	k_{2C}	d_{max}	d_S	k_{1S}	k_{2S}	k_A
10 m	4 m	6 m	0.1 m^{-2}	1	4 m	2 m	0.075 m^{-2}	1.45 $m^{\frac{1}{2}}$	0.1 $s \cdot m^{-1}$

k_E	d_{E1}	d_{E2}	k_F	d_F	d^P_{min}	d^P_C	k^P_{1C}	k^P_{2C}	d^P_{max}	d^P_S
7 $m^{\frac{1}{2}}$	10 m	13 m	0.1	1	3.5 m	5.5 m	0.2 m^{-2}	1.5	3.5 m	1.5 m

k^P_{1S}	k^P_{2S}	t_{ESC}	t_{nd}
0.175 m^{-2}	1.95 $m^{\frac{1}{2}}$	30 s	3 s

Table C.1: Parameters for real-world experiments in section UVDAR system - Communication

UVDAR system - without Communication

r_B	d_{min}	d_C	k_{1C}	k_{2C}	d_{max}	d_S	k_{1S}	k_{2S}	k_A
10 m	4 m	6 m	0.1 m^{-2}	1	4 m	2 m	0.075 m^{-2}	1.45 $m^{\frac{1}{2}}$	0.1 $s \cdot m^{-1}$

k_E	d_{E1}	d_{E2}	k_F	d_F	d^P_{min}	d^P_C	k^P_{1C}	k^P_{2C}	d^P_{max}	d^P_S
7 $m^{\frac{1}{2}}$	9.5 m	12 m	0.1	1	3.5 m	5.5 m	0.2 m^{-2}	1.5	3.5 m	1.5 m

k^P_{1S}	k^P_{2S}	t_{ESC}	t_{nd}
0.175 m^{-2}	1.95 $m^{\frac{1}{2}}$	25 s	3 s

Table C.2: Parameters for real-world experiments in section UVDAR system - without Communication

Appendix D

CD Content

In Table D.1 are listed names of all root directories on CD.

Directory name	**Description**
thesis.pdf	the thesis in pdf format
thesis_sources	latex source codes
source_codes	source codes, scripts
videos_sim	videos from simulations in Gazebo simulator
videos_exp	videos from real-world experiments

Table D.1: CD Content

Appendix E

List of abbreviations

In Table E.1 are listed abbreviations used in this thesis.

Abbreviation	**Meaning**
MAV	Micro Aerial Vehicle
GNSS	Global Navigation Satellite System
GPS	Global Positioning System
CTU	Czech Technical University
MRS	Multi-robot Systems
UVDAR	UltraViolet Direction And Ranging
UV	ultraviolet
ROS	Robot Operating System
CNN	Convolutional Neural Network
AAIS	Autonomous Aerial Intercepting Systems
RTK	Real Time Kinematics

Table E.1: Lists of abbreviations